

South Dakota State University

# Open PRAIRIE: Open Public Research Access Institutional Repository and Information Exchange

---

Electronic Theses and Dissertations

---

2023

## Advanced Analytical Techniques for the Analysis of Toxic Inhaled Agent Exposure and Pharmacokinetic Investigation

Sharmin Sultana

Follow this and additional works at: <https://openprairie.sdstate.edu/etd2>



Part of the [Chemistry Commons](#)

---

ADVANCED ANALYTICAL TECHNIQUES FOR THE ANALYSIS OF TOXIC INHALED  
AGENT EXPOSURE AND PHARMACOKINETIC INVESTIGATION

BY

SHARMIN SULTANA

A dissertation submitted in partial fulfillment of the requirements for the

Doctor of Philosophy

Major in Chemistry

South Dakota State University

2023

## DISSERTATION ACCEPTANCE PAGE

Sharmin Sultana

This dissertation is approved as a creditable and independent investigation by a candidate for the Doctor of Philosophy degree and is acceptable for meeting the dissertation requirements for this degree. Acceptance of this does not imply that the conclusions reached by the candidate are necessarily the conclusions of the major department.

Brian Logue

Advisor

Date

Matthew Miller

Department Head

Date

Nicole Lounsbery, PhD

Director, Graduate School

Date

This dissertation is dedicated to my parents, MD Mohidul Islam and Mst Ismot Ara Begum, and my life partner, Dr. A K M Ahsan Ahmed. I am grateful for their love, support, and sacrifices. Without them, I might not be the person I am today.

## ACKNOWLEDGEMENTS

I would like to express my heartfelt appreciation to my advisor, Dr. Brian A. Logue, for his timely assistance, guidance, encouragement, and constructive feedback throughout my South Dakota State University journey. His vast knowledge and experience in analytical chemistry have significantly helped develop the methodology and answer this work's research questions. I am forever grateful to you for considering me as a member of your LARGE group, believing in me, and guiding me through the entire doctoral journey.

My special thanks go to the LARGE research group, my advisory committee members, the Department of Chemistry and Biochemistry, and all the faculty members and the staff for their assistance and their active participation in shaping my success at SDSU. I am also grateful to Dr. Amanda Appel for helping with instrument troubleshooting and Dr. Subrata Bhadra for sharing his experience with DMTS. I would like to thank the collaborators, especially Drs. Gary A. Rockwood and Vikhyat Bebartta for sending the animal samples. My sincere gratitude goes to the funding agencies supporting my research and making completing my degree possible.

I would like to thank my father, MD Mohidul Islam, my mother, MST Ismot Ara Begum, and my sisters, Jesmin Akter and Nasmin Akter, for their love and belief in me. Many thanks to my in-laws for their never-ending support and encouragement. I would like to thank the most special person in my life, my husband, Dr. A K M Ahsan Ahmed, without whom this journey would not have been possible. Thank you for providing me with your constant support, love, and encouragement to make this journey easier.

**TABLE OF CONTENTS**

Abbreviations .....	x
List of Figures .....	xiv
List of Tables .....	xviii
Abstract .....	xix
1 Chapter 1. Introduction and background .....	1
1.1 Overall Significance .....	1
1.2 Project objectives .....	1
1.3 Toxic inhalation agents .....	2
1.4 Pathogenesis of TIAs.....	3
1.5 Exposure to chlorine and cyanide.....	5
2 CHAPTER 2. Verification of chlorine exposure via lc-ms/ms analysis of base hydrolyzed chlorophenols from chlorotyrosine-protein adducts .....	7
2.1 Abstract .....	7
2.2 Introduction .....	8
2.3 Materials and Methods .....	13
2.3.1 Materials.....	13
2.3.2 Biological samples .....	13
2.3.3 Sample preparation.....	14
2.3.4 UHPLC-MS/MS analysis of 2,6-DCP.....	15
2.3.5 Calibration, quantification, and limit of detection.....	16

2.3.6 Recovery and matrix effect .....	18
2.3.7 Stability .....	18
2.4 Results and Discussion .....	19
2.4.1 UHPLC-MS/MS analysis of 2,6-DCP.....	19
2.4.2 Dynamic range, the limit of detection, and sensitivity .....	24
2.4.3 Accuracy and precision .....	25
2.4.4 Matrix effect and recovery .....	27
2.4.5 Stability of 2,6-DCP and chloro-tyrosine adduct .....	28
2.4.6 Verification of chlorine exposure via 2,6-DCP analysis .....	29
2.5 Conclusion .....	31
2.6 Acknowledgment.....	31
<b>3 CHAPTER 3. Development of a rapid fluorescence probe for the analysis of aqueous hypochlorite .....</b>	<b>32</b>
3.1 Abstract .....	32
3.2 Introduction .....	33
3.3 Materials and Methods .....	36
3.3.1 Materials.....	36
3.3.2 Analytical Instruments .....	36
3.3.3 Synthesis of FSH probes .....	37
3.3.3.1 Purification of FSH via preparative HPLC .....	38

3.3.3.2 Evaluation of FSH purity via LC-MS/MS .....	39
3.3.4 Fluorescence analysis of hypochlorite using FSH .....	41
3.3.5 Method limit of detection .....	41
3.4 Results and Discussion .....	42
3.4.1 Synthesis of FSH .....	42
3.4.2 Spectroscopic properties.....	43
3.4.3 Quantification of $\text{ClO}^-$ using FSH .....	46
3.4.4 Selectivity of FSH to hypochlorite .....	48
3.4.5 Analytical applications .....	49
3.5 Conclusions .....	50
3.6 Acknowledgments .....	50
4 CHAPTER 4. Pharmacokinetics of Next Generation Cyanide Antidote Dimethyl Trisulfide Following Intranasal and Intramuscular Administration of DMTS in Rats and Swine.....	51
4.1 Abstract .....	51
4.2 Introduction .....	52
4.3 Materials and Methods .....	55
4.3.1 Materials.....	55
4.3.2 Biological samples .....	56
4.3.2.1 Swine model of DMTS administration .....	56

4.3.2.2 Rat model of DMTS administration .....	58
4.3.3 Preparation of DMTS standards and samples .....	59
4.3.4 Dynamic headspace GC-MS analysis of DMTS .....	60
4.3.5 Pharmacokinetic studies .....	61
4.3.6 Pharmacokinetics & data analysis .....	62
4.4 Results and Discussion .....	62
4.4.1 PK behavior of Intravenous DMTS-treated Swine .....	62
4.4.2 PK behavior of IM-administered DMTS.....	65
4.4.2.1 Rats treated with Intramuscular DMTS.....	65
4.4.2.2 Swine treated with Intramuscular DMTS .....	69
4.4.3 PK behavior of Intranasal-treated DMTS.....	74
4.4.3.1 Rats treated with Intranasal DMTS .....	74
4.4.3.2 Swine treated with Intranasal DMTS .....	77
4.4.4 Discussion (IV, IM, and IN- administered DMTS in rats and swine) .....	81
4.4.5 Comparing current US FDA-approved antidotes with a novel antidote (DMTS) .....	82
4.5 Conclusion.....	85
4.6 Acknowledgments .....	85
5 CHAPTER 5. Conclusions, Broder impacts, and future works .....	86

5.1 Conclusions .....	86
5.2 Broder impacts .....	86
5.3 Future work .....	87
6 REFERENCES .....	88

## ABBREVIATIONS

2-CP: 2-chlorophenol

2,6-DCP: 2,6-dichlorophenol

2,4-DCP-d<sub>3</sub>: 2,4-dichlorophenol-d<sub>3</sub>

ACN: Acetonitrile

ATP: Adenosine triphosphate

AUC: Area under the curve

CE: Collision energy

C<sub>max</sub>: Concentration maximum

Cl-Tyr: 3-chlorotyrosine

Cl<sub>2</sub>-Tyr: 3,5-dichlorotyrosine

CN: Cyanide

CWAs: Chemical warfare agents

CXP: Collision cell exit potential

DI: Deionized

DHS: Dynamic headspace

DHS-GC/MS: Dynamic headspace gas chromatography mass spectrometry

DMTS: Dimethyl trisulfide

DMTS-d<sub>6</sub>: Dimethyl trisulfide-d<sub>6</sub>

DMDS: Dimethyl trisulfide

DMDS-d<sub>6</sub>: Dimethyl disulfide-d<sub>6</sub>

DP: Declustering potential

EDTA: Ethylenediaminetetraacetic acid

EI: Electron impact

EPA: U.S. Environmental protection agency

ESI: Electron spray ionization

FDA: Food and Drug Administration

FSH: Fluorescence thioacid

GC: Gas chromatography

HCN: Hydrogen cyanide

HPLC: High performance liquid chromatography

HPLC-MS-MS: High performance liquid chromatography-tandem mass spectrometry

HS: Headspace

IACUC: Institutional animal care and use committee

IM: Intramuscular

IN: Intranasal

IS: Internal standard

IV: Intravenous

$K_E$ : Elimination rate constant

LC: Liquid chromatography

LD: Lethal dose

LLOQ: Lower limit of quantification

LOD: Limit of detection

LQC: Low-quality control

$\mu\text{M}$ : Micromolar

MAP: Mean arterial pressure

MITC: Methyl isothiocyanate

MPS: MultiPurpose sampler

MQC: Medium quality control

MRM: Multiple reaction monitoring

MS: Mass spectrometry

MS/MS: Tandem mass spectroscopy

MT: Methanethiol

m/z: Mass-to-charge ratio

nM: Nanomolar

N: Theoretical plate

NIH: U.S. National Institute of Health

PRA: Percent residual accuracy

ppm: Parts per million

ppb: Parts per billion

Q1: First quadrupole mass analyzer

Q2: Collision cell

Q3: Third quadrupole mass analyzer

QC: Quality control

ROS: Reactive oxygen species

RSD: Relative standard deviation

R<sub>s</sub>: Resolution

RT: Room temperature

SCN: Thiocyanate

SEM: Standard error of the mean

SIM: Selective ion monitoring

S/N: Signal-to-noise

SPME: Solid phase microextraction

$t_{1/2 \alpha}$ :  $\alpha$ -phase half-life

$t_{1/2 \beta}$ :  $\beta$ -phase half-life

$t_{1/2 \gamma}$ :  $\gamma$ -phase half-life

$t_{\max}$ : Time of maximum concentration

TC: Tube conditioner

TDU: Thermal desorption unit

Tf: Tailing factor

TLV: Threshold limit value

UCD: University of Colorado Denver

ULOQ: Upper limit of quantification

USAMRICD: United States Army Medical Research Institute of Chemical Defense

UV: Ultraviolet

V: Volts

VOCs: Volatile organic chemicals

WWI: World War I

WWII: World War II

## LIST OF FIGURES

- Figure 1.** Scheme of some of the reactions potentially causing the formation of reactive oxygen and nitrogen species in the setting of acute chlorine inhalation..... 6
- Figure 2.** Reaction pathway for the formation of chlorophenols from the reaction of tyrosine residues with chlorine and subsequent base-catalyzed hydrolysis. Tyrosine residues react with the free chlorine residues to form a chlorotyrosine adduct which can undergo base hydrolysis to produce 2-CP and 2,6-DCP..... 10
- Figure 3.** ESI (-) product ion mass spectra of 2,6-DCP (B) and 2,4-DCP-d<sub>3</sub> (D) and 2-CP (F) with suggested structural assignments identification of the abundant ions. Molecular ions of 2,6-DCP and 2,4-DCP-d<sub>3</sub>, and 2-CP [M-H]<sup>-</sup> correspond to 160.9 and 163.8 and 126.9, respectively. Insets, the structures of 2,6-DCP (B) and 2,4-DCP-d<sub>3</sub> (D) and 2-CP (F) with suggested fragmentation are shown. .... 21
- Figure 4.** UHPLC-MS/MS chromatograms of 2,6-DCP spiked (A), NaOCl-spiked (B) and 2,4-DCP-d<sub>3</sub> (C) spiked rat plasma following sample preparation are presented. The 160.9→125 m/z transitions for 2,6-DCP spiked (A) and NaOCl-spiked (B) and 163.8→126.9 m/z transitions for 2,4-DCP-d<sub>3</sub> (C) are plotted. The insets show the magnified baseline of unspiked rat plasma. .... 23
- Figure 5.** UHPLC-MS/MS chromatogram of 2,6-DCP from the plasma of Cl<sub>2</sub>-exposed and non-exposed rats are presented (A). The 160.9 → 125 m/z transition is plotted. Correlation of Cl<sub>2</sub> dose to the concentration of 2,6-DCP from exposed rats (B). The error bars represent the standard error of the mean, \*\* = p<0.01..... 30
- Figure 6.** Chlorine reactions with water. .... 35
- Figure 7.** <sup>1</sup>H-NMR of synthesized probe called fluorescein thioacid (FSH). .... 38

<b>Figure 8.</b> The synthesis pathway of probe (FSH). .....	39
<b>Figure 9.</b> ClO <sup>-</sup> induced oxidation of fluorescent probe (FSH). .....	41
<b>Figure 10.</b> LC-MS/MS chromatogram for FSH and FOH from the crude product and purified fraction by the preparative HPLC. ....	43
<b>Figure 11.</b> Fluorescence spectra of probe (5 μM) in the absence and presence of NaOCl (100 μM) in the deionized water. The inset shows the photographs of the solution of the probe in the absence and presence of NaOCl under black light. ....	44
<b>Figure 12.</b> Time-course of fluorescence intensity at 513 nm for probe (5 μM) in the presence of NaOCl (100 μM). ....	45
<b>Figure 13.</b> pH optimization for the fluorescence at 513 nm for probe (5 μM) in the presence of NaOCl (100 μM). ....	46
<b>Figure 14.</b> (A) Fluorescence response of probe FSH (5 μM) upon addition of various concentration of ClO <sup>-</sup> . (B) Standard curve of fluorescence intensity at 513 nm versus ClO <sup>-</sup> concentration. $\lambda_{ex}/\lambda_{em} = 482/513$ nm. ....	47
<b>Figure 15.</b> Fluorescence intensity of probe (5 μM) in the presence of various analytes (200 μM) at 513 nm in deionized water. ....	49
<b>Figure 16.</b> Schematic representation of the reaction of DMTS and cyanide to form dimethyl disulfide (DMDS) and thiocyanate. ....	54
<b>Figure 17.</b> Blood concentration of DMTS (A) and DMDS (B) after IV administration of 10 mg/kg DMTS (10% aqueous) in non-exposed swine. Error bars represent the standard error of the mean (N=4). ....	64

- Figure 18.** Blood DMTS concentration after IM administration of DMTS with 25 mg/kg (A) and 5 mg/kg (B) in non-exposed rats. Error bars represent the standard error of the mean (N=7 for A, N=6 for B). ..... 67
- Figure 19.**  $C_{max}$  versus dose (25 and 5 mg/kg) of IM administration in non-exposed rats. Error bars represent the standard error of the mean (N=7, for each dose). ..... 68
- Figure 20.** Blood DMTS concentration after IM administration of 25 mg/kg DMTS in CN-exposed (7.5 mg/kg) rats. Error bars represent the standard error of the mean. (N=3 for CN-exposed, N =7 for No-KCN). Inset shows the comparison concentration of CN-exposed and non-exposed rats after 25 mg/kg (data from **Figure 18A**). ..... 68
- Figure 21.** Blood DMTS concentrations after IM administration of DMTS with 25 mg/kg (A) and 12.5 mg/kg (B) in CN-exposed (7.5 mg/kg) swine. (N=1) ..... 70
- Figure 22.** Blood DMTS (A) and DMDS (B) concentrations after IM administration of 10 mg/kg DMTS in CN-exposed (7.5 mg/kg) swine. Error bars represent the standard error of the mean (N=7 for A, N=4 for B). ..... 72
- Figure 23.** Blood DMTS (A) and DMDS (B) concentrations after IM administration of a double dose of DMTS (each dose was 7.5 mg/kg) in CN-exposed (7.5 mg/kg) swine. Error bars represent the standard error of the mean (N= 6). ..... 73
- Figure 24.** Blood DMTS (A) and DMDS (B) concentrations after IN administration of 100 mg/kg DMTS in non-exposed rats. Error bars represent the standard error of the mean (N = 9 for A, N=5 for B). ..... 76
- Figure 25.** Blood DMTS (A) and DMDS (B) concentrations after IN administration of 550  $\mu$ L of neat DMTS in non-exposed swine. Error bars represent the standard error of the mean (N = 4). ..... 78

**Figure 26.** Blood DMDS concentration after IN administration of 550  $\mu$ L of neat DMTS in CN-exposure (7.5 mg/kg) swine. Error bars represent the standard error of the mean (N = 4). Blood DMTS concentration was below LLOQ ( $<0.2 \mu$ M). ..... 80

## LIST OF TABLES

<b>Table 1.</b> Summary of selected studies of acute exposure to chlorine gas .....	4
<b>Table 2.</b> Comparison of methods for the analysis of chlorotyrosine adducts. ....	12
<b>Table 3.</b> MRM transitions, optimized collision energies (CEs), collision cell exit potentials (CXPs), and declustering potentials (DPs) for detection of 2,6-DCP and 2,4-DCP-d3 by MS/MS analysis .....	16
<b>Table 4.</b> Calibration equations, coefficients of determination ( $R^2$ ), and PRA for calibration curves were created over 3 days. ....	26
<b>Table 5.</b> Intra- and interassay accuracy and precision of 2,6-DCP produced by base hydrolysis of $Cl_2$ -tyrosine protein adduct. ....	26
<b>Table 6.</b> Slopes ( $\mu M^{-1}$ ) obtained from non-IS corrected and IS-corrected calibration curves of 2,6-DCP.....	27
<b>Table 7.</b> MRM transitions, optimized collision energies (CEs), collision cell exit potentials (CXPs), and declustering potentials (DPs) for detection of FSH and FOH by MS/MS analysis .....	40
<b>Table 8.</b> The PK parameters of US FDA-approved and novel cyanide antidote (DMTS) .....	84

**ABSTRACT**ADVANCED ANALYTICAL TECHNIQUES FOR THE ANALYSIS OF TOXIC  
INHALED AGENT EXPOSURE AND PHARMACOKINETIC INVESTIGATION

SHARMIN SULTANA

2023

Toxic inhalation agents (TIAs) (i.e., chlorine (Cl<sub>2</sub>), cyanide (HCN), etc.) are highly poisonous. However, they have a variety of industrial uses, such as health, agro-food, building, textiles, transport, leisure activities, cosmetics, etc. In addition, TIAs can be used as chemical agents in terrorist events or conventional warfare. The ability to detect TIAs in biological and environmental samples is important for preparing use, determining individual exposure, limiting hazardous exposure, etc. Therefore, developing simple and sensitive analytical methods for TIAs, TIA metabolites, and antidotes for those toxic agents is very important. The focus of this study was chlorine and cyanide. Chlorine is a poisonous and corrosive industrial chemical that causes irritation and damages the respiratory tract, eyes, and skin. Chlorine is known to form a stable adduct with tyrosine-protein adducts (e.g., 3-chlorotyrosine (Cl-Tyr) and 3,5-dichloro tyrosine (Cl<sub>2</sub>-Tyr)). These adducts are used as biomarkers to confirm chlorine exposure. However, those methods required time-consuming and tedious sample preparation. Therefore, we developed a novel base hydrolysis technique for chloro-tyrosine protein adducts to produce 2,6-dichlorophenol (2,6-DCP). The 2,6-DCP was extracted from the hydrolysate and analyzed via UHPLC-MS/MS analysis of this marker. The method produced excellent sensitivity for 2,6-DCP with the detection limit of 7.8 µg/kg (corresponding to 7.2 nM in the final solution) and calibration curve linearity extending from 0.054 - 54 mg/kg ( $R^2 \geq 0.9997$  and overall %RA

>94). The accuracy and precision ( $100\pm 14\%$ , and  $<15\%$  relative standard deviation, respectively) of the method were good. The validated method successfully detected elevated levels of 2,6-DCP from plasma protein isolated from chlorine-exposed rats. Another method for the analysis of chlorine was developed for aqueous samples. As chlorine is a water-soluble compound, this toxic irritant gas forms hypochlorous acid and hydrochloric acid in an aqueous environment upon exposure. Here, we study hypochlorite anion ( $\text{ClO}^-$ ) in an aqueous solution with the fluorescent probe, as this technique has been known for its high sensitivity, better selectivity, fast response, and ease of use. In this study, we synthesized a probe called fluorescein thioacid (FSH) for rapid and sensitive  $\text{ClO}^-$  detection in an aqueous solution. The probe FSH has shown the selectivity toward  $\text{ClO}^-$  for the strong oxidative property, producing fluorescein. Probe FSH could detect in the range of 5-200  $\mu\text{M}$  with a detection limit of 1.72  $\mu\text{M}$ . The probe FSH is very easy to synthesize with excellent properties, including high selectivity, excellent sensitivity, good water solubility, and fast response. This probe would be beneficial to the analytical researchers for monitoring the  $\text{ClO}^-$  levels in aqueous solutions. Cyanide is a TIA, as with chlorine, but inhibits mitochondrial cytochrome oxidase upon exposure by blocking electron transport and decreasing oxidative metabolism. Because each of the current antidotes, approved by the U.S. Food and Drug Administration (FDA) (i.e., hydroxocobalamin), has significant disadvantages, especially for mass casualty situations, dimethyl trisulfide (DMTS) has recently been developed as a next-generation cyanide antidote. DMTS converts cyanide to a less toxic substance called thiocyanate, which is more effective than thiosulfate and can be administered intramuscularly (IM). Hence, the pharmacokinetic behavior of intranasal (IN) and intramuscular (IM)-administration of DMTS was evaluated. A total of 47 rats and

35 swine were studied for IN and IM administration of DMTS. Generally, the PK characteristics of DMTS were well-suited for the rapid treatment of cyanide poisoning. These results should be helpful in elaborating guidelines for administering DMTS as a cyanide antidote.

## **1 CHAPTER 1. INTRODUCTION AND BACKGROUND**

### **1.1 Overall Significance**

Chlorine and cyanide, known as toxic inhalation agents (TIAs), are widely used in chemical, polymer, agrochemical industries, etc., due to their chemical properties. Chlorine is used in the production of paper and cloth, cleaning products, including household bleach, and in the preparation of chlorinated chemicals. Chlorine and cyanide are common causes of occupational gas exposure hazards and have been used as chemical warfare agents and terrorist agents. Exposure to chlorine can cause severe risks to human health (i.e., pulmonary edema, pulmonary inflammation, respiratory failure, and possible death), and cyanide can cause hypoxia, cytotoxic, cardiac arrhythmias, coma, and death. They both also cause environmental risks. It is, therefore, crucial to develop analytical methods to confirm human exposure. In addition, there is no approved antidote for chlorine, and approved cyanide antidotes have many drawbacks. Therefore, it is important to develop novel therapeutics, including determination of the pharmacokinetic behavior of potential antidotes.

### **1.2 Project objectives**

This research work addresses three main objectives: 1) Develop a rapid and easy method for the analysis of adducts produced from the interaction of chlorine with tyrosine, 2) Develop a selective fluorometric reagent for analysis of hypochlorite produced from chlorine exposure in aqueous solutions and 3) Determine the pharmacokinetics of next-generation cyanide antidote, dimethyl trisulfide (DMTS), following intranasal and intramuscular administration in rats and swine. Chapter 2 describes the successful development of a simple and rapid method for analysis of chlorotyrosine protein adducts

using base hydrolysis, liquid-liquid extraction, and UHPLC-MS/MS analysis, Chapter 3 reports the synthesis and use of a fluorometric reagent for hypochlorite analysis (i.e., chlorine is soluble in water and forms hypochlorite) to confirm the prior interaction of chlorine with an aqueous, Chapter 4 focuses on the analysis of the next generation cyanide antidote, DMTS in rats and swine whole blood to identify its pharmacokinetics behavior.

### **1.3 Toxic inhalation agents**

Inhalation of toxic agents can cause injury to the lung, both airways, and parenchyma. This type of injury is mainly due to exposure to poisonous or irritant gases adsorbed onto particulates at the alveolar level [1]. The inhalation of such gases and vapors can damage the airways and lungs and destroy the function of the respiratory system. Exposures to oxidizing, electrophilic, acidic, or basic gases frequently occur in occupational environments, but these gases have also been used deliberately to cause harm as warfare agents and in terrorist acts [2]. For instance, chlorine, HCN, H<sub>2</sub>S, mustard gas, phosgene, nerve gas, ammonia, carbon monoxide, hydrogen chloride, hydrogen fluoride, and methane are considered TIAs [3, 4].

Exposure to toxic gases or vapors is most likely to occur via inhalation, direct contact with the skin or eyes, or ingestion. It is easy to inhale these substances. However, finely divided mists, aerosols, or dust also can be inhaled. These inhaled substances may damage the pulmonary epithelium at the respiratory tract levels, leading to disorders from tracheitis and bronchiolitis to pulmonary edema [4, 5].

TIAs are widely used industrial chemicals, such as automotive, electronics, disinfectants, metal production, and many others. Therefore, large volumes of TIAs are manufactured and transported globally. This leads to the possibility of unexpected release

during transportation [6]. **Table 1** lists the acute chlorine exposure incidents. For example, a transportation mishap happened for chlorine on January 6, 2005, in Graniteville, South Carolina; a train was accidentally diverted from the main railway and struck a parked train, causing the derailment of both near a textile mill. Immediately, the textile workers, railroad employees, and initial emergency responders began having respiratory difficulties at the scene—many ensuing patients presented with eye irritation, cough, dyspnea, chest pain, and pulmonary edema [7].

TIAs have also been used as chemical warfare agents by many military and terrorist groups to kill and injure civilian populations. An attack occurred at Ypres on the Russian Front on 22nd April of 1915, releasing 5,730 cylinders with 180,000 kg of chlorine gas into a six-kilometer-long front for 5 mins. It was reported this attack caused 15,000 French casualties, 800 who were killed, and 2500 to 3000 who were incapacitated by the chlorine gas [8, 9]. A large-scale incidence of chemical terrorism happened in the U.S. in 1982 in Chicago, where seven people died by consumption of CN-laced Tylenol [10]. The perpetrator collected the drugs from the store, added CN (60-100 mg per capsule), and returned them to the store [11]. The Jonestown massacre in Guyana in 1978, resulted in the death of more than 900 people, including children, because of toxic CN ingestion [12].

#### **1.4 Pathogenesis of TIAs**

The effect of inhaled substances on the respiratory system depends on various factors, such as the substance's nature (water solubility and particle size), the concentration of inhaled toxin, the environment (whether exposure occurred in an enclosed space or open space), and host factors (elderly or younger patient, history of smoking and underlying lung debilitating illness, underlying reactive airway disease or lung disease, etc.) [13, 14].

**Table 1.** Summary of selected studies of acute exposure to chlorine gas

No. cases	Cohort type	Time of study <sup>1</sup>	Findings <sup>2</sup>	References
605	Train derailment	hours	9 deaths occurred, 72 were hospitalized, 525 were examined in hospital emergency departments.	Duncan et al. [15]
133	Cylinder leak	hours	Cough (96%), chest tightness (97%), 33 hospitalized with bronchitis, pulmonary edema	Chasis et al. [16]
100	Train derailment	hours	Severe mucosal irritation; respiratory distress in 65 hospitalized	Joyner et al. [17]
76	Reservoir leak	1 hour	Mucosal irritation, respiratory distress	Fleta et al. [18]
19	Rail car leak	1 day	FEV1/ FVC < 75% in 53% of cases	Charan et al. [19]
18	Storage tank leak	a. 18 hours b. 14 days	FEV1/ FVC 66%; chief complaints cough, dyspnea FEV1/ FVC 85% in those with cough, 74% in those with dyspnea	Hasan et al. [20]
18	Storage tank leak	1 day	FEV1% ≤75% in 16%; RV > 120% in 38%; MMF < 75% in 38%	Kaufman et al. [21]
12	Train car puncture	hours	All hospitalized; 85% pulmonary edema, 81% bronchitis; 55% hemoptysis	Weil et al. [22]
7	Inadvertent gassing, several factories	2 days- 10 weeks	FEV1/ FVC at 8 weeks; ≥90% in 6/7 75% in 1 with pulmonary edema	Beach et al. [23]
4	Public swimming pool leak	a) hours b) 1 month	a) FEV1/ FVC 68-82%; TLC 94-99% b) FEV1/ FVC 93-133%; TLC 105-126%	Ploysongsang et al. [24]

<sup>1</sup>Time of study following chlorine gas exposure; <sup>2</sup>% for pulmonary function refers to percent height, age, gender predicted normal for that study; FEV1 = forced expiratory volume in one second; FVC = forced vital capacity; TLC = total lung capacity; MMF = maximum mid-expiratory flow rate; RV = residual volume

The most vital factors include the intensity and duration of exposure and the quality of ventilation in the space. Generally, the greater exposure dose (defined as the product of the exposure concentration and duration of exposure) is associated with greater potential harm. For example, with exposure to high concentrations, mild toxic compounds may cause damage to health; on the other hand, some compounds may not be harmful with low concentrations or short duration of exposure [1–4, 12].

High water-soluble gases and vapors are primarily deposited in the upper airways. These compounds produce rapid upper airway irritation (e.g., eye and mucous membrane), and several symptoms may occur, including progressive coughing, wheezing, or stridor. On the other hand, low water-soluble compounds can reach to the lower respiratory tract and cause a slow onset of the symptoms. Intermediate water-soluble (e.g., chlorine) may cause fast irritation after a massive exposure and may cause slow pulmonary edema.

### **1.5 Exposure to chlorine and cyanide**

Chlorine and cyanide exposure can occur via inhalation, ingestion, or skin penetration. Chlorine is fairly soluble in water. When it contacts the mucosal surfaces and airways (**Figure 1**), it dissolves into the airway surface liquid to form hypochlorous acid and hydrochloric acid [25]. HCl is a strong acid, and HOCl is a strong oxidant that can produce different types of highly reactive oxidants and reactive oxygen species [26]. Exposure to chlorine may cause instant oxidative injury to the epithelium; additionally, with migration and activation of inflammatory cells such as neutrophils, damage to the epithelium may occur. Chlorine exposure also can damage eyes, skin, and upper airways by affecting the nose to the level of the bronchi [27], using the same mechanism as for lower airways [28]. Complete recovery of the airway epithelium may not restore normal

activities, as subepithelial fibrosis, mucous hyperplasia, and nonspecific airway hyperresponsiveness have been reported after recovery from chlorine injury [27, 29, 30].

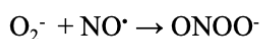
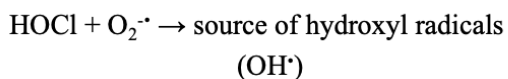
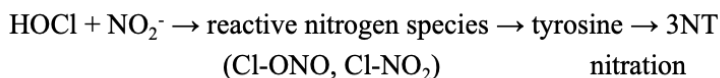
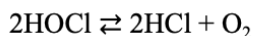
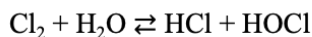


**Figure 1.** Scheme of some of the reactions potentially causing the formation of reactive oxygen and nitrogen species in the setting of acute chlorine inhalation.

Following exposure, cyanide distributes quickly throughout the body. It reacts with cytochrome c oxidase and interrupts the oxidative phosphorylation process [31-34]. Therefore, the ability to utilize oxygen is diminished, the electron transport chain is disrupted, ATP production is reduced, and cellular hypoxia, hyperlactatemia, metabolic acidosis, cytotoxic anoxia, cardiac arrest, and potential death [35-38] result. In addition, cyanide also can damage essential enzymes (e.g., succinic dehydrogenase, superoxide dismutase, and carbonic anhydrase), slow the formation of fumarate in the Krebs cycle, obstruct the removal of harmful reactive oxygen species (ROS), and interrupt the interconversion of carbon dioxide and carbonic acid [39, 40].

## 2 CHAPTER 2. VERIFICATION OF CHLORINE EXPOSURE VIA LC-MS/MS ANALYSIS OF BASE HYDROLYZED CHLOROPHENOLS FROM CHLOROTYROSINE-PROTEIN ADDUCTS

### 2.1 Abstract

Inhalation of chlorine gas at high enough levels can cause pulmonary edema (i.e., fluid build-up in the lungs), pulmonary inflammation (with or without infection), respiratory failure, and death. The toxicity of inhaled chlorine is due to the hydrolysis of chlorine gas in the lungs to form hydrochloric acid (HCl) and hypochlorous acid (HOCl), which damages lung tissues. The resulting HOCl is known to produce stable tyrosine adducts via electrophilic aromatic substitution, resulting in 3-chlorotyrosine (Cl-Tyr) and 3,5-dichlorotyrosine (Cl<sub>2</sub>-Tyr). While several analysis methods are available for determining Cl-Tyr and Cl<sub>2</sub>-Tyr, they each have significant disadvantages, including long and tedious sample preparation. Hence, in this study, a simple and sensitive ultra-high performance liquid chromatography-tandem mass spectroscopy (UHPLC-MS/MS) method was developed for the determination of chlorotyrosine adducts. The sample preparation involves base hydrolysis of isolated plasma proteins to form 2-chlorophenol (CP) from Cl-Tyr and 2,6-dichlorophenol (2,6-DCP) from Cl<sub>2</sub>-Tyr as markers of chlorotyrosine adducts with subsequent liquid-liquid extraction prior to UHPLC-MS/MS analysis. The method produced excellent sensitivity for 2,6-DCP with a limit of detection of 2.2 µg/kg and calibration curve linearity extending from 0.054 - 54 mg/kg ( $R^2 \geq 0.9997$  and %RA >94). The sensitivity of the method for 2-CP was relatively poor, so it was used only as a secondary marker for severe chlorine exposure. The accuracy and precision (100±14%, and <15% relative standard deviation, respectively) of the method for 2,6-DCP

were good. The method successfully detected elevated levels of 2,6-DCP from hypochlorite-spiked plasma protein and was further used to detect significantly elevated 2,6-DCP levels from plasma protein isolated from chlorine-exposed rats.

## **2.2 Introduction**

Chlorine is a dense yellow-green gas at room temperature. It has a pungent, irritating odor characteristic of bleach [41]. It is slightly water soluble but reacts quickly with moisture to form hypochlorous acid (HOCl) and hydrochloric acid (HCl). Chlorine is used in a variety of industries, such as health, agro-food, textiles, transport, cosmetics, etc. [8, 42]. Chlorine is also used for plastic production, pulp and paper production, water purification, and chemical synthesis, including pharmaceuticals and chlorinated solvents [8].

While chlorine has many industrial uses, it is also toxic and exposure to chlorine can be historically divided into a number of categories [27]: chlorine gas as a chemical warfare agent in military applications (e.g., Cl<sub>2</sub> was successfully used during the First World War at Ypres in April 1915) [8, 9]; occupational exposure of industrial workers [43-46]; leaks or spills of chlorine including transportation mishaps [16, 17]; and civilian accidents with commercially available chlorine-containing products, such as pool chemicals or laundry bleach [47-58]. Chlorine has a toxic threshold limit value (TLV) of 0.1 ppm (i.e., the TLV is the concentration of the compound in the air that can be breathed for five consecutive eight-hour working days by people without significant damage to the health) [59, 60]. At approximately 30 - 50 ppm, chlorine causes immediate substernal chest pain, shortness of breath, cough, a toxic pneumonitis with acute pulmonary edema [25]. Higher level exposures (> 400 ppm) result in asphyxia with respiratory failure, pulmonary

edema, acute pulmonary hypertension, cardiomegaly, pulmonary vascular congestion, and acute burns of the upper and proximal lower airways and can result in death [25, 27, 61]. Although chlorine is toxic, its strong odor can be detected by humans at 0.1-0.3 ppm, and mucus membranes become irritated at >1 ppm. This results in limited harm during most exposure events, but large-scale and/or sudden exposure is still very concerning. Additionally, chronic exposure is another concern.

Chlorine toxicity is based on the formation of HOCl and HCl following contact with surface liquid on mucosal surfaces and airways [25]. They may produce highly reactive oxidants via combination with reactive oxygen species and other airway constituents [26]. This causes instant oxidative injury to the epithelium and migration and activation of inflammatory cells such as neutrophils. Chlorine exposure can damage eyes, skin, and upper airways from the nose to the bronchi [27, 28]. Furthermore, subepithelial fibrosis, mucous hyperplasia, and nonspecific airway hyperresponsiveness have been reported following chlorine injury [27, 29, 62, 63].

Exposure to chlorine gas results in chlorine adducts with proteins, specifically at tyrosine residues (see **Figure 2**) [64, 65]. Chlorine modifies these residues via electrophilic aromatic substitution at the *ortho* position, causing the formation of 3-chlorotyrosine (Cl-Tyr) and 3,5-dichlorotyrosine (Cl<sub>2</sub>-Tyr) [66]. These adducts can be utilized as biomarkers to confirm chlorine exposure. For example, both biomarkers were readily detected in rat nasal tissue following exposure to chlorine gas (e.g., rats were exposed for 90 min to various doses of Cl<sub>2</sub>) [67]. Moreover, the chlorotyrosine adducts have been broadly studied as a biomarker for inflammation and oxidative tissue damage resulting from neutrophil myeloperoxidase in cases of chronic inflammatory disease [65, 68-71]. Specifically,

increased levels of Cl-Tyr have been linked to renal failure [72], atherosclerosis (ATH) [71], myocardial infarction [73], and cystic fibrosis (CF) [74]. The higher-order chlorination product, Cl<sub>2</sub>-Tyr, is produced at lower concentrations but may prove to be the more specific biomarker when separating acute chlorine exposure from chronic inflammatory disease [75].

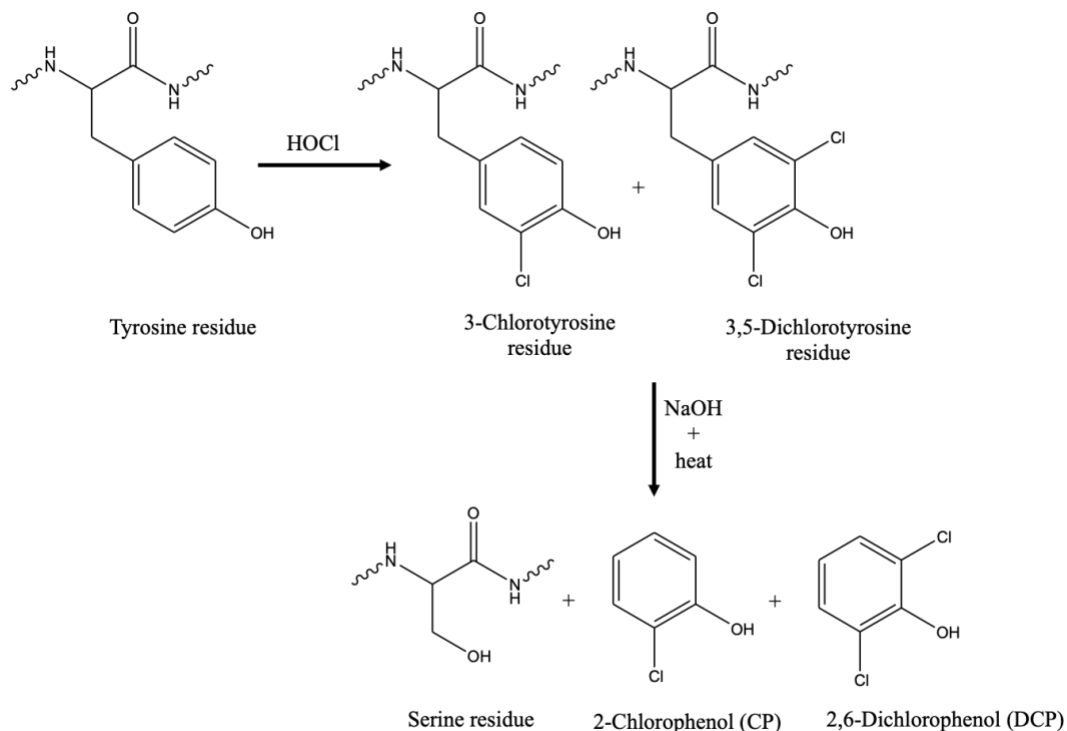


**Figure 2.** Reaction pathway for the formation of chlorophenols from the reaction of tyrosine residues with chlorine and subsequent base-catalyzed hydrolysis. Tyrosine residues react with the free chlorine residues to form a chlorotyrosine adduct which can undergo base hydrolysis to produce 2-CP and 2,6-DCP.

The analysis of chlorotyrosine residues is important for verifying and evaluating the extent of chlorine exposure and chronic inflammatory disease. Previously published methods for the analysis of chlorotyrosine adducts are listed in **Table 2** along with comparison of some important parameters. Acid hydrolysis is the earliest and most common technique used to prepare chlorotyrosine adducts. Acid hydrolysis is achieved via

hydrolysis of protein with a strong acid (~ 6 N HBr or methane sulfonic acid containing 1% phenol) at high heat (~110 °C for ~ 18 h) to produce Cl-Tyr and Cl<sub>2</sub>-Tyr for analysis. Another approach for chlorotyrosine adduct analysis is enzymatic hydrolysis, achieved by 24-hr incubation with pronase at 37 °C. The markers of chlorinated tyrosine adducts following acid hydrolysis have been analyzed by GC-MS [67, 68, 70-75], HPLC–UV [69], and LC-MS/MS [76] (see **Table 2**). These methods involved more than 20 steps and over 24 h of sample preparation and required a relatively large amount of organic waste and energy. Because each of the available methods has significant drawbacks, there is a need to develop a simple and sensitive sample preparation method to analyze protein adducts of chlorotyrosine to verify exposure to chlorine.

This study aimed to utilize strong base hydrolysis of chlorine-adducted tyrosine plasma protein residues to form the phenolic hydrolysis products 2-CP and 2,6-DCP and to analyze them with a simple UHPLC-MS/MS method to verify acute exposure to chlorine. Note that 2-CP produced limited sensitivity, so was considered a secondary marker of chlorotyrosine adducts.

**Table 2.** Comparison of methods for the analysis of chlorotyrosine adducts.

Analyte	Sample preparation	Analysis technique	Steps	Approximate estimated time (h)	Year	Reference
Cl-Tyr	Acid hydrolysis, SPE, derivatizations	NCI GC-MS	>20	>24	1996	Hazen et al. [68]
Cl-Tyr	Acid hydrolysis, SPE, derivatizations	NCI GC-MS	>20	>24	1997	Hazen et al. [71]
Cl-Tyr	Acid hydrolysis, SPE, derivatizations	NCI GC-MS	>20	>24	2001	Himmelfarb et al. [72]
Cl-Tyr	Acid hydrolysis, SPE, derivatizations	GC-MS	>20	>24	2007	Mocatta et al. [73]
Cl-Tyr & Cl <sub>2</sub> -Tyr	Acid hydrolysis, SPE, derivatizations	GC-MS	>20	>24	2004	Kettle et al. [74]
Cl-Tyr & Cl <sub>2</sub> -Tyr	Acid hydrolysis, RP-HPLC, derivatizations	GC-MS	>20	>24	2000	Chapman et al. [75]
Cl-Tyr & Cl <sub>2</sub> -Tyr	Acid hydrolysis, SPE, derivatizations	GC-MS	> 20	>24	2008	Sochaski et al. [67]
Tyr & Cl-Tyr	Enzymatic hydrolysis, derivatizations	RP-HPLC-UV	>20	>24	1996	Kettle et al. [69]
Cl-Tyr & Cl <sub>2</sub> -Tyr & CHPA & DCHPA	Acid hydrolysis, derivatizations	RP-HPLC-UV	>20	>24	2000	Davies et al. [77]
Cl-Tyr & Cl <sub>2</sub> -Tyr	Enzymatic hydrolysis, SPE	RP-HPLC-MS/MS	>20	>24	2022	Bruin-Hoegge et al. [76]
2-CP & 2,6-DCP	Base hydrolysis, LLE	RP-UHPLC-MS/MS	12	4	2023	Current study

Cl-Tyr = 3-chlorotyrosine, Cl<sub>2</sub>-Tyr = 3,5-dichlorotyrosine, Tyr = tyrosine, CHPA = 3-chloro-4-hydroxyphenylacetaldehyde, DCHPA = 3,5-dichloro-4-hydroxyphenylacetaldehyde, 2-CP = 2-chlorophenol, 2,6-DCP = 2,6-dichlorophenol, NCI-GC-MS = negative chemical ionization-gas chromatography-mass spectrometry, RP-HPLC-MS/MS = reversed phase high performance liquid chromatography-tandem mass spectrometry, RP-HPLC-UV = reversed phase high performance liquid chromatography-ultraviolet, SPE = solid-phase extraction, LLE = liquid-liquid extraction

## **2.3 Materials and Methods**

### **2.3.1 Materials**

All reagents and solvents were at least HPLC grade unless otherwise stated. Ammonium Acetate (LC/MS grade), sodium hydroxide, cyclohexane (Certified ACS), acetonitrile, and ammonium hydroxide were purchased from Fisher Scientific (Fair Lawn, NJ, USA). Water used for this study was purified by reverse osmosis and filtered through a Lab Pro polishing unit from Labconco (Kansas City, KS, USA) and had a resistivity of 18.2 M $\Omega$ -cm (referred to as deionized (DI) water). Hydrochloric acid, 2-chlorophenol (2-CP), and 2,6-dichlorophenol (2,6-DCP) were obtained from Sigma-Aldrich (St. Louis, MO, USA). In addition, isotopically labeled 2,4-dichlorophenol (ring-d3, 98%) was purchased from Cambridge Isotope Laboratories, Inc. (Tewksbury, MA, USA). A freshly prepared mixture of 2-CP and 2,6-DCP was prepared as a stock solution in methanol (10 mM) for each experiment, and the stock solution was kept in the dark at ambient temperature. The as-received internal standard solution was diluted in methanol to produce a stock solution of 10 mM, which was further diluted to 1 mM in DI water and stored in a -80 °C freezer (So-Low Ultra-Low Freezer, Ohio, USA). The nitrogen gas generator (Parker Balston) with a pierce Reacti-Therm heating module was used for solvent evaporation.

### **2.3.2 Biological samples**

Sprague Dawley rat plasma (3.2% NaCit) was purchased for method development and validation from BioIVT (Westbury, NY, USA) and immediately stored at -80 °C until used. This plasma was used for protein collection, NaOCl spikes, and other procedures necessary to develop and optimize the method.

To verify the method's ability to detect 2,6-DCP as a marker of chlorine exposure, rats were exposed to chlorine, and plasma was sampled for 2,6-DCP analysis. This work was done in collaboration with the University of Colorado Denver. Rat plasma was fractionated by centrifugation of whole blood at 3000 x g for 15 min at 4 °C. Plasma was removed, and aliquots (0.5-1 mL) of blood plasma were immediately frozen and stored at -80 °C. The frozen plasma samples were then shipped to South Dakota State University on dry ice and stored at -80 °C until analysis.

### **2.3.3 Sample preparation**

Plasma protein precipitation was achieved by following the method by Logue et al [78]. Briefly, plasma samples (250 µL) were added to a 2-mL centrifuge tube, and acetonitrile was added to the plasma samples with a 3:1 volume ratio of acetonitrile to plasma. The mixture was vortexed and centrifuged at 13000 x rpm for 10 min at 5 °C. The supernatant was discarded, the precipitate was collected, the pellet was broken, and the protein was rewashed with the same volume of acetonitrile. The mixture was vortexed and centrifuged, and the supernatant was discarded as above. The residue was dried in a centrifugal evaporator (Labconco, Kansas City, USA) equipped with a rotary vacuum pump (Edwards, Glenwillow, USA) at 30 °C until dry. The precipitate was stored at -80 °C until further analysis. Next, the precipitated plasma protein (15 mg) was added to a clean 2-mL centrifuge tube, and aqueous NaOH (200 µL of 1 M) was added to the plasma protein for base hydrolysis. The internal standard (2,4-dichlorophenol-ring d<sub>3</sub>; 2,4-DCP-d<sub>3</sub>) was spiked (100 µL, 2 µM) into the mixture. The mixture was then vortexed and heated at 75 °C for 2 hr. The sample was removed from heat and cooled to room temperature. To neutralize the base, HCl (100 µL, 3 M) was added to the solution. Cyclohexane (1.2 mL)

was added to the mixture to extract 2,6-DCP, and the resulting mixture was capped, vortexed, and centrifuged at 13000 x rpm for 20 min at 5 °C. An aliquot of the organic layer (1 mL) was then transferred into a 4-mL glass screw-top vial and nitrogen dried for 13 min at room temperature. The dried samples were reconstituted with 100  $\mu$ L of 50% acetonitrile in ammonium acetate buffer (0.1 mM, pH 10.0), mixed thoroughly, filtered with a 0.22  $\mu$ m nylon syringe filter, and analyzed using UHPLC-MS/MS.

#### **2.3.4 UHPLC-MS/MS analysis of 2,6-DCP**

UHPLC analysis was performed on a Shimadzu UHPLC with an LC-20ADXR controller. The column used for chromatography was a Waters reversed-phase column, charged surface hybrid (CSH) C18 (3.0 x 75 mm, 2.5  $\mu$ m, part #: 186006106). The chromatographic separation was achieved using isocratic elution at a flow rate of 0.3 mL/min at 90% B for 5 min. Mobile phases A and B were ammonium acetate buffer in water (0.1 mM, pH 10.0) and acetonitrile, respectively. The column was equilibrated for 1 min, and a volume of 10  $\mu$ L was injected for UHPLC-MS/MS analysis.

For MS analysis, a tandem mass spectrometer (Sciex Q-Trap 5500 MS) equipped with an electrospray ionization interface in the negative mode was used to detect 2,6-DCP and 2,4-DCP-d<sub>3</sub>. Mass spectrometric conditions were optimized by directly infusing a standard solution of 2,6-DCP and 2,4-DCP-d<sub>3</sub> into the spectrometer at a flow rate of 10  $\mu$ L/min. After infusion of standard solutions of 2,6-DCP and 2,4-DCP-d<sub>3</sub> into ESI, molecular ions of m/z 160.9 ([M-H]<sup>-</sup>) and m/z 163.8 ([M-H]<sup>-</sup>), respectively, were identified. Multiple reaction monitoring (MRM) parameters for 2,6-DCP and 2,4-DCP-d<sub>3</sub> were optimized and are outlined in **Table 3**, which reports the MRM transitions, optimized collision energies (CEs), collision cell exit potentials (CXPs), and declustering potentials

(DPs) for detection of 2,6-DCP and 2,4-DCP-d<sub>3</sub> by MS/MS analysis. Nitrogen (20 psi) was used as the curtain and nebulization gas. The ion spray voltage was 4,500 V, the source temperature was 600 °C, and the nebulizer (GS1) and heater (GS2) gas pressure were 30 psi. The collision cell was operated at a “medium” collision gas flow rate. The total mass spectrometry acquisition time was 5 min.

**Table 3.** MRM transitions, optimized collision energies (CEs), collision cell exit potentials (CXPs), and declustering potentials (DPs) for detection of 2,6-DCP and 2,4-DCP-d<sub>3</sub> by MS/MS analysis

Compounds	Q1 (m/z)	Q3 (m/z)	Dwell Time (msec)	CE (V)	CXP (V)	DP (V)
2,6-DCP (quantification)	160.9	125.0	100	-24.81	-8.34	-85.86
2,6-DCP (identification)	160.9	89.0	100	-38.98	-9.71	-65.02
2,4-DCP-d <sub>3</sub> (quantification)	163.8	126.9	100	-24.51	-8.94	-37.27
2,4-DCP-d <sub>3</sub> (identification)	163.8	90.0	100	-30.06	-8.23	-39.34

### 2.3.5 Calibration, quantification, and limit of detection

Food and Drug Administration guidelines were used to validate the method [79, 80]. The limit of detection (LOD) was determined by analyzing multiple concentrations of 2,6-DCP below the lower limit of quantification (LLOQ) in plasma protein utilizing the sample preparation method described above (Section 2.3.3). The LOD is generally defined as the lowest concentration, which reproducibly produces a signal-to-noise ratio of at least 3. Since endogenous levels of chlorinated protein residues in plasma protein are known to be present from natural sources [81, 82]. A “true” limit of detection for the method was calculated using Equation ((2.1).

$$LOD_{signal} = \bar{x}_{blank} + 3S_{blank} \quad (2.1)$$

where  $LOD_{\text{signal}}$  is the signal LOD,  $x_{\text{blank}}$  is the average signal of blank, and  $S_{\text{blank}}$  is the standard deviation of blank measurement. The  $x_{\text{blank}}$  was calculated using the blank signal 1 min prior to and after the elution of 2,6-DCP. Calibrators (0.05, 0.1, 0.2, 0.5, 1, 2, 5, 10, 20, and 50  $\mu\text{M}$ ) and quality control (QC) standards (0.3, 3, and 30  $\mu\text{M}$ ) were prepared from a stock solution of 2,6-DCP in 50% acetonitrile: ammonium acetate buffer. Aliquots (100  $\mu\text{L}$  each) of 2,6-DCP and 2,4-DCP-d3 were spiked into plasma protein to create calibration standards utilizing the sample preparation method described above. The aqueous standards (0.3, 3, and 30  $\mu\text{M}$ ) were also prepared from the same stock solution. The QC standards were not included in the calibration curve. Each calibration standard was prepared in triplicate, and QC standards were quintuplicated. After analysis of the calibration standards, calibration curves were plotted using the average signal ratios of 2,6-DCP and 2,4-DCP-d3 as a function of 2,6-DCP nominal concentration. Based on the criteria of <15% relative standard deviation (%RSD, as a measure of precision) and a percent error (as a measure of accuracy) of  $100\pm 15\%$ , the LLOQ and upper limit of quantification (ULOQ) were established. The percent error was calculated based on comparing the 2,6-DCP concentration back-calculated from the calibration curve to the nominal 2,6-DCP concentration of the QC standard. The percent residual accuracy (PRA) was used to determine the goodness-of-fit of the calibration curves (i.e., PRA values  $\geq 90\%$  are indicative of a good fit) [83]. Intraassay precision and accuracy were calculated from each day's analysis, and interassay precision and accuracy were calculated by comparing the data gathered over three separate days.

### **2.3.6 Recovery and matrix effect**

The recovery of 2,6-DCP was determined by analyzing five QC replicates (low, medium, and high concentrations) prepared in an aqueous solution compared with equivalent concentration QCs in plasma protein. Recovery (which was calculated as a percentage) was determined by dividing the peak area of the 2,6-DCP signal in plasma protein by the peak area of the equivalent concentration of aqueous QC standards containing 2,6-DCP reconstituted in mobile phases (50% acetonitrile in ammonium acetate buffer). Recovery calculated in this manner is influenced by the plasma matrix effects and, therefore, may not reflect the true recovery. However, it may be better estimated by accounting for matrix effects. Matrix effects for the analysis of 2,6-DCP in plasma protein were evaluated by comparing an aqueous calibration curve with a calibration curve in plasma protein. The ratio of calibration curve slopes, using plasma protein matrix versus aqueous calibration standards, was used to quantify the matrix effect. A slope ratio (plasma protein slope/aqueous slope) equal to one indicates no matrix effect, less than 1 represents the suppression of the analyte signal, and greater than 1 represents an enhancement effect by the plasma protein. The effectiveness of IS to compensate for the matrix effect and limited recovery was also evaluated by comparing the ratio of IS-corrected values.

### **2.3.7 Stability**

Both short- and long-term stability of 2,6-DCP in plasma protein matrix was evaluated in triplicate using low and high QCs stored at various temperatures at multiple time periods. For short-term stability, low and high QCs were evaluated in an autosampler. Prepared samples were placed on the auto-sampler (ambient temperature) and analyzed at approximately 0, 1, 2, 4, 8, 12, and 24 h following preparation. The internal standard was

not considered when evaluating the autosampler stability, as it would correct for the loss of 2,6-DCP in the plasma protein matrix during the analysis. To evaluate the benchtop stability of the chlorotyrosine-protein adduct, hypochlorite was initially spiked in rat plasma at concentrations that produced 2,6-DCP signals similar to the low and high QCs: 1.7  $\mu\text{mol/g}$  and 25  $\mu\text{mol/g}$ , respectively. The hypochlorite-spiked rat plasma protein samples were vortexed and placed at room temperature for 2 h. The samples were then stored on the benchtop for 0, 1, 2, 4, 8, 12, and 24 h. The samples were subsequently precipitated, dried, and stored in a  $-80\text{ }^{\circ}\text{C}$  freezer until all samples were ready for analysis. During analysis, samples were prepared using the sample preparation steps outlined above and analyzed using the developed UHPLC-MS/MS method. Sample preparation was carried out for long-term stability as with the benchtop stability, except that samples were stored at room temperature,  $4\text{ }^{\circ}\text{C}$ ,  $-20\text{ }^{\circ}\text{C}$ , and  $-80\text{ }^{\circ}\text{C}$  for 0, 1, 2, 5, 15, and 30 days.

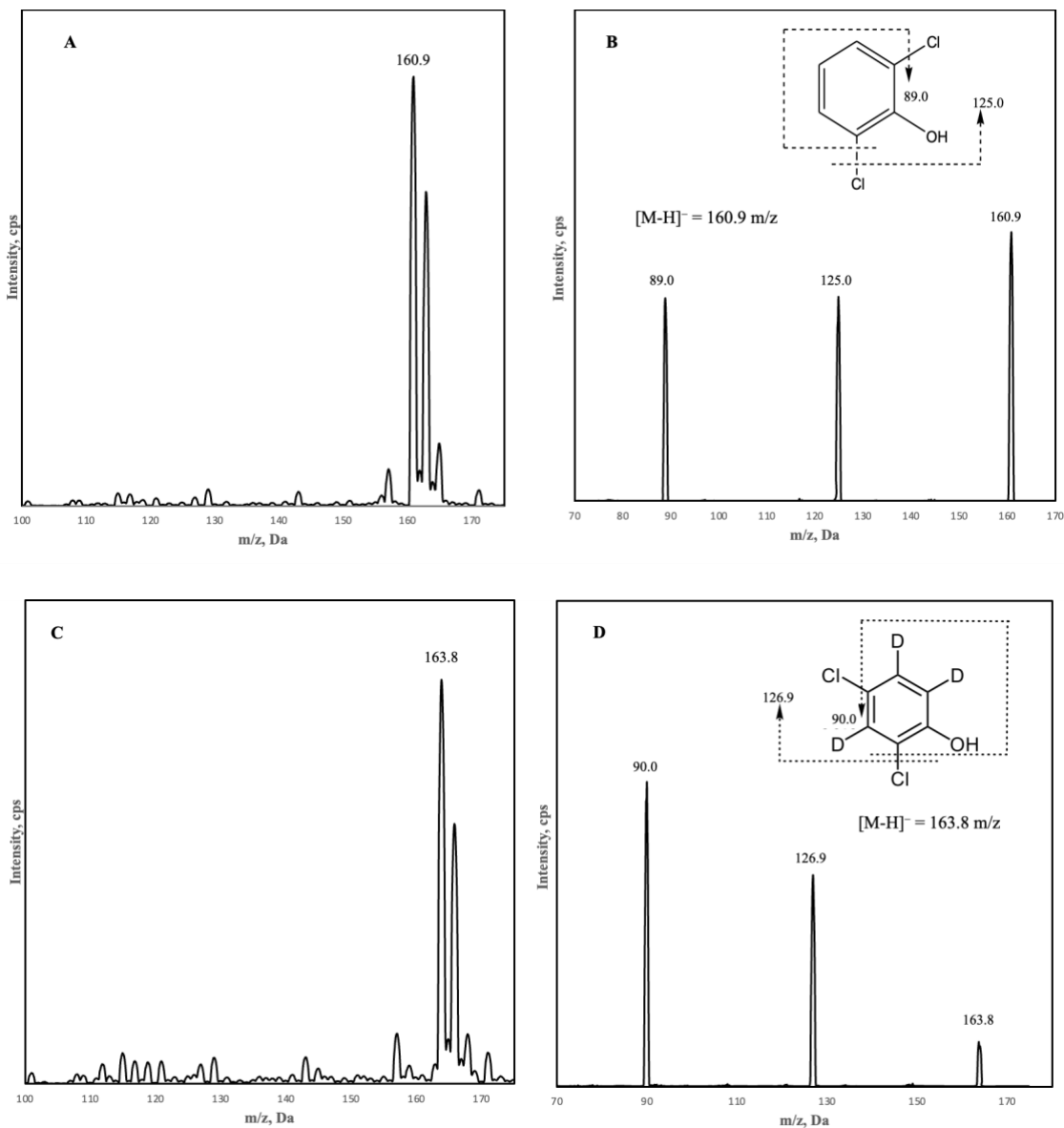
## **2.4 Results and Discussion**

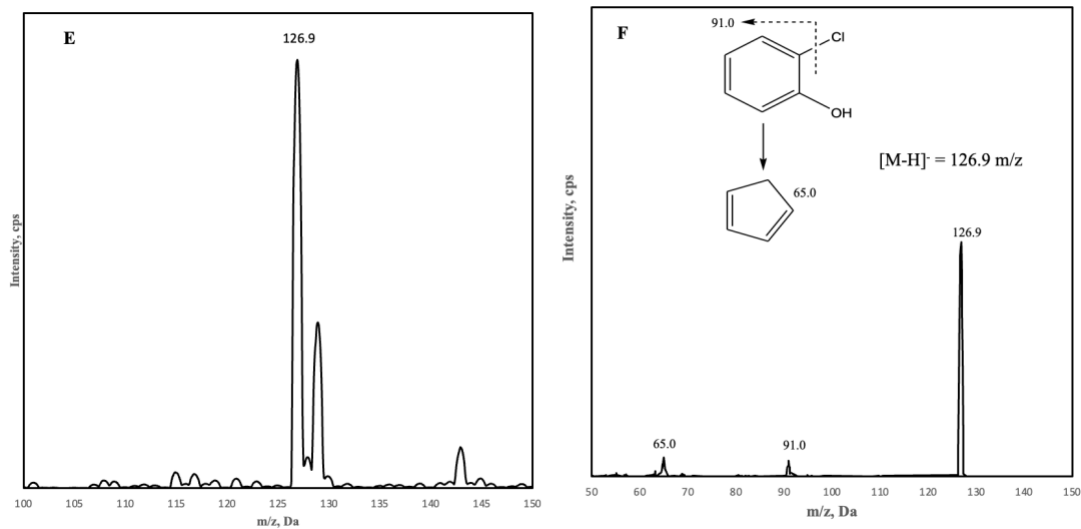
### **2.4.1 UHPLC-MS/MS analysis of 2,6-DCP**

Donkor et al [84] utilized base hydrolysis of methyl isocyanate-adducted tyrosine residues to produce phenylmethyl carbamate for simple analysis of MIC-adducted proteins. We hypothesize that chlorotyrosine adducts would behave similarly to produce 2-CP and 2,6-DCP.

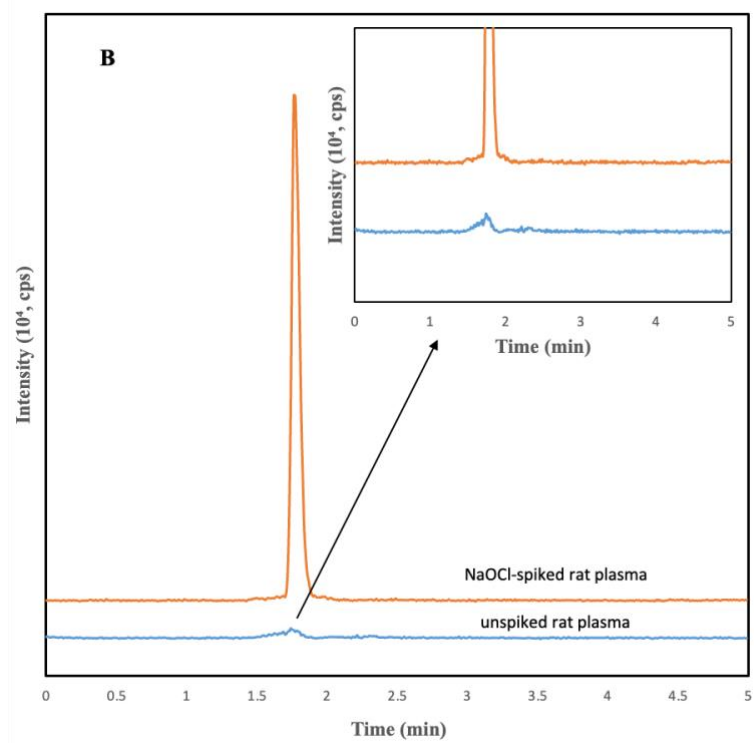
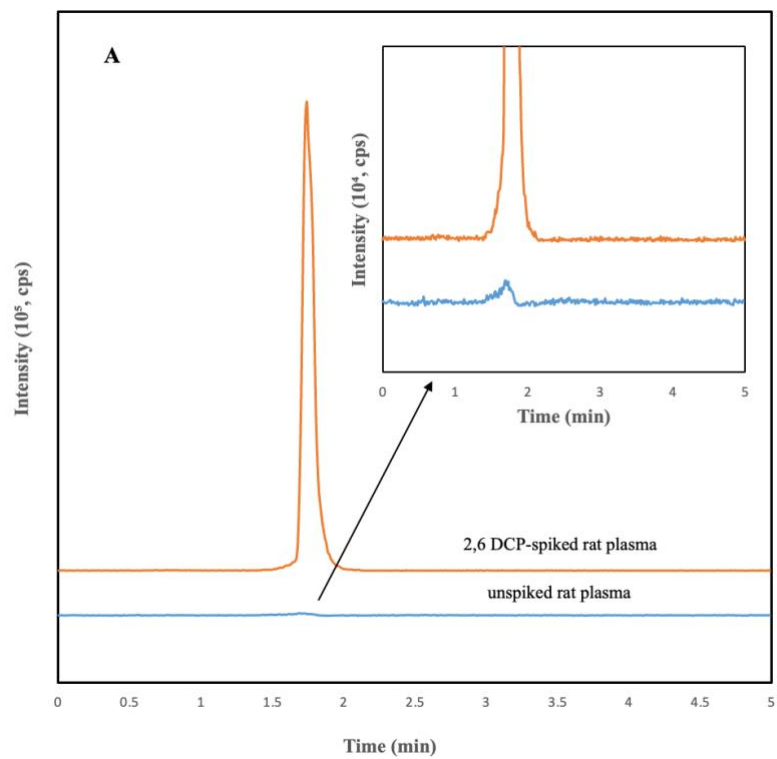
To confirm the formation of these compounds from chlorine exposure, an analytical method was developed to detect and quantify both 2-CP and 2,6-DCP from the hydrolysis of chlorine-adducted plasma protein. Note that while the method was initially developed for both analytes, the sensitivity of 2-CP was severely limited. Therefore, the development of the method continued for 2,6-DCP alone. The mass spectra of 2,6-DCP and 2,4-DCP- $d_3$

produced by ESI (-) MS are shown in **Figure 3**, with abundant ions identified. For 2,6-DCP and 2,4-DCP-d<sub>3</sub>, the proposed major MS fragmentation occurs at two C-Cl bonds [85, 86]. The quantification and identification transitions of 2,6-DCP and 2,4-DCP-d<sub>3</sub> are listed in **Table 3**.





**Figure 3.** ESI (-) product ion mass spectra of 2,6-DCP (B) and 2,4-DCP-d<sub>3</sub> (D) and 2-CP (F) with suggested structural assignments identification of the abundant ions. Molecular ions of 2,6-DCP and 2,4-DCP-d<sub>3</sub>, and 2-CP [M-H]<sup>-</sup> correspond to 160.9 and 163.8 and 126.9, respectively. Insets, the structures of 2,6-DCP (B) and 2,4-DCP-d<sub>3</sub> (D) and 2-CP (F) with suggested fragmentation are shown.



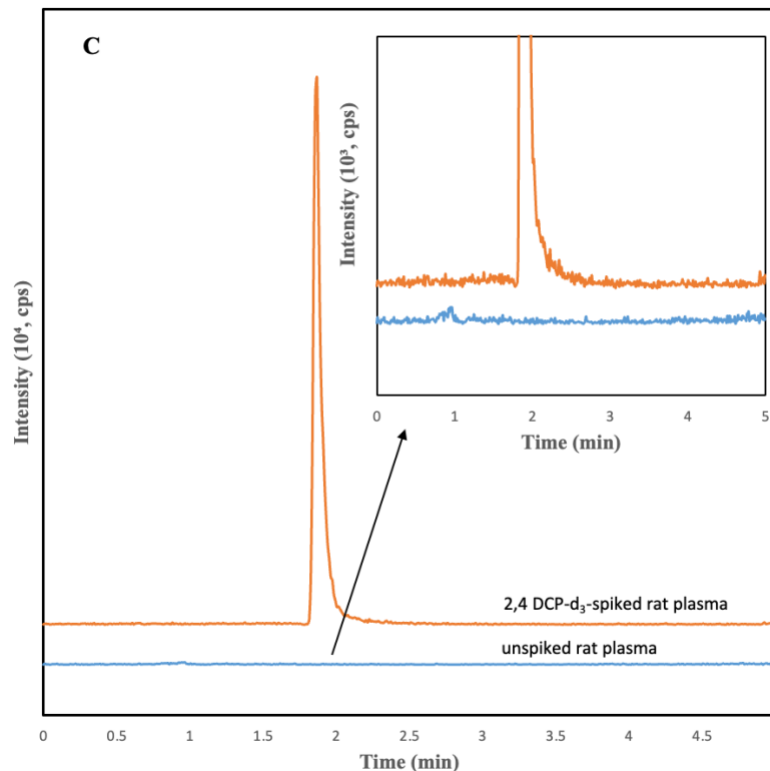


**Figure 4.** UHPLC-MS/MS chromatograms of 2,6-DCP spiked (A), NaOCl-spiked (B) and 2,4-DCP-d<sub>3</sub> (C) spiked rat plasma following sample preparation are presented. The 160.9→125 m/z transitions for 2,6-DCP spiked (A) and NaOCl-spiked (B) and 163.8→126.9 m/z transitions for 2,4-DCP-d<sub>3</sub> (C) are plotted. The insets show the magnified baseline of unspiked rat plasma.

The analytical method for 2,6-DCP presented here features simple sample preparation compared to existing methods used to analyze chlorotyrosine protein adducts. The method consists of plasma precipitation, followed by strong base hydrolysis of chlorotyrosine adducts from isolated plasma protein to form 2,6-DCP, rapid liquid-liquid extraction, and analysis via liquid chromatography-tandem MS analysis. To our knowledge, this is only the second study that utilizes strong base hydrolysis to cleave tyrosine residues at the  $\alpha$ -carbon bond to produce phenolic analytes and utilize them as markers of protein modification. This chemistry produces a relatively simple analysis of

tyrosine adducts. For example, the sample preparation, including protein precipitation, washing, drying, and UHPLC–MS/MS analysis, required 12 steps and lasted approximately 4 hr, with the chromatographic analysis time being approximately 7 min per sample. This produced far shorter analysis times and reduced efforts than previous acid hydrolysis and enzymatic digestion methods (**Table 2**). While being effective at determining chlorine exposure, using this method, roughly 90 parallel samples could be processed and analyzed in a 24-h period. The UHPLC–MS/MS chromatograms of 2,6-DCP and 2,4-DCP-d<sub>3</sub> were prepared and analyzed from 2,6-DCP, and 2,4-DCP-d<sub>3</sub> spiked rat plasma protein (**Figure 4**). 2,6-DCP, eluting at about 1.7 min, and 2,4-DCP-d<sub>3</sub>, eluting at about 2 min, were detected from the protein precipitate of spiked rat plasma. Following preparation, UHPLC-MS/MS analysis of 2,6-DCP and 2,4-DCP-d<sub>3</sub> produced a sharp and symmetrical peak with peak asymmetry factors of <1.1 and <1.3, respectively, showed excellent efficiency, and were resolved from other components in the plasma matrix.

#### **2.4.2 Dynamic range, the limit of detection, and sensitivity**

Initially, the linearity of the method was evaluated in the range of 0.01–100  $\mu\text{M}$  in plasma protein. Multiple calibration curves were constructed to analyze the calibration behavior of 2,6-DCP by plotting the concentration of 2,6-DCP versus the signal ratio (i.e., the peak area of 2,6-DCP at 160.9/125 divided by the corresponding peak area of 2,4-DCP-d<sub>3</sub> at 163.8/126.9) as a linear relationship over multiple calibration ranges. We confirmed that the calibration behavior was best described by non-weighted linear least-squares regression. The 0.01, 0.02, and 100  $\mu\text{M}$  calibration standards were evaluated, and they fell outside the linear range when the inclusion criteria were  $100 \pm 15\%$  for accuracy and  $\leq 15\%$  for precision. Therefore, the method had a linear range of 0.05–50  $\mu\text{M}$ . The lower limit of

quantification (LLOQ) and upper limit of quantification (ULOQ) were 0.05 and 50  $\mu\text{M}$ , respectively. Calibration curve equations of three separate calibration curves prepared over a 3-day period with their corresponding  $R^2$  and PRA values shown in **Table 4**. All three calibration curves were found to be highly reproducible in terms of slope,  $R^2$ , PRA, accuracy, and precision. While calibration curve goodness-of-fit, accuracy, and precision were consistently outstanding, the %RSD of the slope for the three calibration curves was <15 %. Therefore, it is recommended the calibration curve be prepared daily for accurate calculation of 2,6-DCP concentrations.

The LOD was 7.8  $\mu\text{g}/\text{kg}$ , as calculated by equation (2.1) and converted to concentration. This LOD corresponds to 7.2 nM in the base hydrolysate. This high sensitivity is very important to accurately quantify 2,6-DCP in plasma protein samples [75].

### 2.4.3 Accuracy and precision

The accuracy and precision of the method were established by quintuplicate analysis of three QC standards: low, medium, and high (0.3, 3, and 30  $\mu\text{M}$ ) on three days within 7 calendar days. FDA method validation guidelines were followed to evaluate the results [80, 87, 88]. The precision and accuracy of the method were excellent (**Table 5**), with interassay and intraassay accuracies within  $100 \pm 6\%$  and  $100 \pm 13\%$  (Note: one data point was  $\pm 13\%$  and all other were <8%), respectively. The interassay and intraassay precisions were also within  $\leq 6.6\%$  and  $\leq 12\%$  of the nominal concentration, respectively.

**Table 4.** Calibration equations, coefficients of determination ( $R^2$ ), and PRA for calibration curves were created over 3 days.

Day	Calibration Equation	$R^2$	PRA(%)	Accuracy (%)	Precision (%RSD)
1	$y = 0.5646x - 0.0033$	1.00	95.3	$100 \pm 14.02$	<15
2	$y = 0.7134x - 0.0091$	0.9997	94.7	$100 \pm 9.4$	<10
3	$y = 0.6953x - 0.0058$	0.9998	94.8	$100 \pm 8.6$	<8.5

**Table 5.** Intra- and interassay accuracy and precision of 2,6-DCP produced by base hydrolysis of  $Cl_2$ -tyrosine protein adduct.

Nominal concentration ( $\mu$ M)	Intraassay accuracy (%) <sup>b</sup>			Intraassay precision (%RSD) <sup>b</sup>			Interassay accuracy (%) <sup>a</sup>	Interassay precision (%RSD) <sup>a</sup>
	Day 1	Day 2	Day 3	Day 1	Day 2	Day 3		
0.3	$100 \pm 13$	$100 \pm 5.4$	$100 \pm 1.5$	9.2	3.1	6.9	$100 \pm 5.4$	< 6.6
3	$100 \pm 7.5$	$100 \pm 2.7$	$100 \pm 4.02$	10.9	9.5	8.8	$100 \pm 0.25$	< 6.3
30	$100 \pm 1.6$	$100 \pm 6.3$	$100 \pm 0.91$	11.6	8.5	6.4	$100 \pm 1.3$	< 4.5

<sup>a</sup> QC method validation (N=5). <sup>b</sup> Mean of three different days of QC method validation (N=15).

#### 2.4.4 Matrix effect and recovery

To evaluate the matrix effect, two calibration curves were constructed (non-IS corrected and IS-corrected curves) in plasma protein and aqueous samples. The ratio of slopes ( $m_{\text{plasma}}/m_{\text{aq}}$ ) was 0.88 (**Table 6**). Therefore, a minor matrix effect indicates approximately 12% suppression of 2,6-DCP signals in the rat plasma matrix. Moreover, the IS-corrected slope ratio ( $m_{\text{plasma}}/m_{\text{aq}}$ ) was 0.96, revealing the importance of IS for correcting the modification of the analyte signal due to matrix effects.

**Table 6.** Slopes ( $\mu\text{M}^{-1}$ ) obtained from non-IS corrected and IS-corrected calibration curves of 2,6-DCP

Calibration curve	$m_{\text{plasma}}$	$m_{\text{aq}}$	$m_{\text{plasma}}/m_{\text{aq}}$	Remark
Non-IS corrected	0.9595	1.0838	0.88	Minor matrix effect
IS-corrected	0.9977	1.0343	0.96	Corrected matrix effect

The recoveries (determined by dividing the peak area of the 2,6-DCP signal in plasma protein by the peak area of the equivalent concentration of aqueous QC standards containing 2,6-DCP reconstituted in mobile phases) for low, medium, and high QCs were 38.9%, 40.9%, and 41.7%, respectively. The loss of 2,6-DCP during the sample preparation steps is most likely due to the incomplete extraction (part of the analytes remain in the aqueous layer) of 2,6-DCP from the plasma matrix into the organic layer. Since the recovery reported is the combination of matrix effect and recovery, the minor matrix effect in rat plasma slightly contributes to recoveries <100%, but the loss of 2,6-DCP is the major contributor to the loss of signal than matrix suppression. To investigate the ability of the internal standard to correct for the low recovery and matrix effect, the internal standard was used to correct the signals for the recovery experiment. The internal standard corrected for the signal loss from these two sources. Internal standard corrected accuracy of the low

(LQC), medium (MQC), and high QC (HQC) standards being 98.8%, 96.7%, and 97.6%, respectively. It is, therefore, essential to use internal standards to correct for the loss of 2,6-DCP during sample preparation and matrix effects to ensure accurate quantification of 2,6-DCP.

#### **2.4.5 Stability of 2,6-DCP and chloro-tyrosine adduct**

The stabilities of 2,6-DCP and Cl<sub>2</sub>-Tyr (i.e., the chlorotyrosine adduct) were evaluated under multiple storage conditions. To determine the stability of 2,6-DCP in prepared samples in the autosampler at 15 °C, LQC and HQC standards were placed in the autosampler after they were processed using the sample preparation described and were subsequently analyzed after 0, 1, 2, 4, 8, 12 and 24 h. 2,6-DCP signals for both LQC and HQC samples were stable for all times tested. We also investigated the stability of the chlorotyrosine adducts on the benchtop. Samples were prepared and analyzed after 0, 1, 2, 4, 8, 12, and 24 h of storage. Both LQC and HQC concentrations of chloro-tyrosine adducted protein were stable for the entire period tested.

For long-term stability, the chloro-tyrosine adducted protein was stored at room temperature, 4 °C, -20 °C, and -80 °C. Samples were prepared and analyzed after 0, 1, 2, 5, 15, and 30 days. At room temperature and 4 °C, samples were stable for 5 and 15 days, respectively. However, samples stored at lower temperatures (-20 °C and -80 °C) were stable for at least 30 days (i.e., the most extended period tested). Based on the aggregate results of the stability studies, we suggest storage of samples at -20 °C or -80 °C. Once thawed, samples should be stable during processing and on an autosampler (at 15 °C) for at least 24 hr each.

#### 2.4.6 Verification of chlorine exposure via 2,6-DCP analysis

The ability of the method to verify exposure to chlorine was confirmed by the detection of 2,6-DCP from base-hydrolyzed plasma proteins of Cl<sub>2</sub>-exposed rats compared to non-exposed (naïve) rats. **Figure 5** shows the representation of 2,6-DCP chromatograms of these two groups of rats (A) and the mean 2,6-DCP produced by these groups (B). **Figure 5B** shows the mean amount of 2,6-DCP generated from hydrolysis of plasma protein, non-exposed (N=5), and 600 ppm (N=8). The dose of chlorine was modeled after a large-dose acute exposure which may be produced in a mass-casualty situation. For this study, 2,6-DCP was detected over the concentration range of 0.15 to 0.97 mg/kg (0.14 to 0.9 μM) from the exposed rats and between 0.023 to 0.038 mg/kg (0.021 to 0.035 μM) for the non-exposed rats. It was expected that 2,6-DCP would be detected in naïve rats since endogenous levels of chlorinated protein residues in plasma protein are known to be present from natural sources [81, 82]. While endogenous levels of 2,6-DCP were detected in the non-exposed rats, the maximum concentration detected, 0.038 mg/kg (0.035 μM), was well below the minimum 2,6-DCP detected for exposed rats. Differences in the aggregated groups (non-exposed and 600 ppm) were evaluated using a one-way t-test analysis. The p-value obtained was < 0.0040, indicating a significant difference between the groups. The relationship shown in **Figure 5** is very promising for using 2,6-DCP as a biomarker to confirm chlorine exposure utilizing this method.

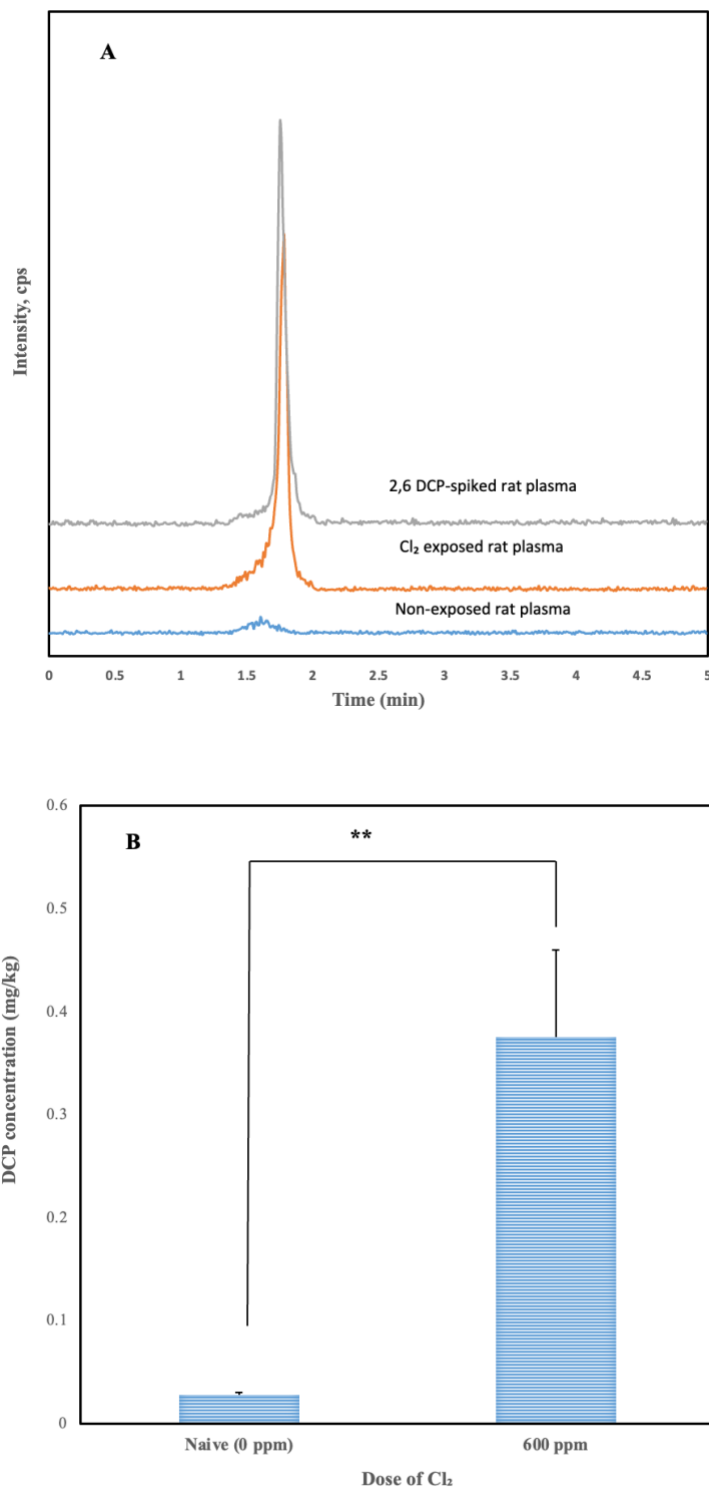


**Figure 5.** UHPLC-MS/MS chromatogram of 2,6-DCP from the plasma of Cl<sub>2</sub>-exposed and non-exposed rats are presented (A). The 160.9 → 125 m/z transition is plotted. Correlation of Cl<sub>2</sub> dose to the concentration of 2,6-DCP from exposed rats (B). The error bars represent the standard error of the mean, \*\* = p<0.01.

## **2.5 Conclusion**

A novel marker of chlorinated tyrosine protein adducts, 2,6-DCP, was discovered on base hydrolysis of these adducts. A simple and rapid UHPLC–MS/MS method with excellent sensitivity to 2,6-DCP was successfully developed to verify chlorine exposure. The detection of chlorophenol in plasma protein isolated from chlorine-exposed rats indicates that 2,6-DCP is a promising biomarker of chlorine exposure.

## **2.6 Acknowledgment**

We gratefully acknowledge support from the CounterACT Program, National Institutes of Health Office of the Director, and the National Institute of Environmental Health Sciences (NIEHS), Grant number U54 ES027698 (CWW). The opinions or assertions contained herein are the private views of the authors. They are not to be construed as official or as reflecting the views of the National Institutes of Health or the CounterACT Program.

### 3 CHAPTER 3. DEVELOPMENT OF A RAPID FLUORESCENCE PROBE FOR THE ANALYSIS OF AQUEOUS HYPOCHLORITE

#### 3.1 Abstract

When assessing risk and clinical treatment plans for harmful chemical exposure, it is ideal to identify the chemical involved in an incident and the extent of exposure to take necessary actions. Chlorine exposure is of particular concern because of its widespread use in industry. The interaction of chlorine with an aqueous environment, including the mucosa and alveolar fluid in the lungs, causes the transformation of the chlorine to hypochlorous acid and hydrochloric acid. Contact of HOCl and HCl with cells via inhalation, ingestion, or dermal contact causes cell ulcer damage and can produce systemic toxicity. In this study, we investigate the detection of hypochlorite anion ( $\text{ClO}^-$ ) from aqueous solutions. There are multiple techniques to monitor the hypochlorite from various matrices, however, growing attention has been paid to fluorescent probes for tracking  $\text{ClO}^-$  because of their high sensitivity, better selectivity, fast response, and ease of use. In this article, we synthesized a water-soluble probe by a one-step procedure called fluorescein thioacid (FSH) for the rapid and sensitive detection of  $\text{ClO}^-$  in aqueous solutions. FSH exhibited an excellent selectivity toward  $\text{ClO}^-$  based on its strong oxidative properties, reacting with FSH to produce fluorescein. Probe FSH could detect  $\text{ClO}^-$  quantify in the range of 1-200  $\mu\text{M}$  with a detection limit of 0.1  $\mu\text{M}$ . The probe is extremely simple to synthesize, yet its properties, including high selectivity, excellent sensitivity, good water solubility, and fast response, lend this probe to be of great benefit to analytical researchers for monitoring the  $\text{ClO}^-$  levels in aqueous solutions.

### 3.2 Introduction

Chlorine is a denser-than-air gas that is a highly toxic irritant gas to the skin, and especially to the eyes, nose, throat, and respiratory system. Although it is toxic, chlorine is one of the most widely used chemicals in health, agro-food, building, textiles, transport, leisure activities, cosmetics, etc. [8, 42]. Because of its industrial uses, it is transported and stored in many locations, leading to a relatively large number of accidental releases (see **Table 1**).

The effects of human exposure to chlorine are well known insofar as the nature of the toxic response is concerned. However, there is a substantial disagreement on the quantitative relationship between exposure, in terms of concentration and duration, and the incidence of acute health effects in the exposure population [89]. Chlorine concentration above 1 ppm causes mucus membrane irritation; at about 10 to 30 ppm causes cough, chest pain, and shortness of breath. Higher level exposures (> 400 ppm) result in asphyxia with respiratory failure, pulmonary edema, acute pulmonary hypertension, cardiomegaly, pulmonary vascular congestion, and acute burns of the upper and proximal lower airways, which can ultimately result in death [25, 27, 61].

There have been many incidents of chlorine exposure (see **Section 2.2**) during chlorine transportation [16, 17], occupational exposure [43-46], civilian accidents with chlorinated commercial products [47-58], and using chlorine in chemical weapon [8, 9]. For instance, an accidental release of chlorine happened on August 2, 2019; a worker was preparing disinfectant by mixing unknown chemicals, which generated chlorine formation as high as 301,964 ppm (estimated) [90]. Another incidental release happened during the transportation of chlorine on January 6, 2005, in Graniteville, South Carolina, where a train

was accidentally diverted from the central railway and struck a parked train, causing the derailment. People near the incident were seeking treatment for exposure to the unidentified gas [7]. Therefore, it is essential to identify the substance of harmful exposure to take the necessary steps.

Upon exposure, chlorine contact with mucosal and lungs fluid and forms hypochlorous acid and hydrochloric acid [25], which then produce highly reactive oxidants via combination with reactive oxygen species and other airway constituents [26], results in instant oxidative injury to the epithelium and migration and activation of inflammatory cells such as neutrophils. Therefore, chlorine exposure can damage the eyes, skin, and upper airways from the nose to the bronchi [27, 28]. In addition, there have been reported subepithelial fibrosis, mucous hyperplasia, and nonspecific airway hyperresponsiveness following chlorine injury [27, 29, 62, 63].

Chlorine mixes with water, and produces hypochlorous acid (HOCl) and HCl [91, 92]. High concentrations of both HCl and HOCl are toxic. While HOCl is considered a weak acid, it is a strong oxidizer. The measurement of hypochlorous acid (HOCl) and hypochlorite ion (OCl<sup>-</sup>) is called free chlorine residual (**Figure 6**). For HOCl as an acid, the acid dissociation occurs slightly into hydrogen and hypochlorite ions between a pH of 6.5 and 8.5, where both HOCl and OCl<sup>-</sup> species are present [92]. Below a pH of 6.5, no dissociation of HOCl occurs, while above a pH of 8.5, complete dissociation to OCl<sup>-</sup> occurs [93].

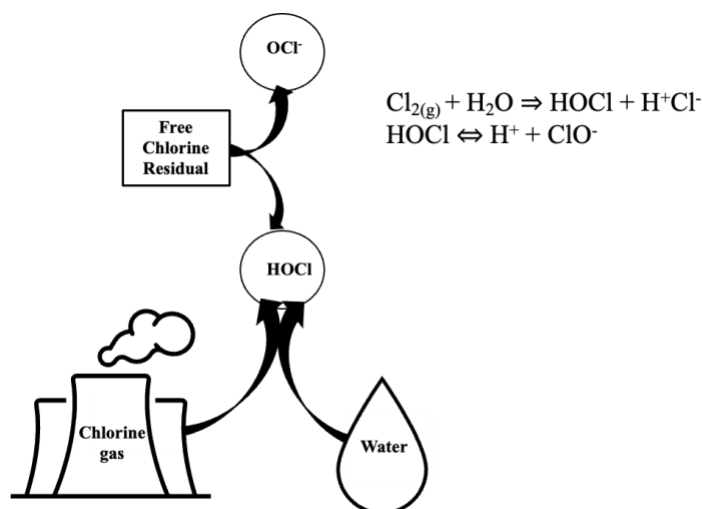


**Figure 6.** Chlorine reactions with water.

Experimental measurements of  $\text{Cl}_2$  uptake on groundwater [94, 95], soil [96-98] and plant [99-104] have been noted in several reports of accidental releases. However, given this context of interest, the exposure periods of interest are very long compared with the likely durations of accidental exposures [105]. Therefore, a fast technique to determine chlorine exposure is continuously investigated.

There are methods available to analyze HOCl, such as the colorimetric [106, 107], electrochemical [108-114], chemiluminescence [115], and fluorescent methods [116-123]. Among those reported methods, fluorescent probe detection is promising for detecting  $\text{ClO}^-$  due to high sensitivity, better selectivity, fast response, simplicity, potential spatial resolution (e.g., for imaging), and ease of detection [119, 124]. So far, many fluorescent probes for the recognition and detection of  $\text{ClO}^-$  have been identified. Although multiple probes have been developed, they typically require lengthy and complex synthesis. Additionally, commercially available fluorescent probes are costly and often don't function well for the  $\text{ClO}^-$  (e.g., unstable baseline signals). Therefore, efforts to enhance the

sensitivity, water solubility, and signal intensities of fluorescent probe performance with a simple synthetic route is needed [120].

The objectives of this study were to develop a simple turn-on fluorescent probe and evaluate its ability to detect  $\text{ClO}^-$ . The requirements of the probe were high selectivity, rapid response, high sensitivity, and amenability to aqueous systems.

### **3.3 Materials and Methods**

#### **3.3.1 Materials**

All chemicals were of HPLC grade and used as received without further purification. 2-benzothiophene-1,3-dione was purchased from Millipore Sigma (St. Louis, MO, USA). Resorcinol was obtained from Acros Organics (New Jersey, USA). Chloroform-d with TMS as an internal standard, was purchased from Millipore Sigma (St. Louis, MO, USA). Sulfuric acid, acetone, methanol, and formic acid were purchased from Fisher Scientific (Fair Lawn, New Jersey, USA). Deionized water was obtained from a polisher at 18 M $\Omega$ -cm resistivity. The sodium hypochlorite stock solution (10-15 %) was obtained from Millipore Sigma (St. Louis, MO, USA), stock solutions of NaOCl (10 mM) were prepared in deionized water.

#### **3.3.2 Analytical Instruments**

NMR spectra were obtained from Bruker AVANCE-600 MHz NMR spectrometer (Billerica, Massachusetts, USA) in deuterated solvent  $\text{CDCl}_3$  for  $^1\text{H}$  NMR and  $^{13}\text{C}$  NMR with chemical shifts reported as ppm. Electrospray ionization-mass spectra (ESI-MS) were obtained from AB SCIEX QTRAP 5500 MS (Applied Biosystems, Foster City, CA, USA). Mass spectra were obtained by using Analyst software. Fluorescence spectra were obtained from a FluoroMax-4, HORIBA Scientific spectrofluorometer (Knightsbridge Road,

Piscataway, New Jersey, USA) using a polystyrene cuvette (Fisher Scientific, Pittsburgh, PA, USA). The pH of each sample solution was recorded by pH meter (Thermo Fisher Scientific, USA).

### 3.3.3 Synthesis of FSH probes

The fluorescein thioacid (FSH) was synthesized according to the previously published procedure by Guetzloff et al. Briefly, a mixture of 2-benzothiophene-1,3-dione (23 mg, 0.14 mmol) and resorcinol (40 mg, 0.36 mmol) in sulfuric acid (18 M, 3-6 drops) was heated at 150 °C for 30 min (**Figure 8**). The reaction mixture was then poured into 40 mL dichloromethane and 50 mL of 1M NaOH was added. The layers were separated, and the organic layer was collected. The organic layer was dried over MgSO<sub>4</sub> and concentrated using N<sub>2</sub> gas. The crystalline product was a mixture of both FSH and fluorescein (FOH). This crude product was reconstituted in 2 mL of water/methanol (50/50, w/w) and further purified by preparative HPLC (Dr. Fathi T. Halaweish's lab from the Department of Chemistry and Biochemistry, South Dakota State University, Brookings, SD, USA) with the mixture of water and methanol as mobile phase (50:50, v/v) to yield probe FSH.

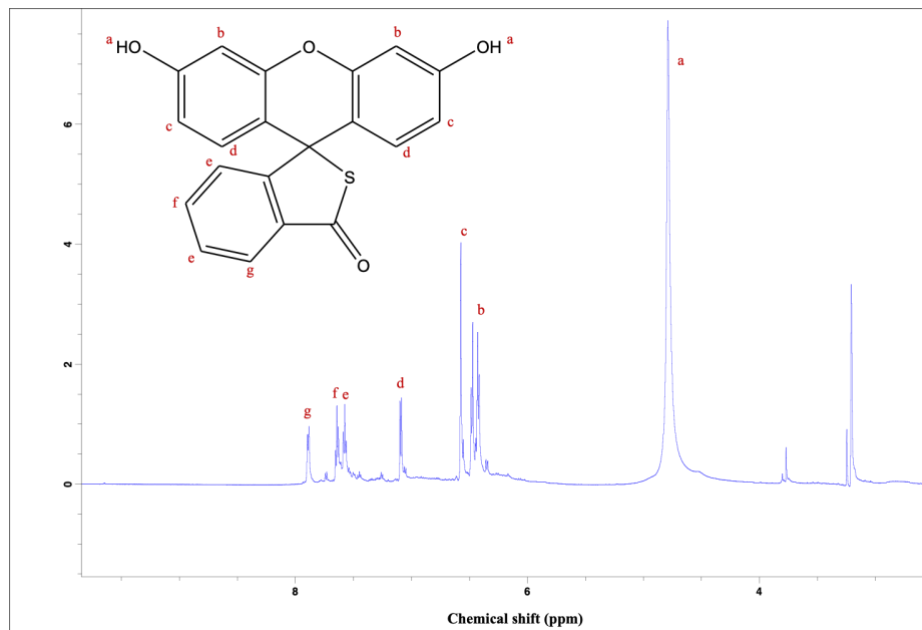


**Figure 7.**  $^1\text{H-NMR}$  of synthesized probe called fluorescein thioacid (FSH).

### 3.3.3.1 Purification of FSH via preparative HPLC

A Dynamax liquid chromatograph (Varian chromatography systems) and dual pump solvent delivery system, model SD-200 with PDA-2 photodiode array UV detector using the Dynamax PC Chromatography Data System (v. 1.9) software were used. The 200  $\mu\text{L}$  of the reconstituted crude sample was injected into an Econosil C18 (Alltech; 250 mm x 22 mm, 10  $\mu\text{m}$ , Part No: 6251) preparative column at a constant 11 mL/min flow. Gradient elution started at 60% B and increased to 90% B over 8 minutes, held constant for 4 minutes, and decreased to 60% B over 3 minutes. Mobile phase A was 0.1% formic acid prepared in 5% methanol in DI water, and solvent B was 100% methanol. The total run time was 15 minutes, with elution time of FSH (226 nm) at 11.5 minutes and FOH (234 nm) at 10 minutes. The FSH fraction was collected, and evaporated the solvents using Rotavapor.

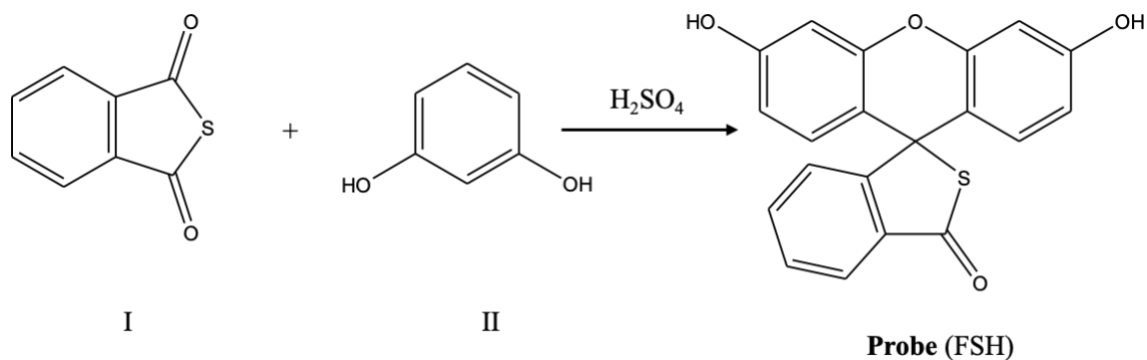


**Figure 8.** The synthesis pathway of probe (FSH).

### 3.3.3.2 Evaluation of FSH purity via LC-MS/MS

After the FSH was separated from FOH, the collected eluent was dried and reconstituted with water/methanol (50/50, v/v). The prepared sample was filtered using a 0.22  $\mu\text{m}$  PVDF syringe filter and transferred the solution into a 2 mL LC-MS vial. The sample was analyzed using the LC-MS/MS.

LC analysis was performed on a Shimadzu UHPLC with an LC-20ADXR controller. The column used for chromatography was an Eclipse XDB-C18 (4.6 x 150 mm, 5  $\mu\text{m}$ ). The chromatographic separation was achieved using gradient elution at a flow rate of 0.5 mL/min starting at 60 %B and increased to 90 % B over 8 minutes, held constant for 4 minutes and decreased to 60% B over 3 minutes (total run time was 15 minutes). Mobile phase A was 0.1% formic acid prepared in 5% methanol in DI water, and solvent B was 100% methanol. The column was equilibrated for 1 min, and a volume of 10  $\mu\text{L}$  was injected for LC-MS/MS analysis. For MS analysis, a tandem mass spectrometer (Sciex Q-Trap 5500 MS) equipped with an electrospray ionization interface in the positive mode was used to detect FSH and FOH. Mass spectrometric conditions were optimized by directly infusing a standard solution of FSH and FOH into the spectrometer at a flow rate of 10

$\mu\text{L}/\text{min}$ . After infusion of standard solutions of FSH and FOH into ESI, molecular ions of  $m/z$  349 ( $[\text{M}+\text{H}]^+$ ) and  $m/z$  333 ( $[\text{M}+\text{H}]^+$ ), respectively, were identified. Multiple reaction monitoring (MRM) parameters for FSH and FOH were optimized and are outlined in **Table 7**. Nitrogen (20 psi) was used as the curtain and nebulization gas. The ion spray voltage was 4,500 V, the source temperature was 600 °C, and the nebulizer (GS1) and heater (GS2) gas pressure was 30 psi. The collision cell was operated at a “medium” collision gas flow rate. The product was considered pure if the % of FOH was < 2% of the total peak area of FSH + FOH combined.

**Table 7.** MRM transitions, optimized collision energies (CEs), collision cell exit potentials (CXPs), and declustering potentials (DPs) for detection of FSH and FOH by MS/MS analysis

Compounds	Q1 (m/z)	Q3 (m/z)	Dwell Time (msec)	CE (V)	CXP (V)	DP (V)
FSH (quantification)	349	287.1	100.0	53.01	22.70	185.10
FSH (identification)	349	271.0	100.0	182.91	37.03	45.69
FOH (quantification)	333	289.1	100.0	57.13	23.90	249.12
FOH (identification)	333	271.0	100.0	62.89	19.06	180.99

### 3.3.4 Fluorescence analysis of hypochlorite using FSH

For measuring the FSH probe's response to  $\text{ClO}^-$ , a working solution (200  $\mu\text{M}$ ) was freshly prepared in deionized water. Test solutions of NaOCl were prepared by placing 50  $\mu\text{L}$  of the probe (5  $\mu\text{M}$ ) solution into a polystyrene (1.2 cm x 1.2 cm x 4.5 cm) cuvette and adding 1450  $\mu\text{L}$  of NaOCl solution at the desired concentration. All measurements were made within 5 min at room temperature (25  $^\circ\text{C}$ ). The fluorescence spectra were measured by a HORIBA scientific fluorescence spectrometer. The excitation wavelength was optimized at 482 nm and the emission spectra were gathered from 492 nm to 600 nm with excitation and emission slit width both set at 5 nm.

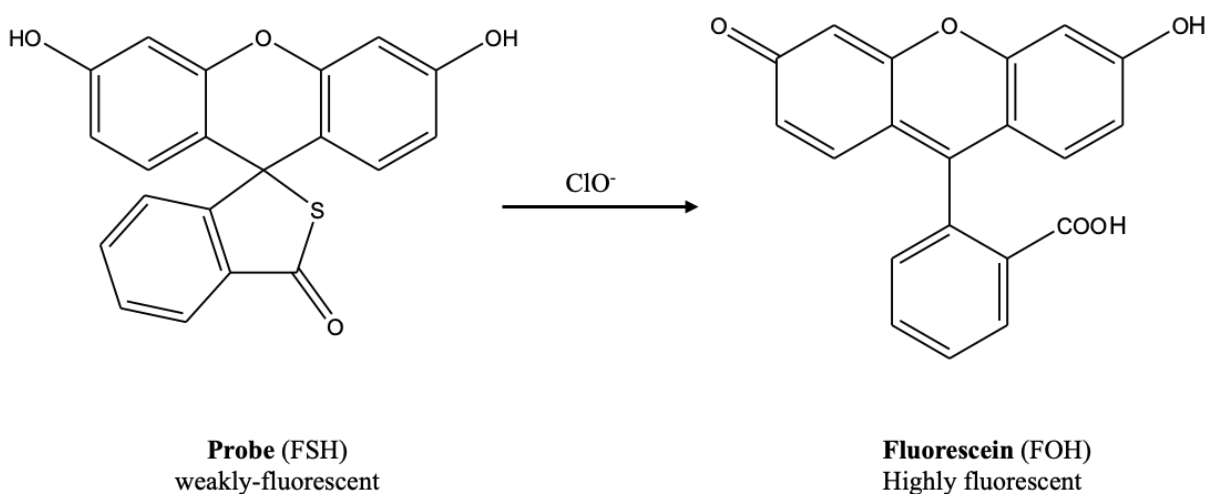


**Figure 9.**  $\text{ClO}^-$  induced oxidation of fluorescent probe (FSH).

### 3.3.5 Method limit of detection

The limit of detection (LOD) was calculated based on previous work [125]. Briefly, the fluorescence emission spectrum of the probe solution (i.e., the blank) was measured

five times. The intensity of the blank at 513 nm was measured for each blank replicate. The average signal and standard deviation of the blank were calculated.

The signal LOD was calculated by multiplying the standard deviation of the blank signal by 3 and adding this value to the average blank signal. To determine the concentration LOD, a calibration curve was created near the signal LOD and the signal LOD was converted to a concentration-based LOD.

### **3.4 Results and Discussion**

#### **3.4.1 Synthesis of FSH**

FSH was easily synthesized from known and commercially available compounds (I and II according to the route outlined in **Figure 8.** Specifically, a mixture of two solids, 2-benzothiophene-1,3-dione (23 mg, 0.14 mmol) and resorcinol (40 mg, 0.36 mmol), was heated in the presence of sulfuric acid (18 M, 3-6 drops). To ensure purity, the probe was characterized by LC-MS/MS. **Figure 10.** shows chromatograms for FSH and FOH. The fraction collected for FSH shows no signal for FOH, which confirms FSH's isolation from FOH and the probe's purity.

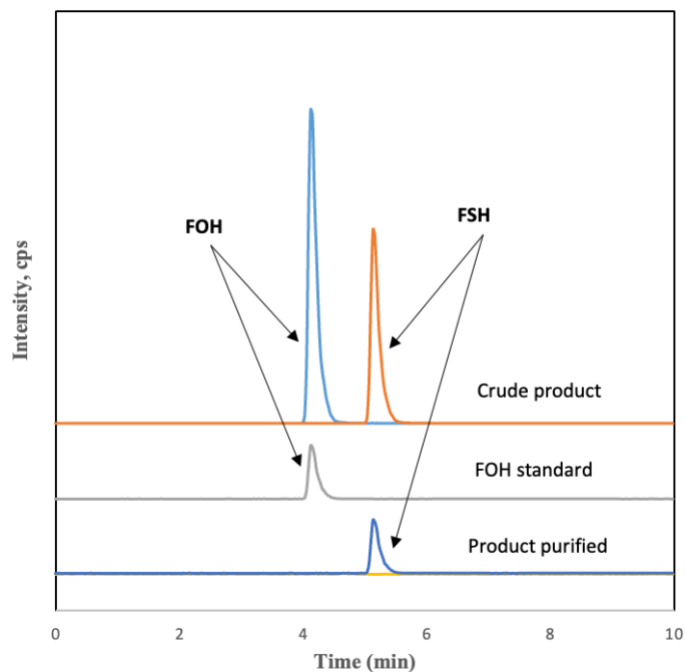


**Figure 10.** LC-MS/MS chromatogram for FSH and FOH from the crude product and purified fraction by the preparative HPLC.

### 3.4.2 Spectroscopic properties

The fluorescence intensity of the FSH was measured in deionized water both in the absence and presence of NaOCl. As shown in **Figure 11.**, the probe displayed a major fluorescence band centered at 513 nm, accompanied by a change in the color of the solution from light green to dark green (**Figure 11.**, inset) was observed in the dark under black light when in the presence of NaOCl. This is attributed to the structural oxidization of the probe sulfur, yielding the green-colored and highly fluorescent compound.

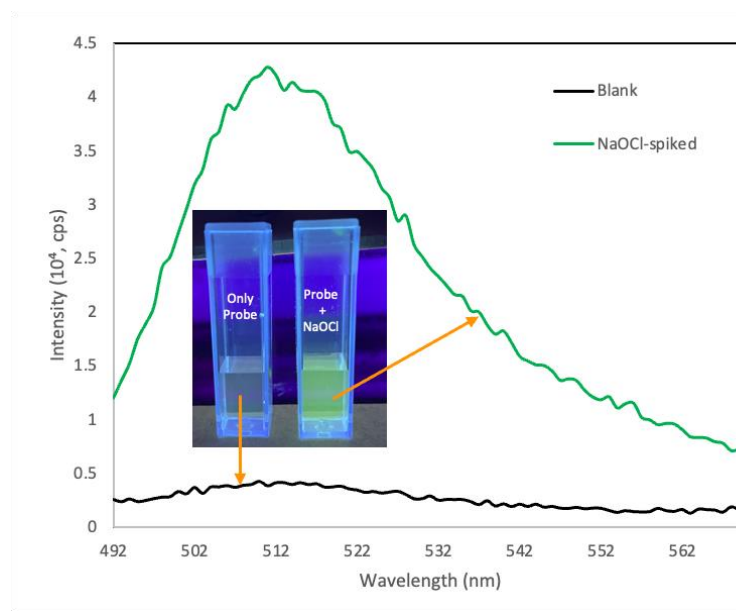


**Figure 11.** Fluorescence spectra of probe (5  $\mu\text{M}$ ) in the absence and presence of NaOCl (100  $\mu\text{M}$ ) in the deionized water. The inset shows the photographs of the solution of the probe in the absence and presence of NaOCl under black light.

To demonstrate the stability of the probe, we measured fluorescence intensity at 513 nm for 24 hours (**Figure 12.**). The results showed that our proposed probe maintained 82% intensity for 24 hours. Our proposed probe is very stable.

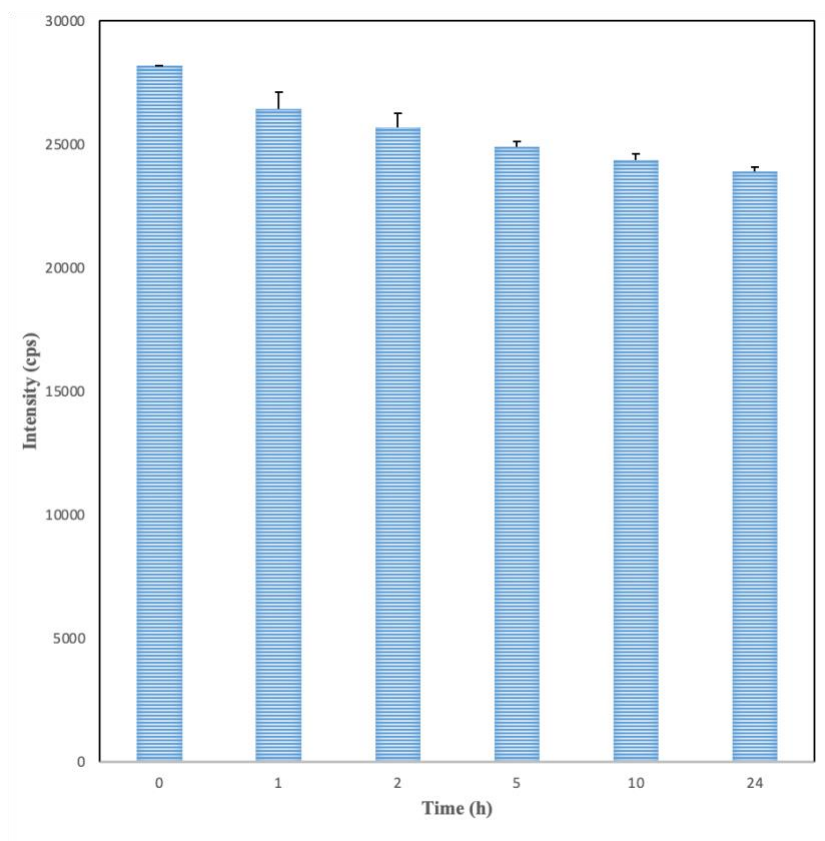


**Figure 12.** Time-course of fluorescence intensity at 513 nm for probe (5  $\mu\text{M}$ ) in the presence of NaOCl (100  $\mu\text{M}$ ).

The pH of a solution can have major effects on the fluorescence properties of a fluorescent probe, especially fluorescence-based probes. For example, FOH does not fluoresce at low pH values but strongly fluoresces above pH 3 [126-128].

The effect of pH on the detection of  $\text{ClO}^-$  for the FSH probe is shown in **Figure 13.** The fluorescence intensity of the FSH probe itself (i.e., an aqueous solution of the probe itself without  $\text{ClO}^-$ ), labeled “blank” in **Figure 13.**, shows very little fluorescence at pH values below 5 relative to pH values  $\geq 5$ . In the presence of  $\text{ClO}^-$ , the fluorescence intensity of the FSH probe showed a massive increase in fluorescence from pH 3 to 4, with fairly consistent fluorescence from 4 to 11. The difference in fluorescence between blank

and NaClO spikes probe FSH can be used to detect ClO<sup>-</sup> over a wide pH range. The optimum pH, which produces the maximum sensitivity to NaClO, is about 4.

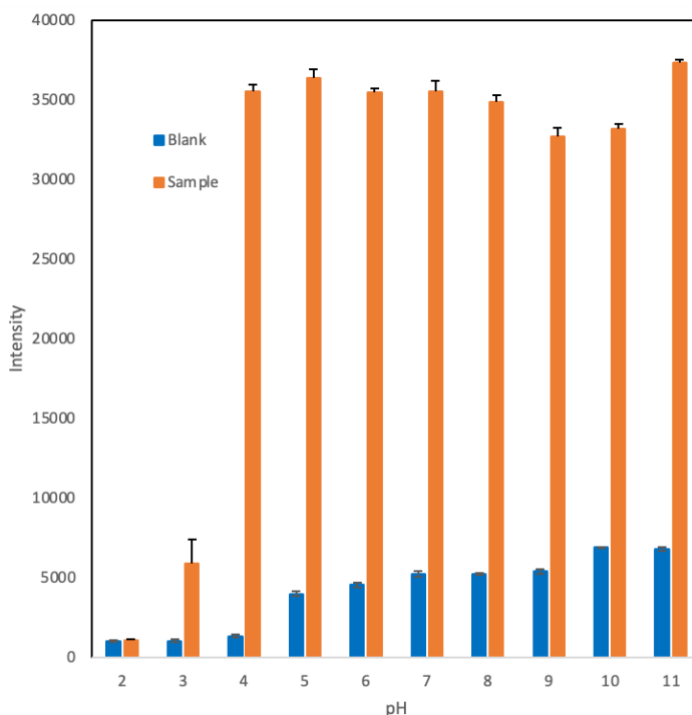


**Figure 13.** pH optimization for the fluorescence at 513 nm for probe (5  $\mu$ M) in the presence of NaOCl (100  $\mu$ M).

### 3.4.3 Quantification of ClO<sup>-</sup> using FSH

The limit of detection (LOD) of ClO<sup>-</sup> was calculated to be 0.1  $\mu$ M, and the sensitivity of our proposed system is superior to the previous reports [117]. The addition of a series of ClO<sup>-</sup> concentrations to the solution of the probe resulted in a gradual increase of the fluorescence intensity at 513 nm (**Figure 14.A**). Importantly, there was good linearity between the intensity and concentrations of ClO<sup>-</sup> in the range of 1-200  $\mu$ M, and the linear equation is  $y = 178.33x$  (ClO<sup>-</sup>,  $\mu$ M) + 2825.2 (correlation coefficient  $R^2 = 0.9987$ )

(Figure 14.B). The result demonstrated that probe FSH could detect  $\text{ClO}^-$  qualitatively and quantitatively.

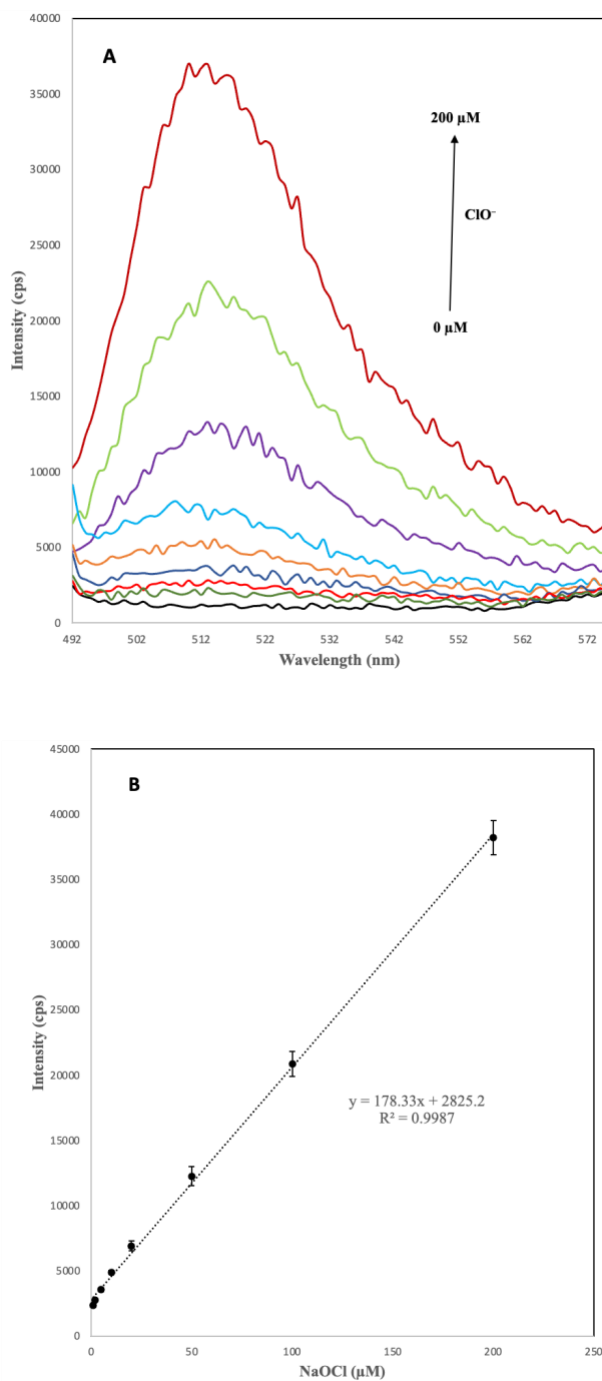


**Figure 14.** (A) Fluorescence response of probe FSH (5 μM) upon addition of various concentration of  $\text{ClO}^-$ . (B) Standard curve of fluorescence intensity at 513 nm versus  $\text{ClO}^-$  concentration.  $\lambda_{\text{ex}}/\lambda_{\text{em}} = 482/513$  nm.

#### 3.4.4 Selectivity of FSH to hypochlorite

High selectivity is desirable in a fluorescent probe. Therefore, various common ions and oxidants were evaluated as potential interferents.  $\text{ONOO}^-$ ,  $\text{NO}_2^-$ ,  $\text{CN}^-$ , and  $\text{H}_2\text{O}_2$  were evaluated as potential interferences by adding 200  $\mu\text{M}$  concentrations into the FSH probe solution, and the fluorescence intensity was measured. None of these potential interferents produced a fluorescence signal from FSH above (**Figure 15.**), show that probe FSH possesses high selectivity toward  $\text{ClO}^-$ .

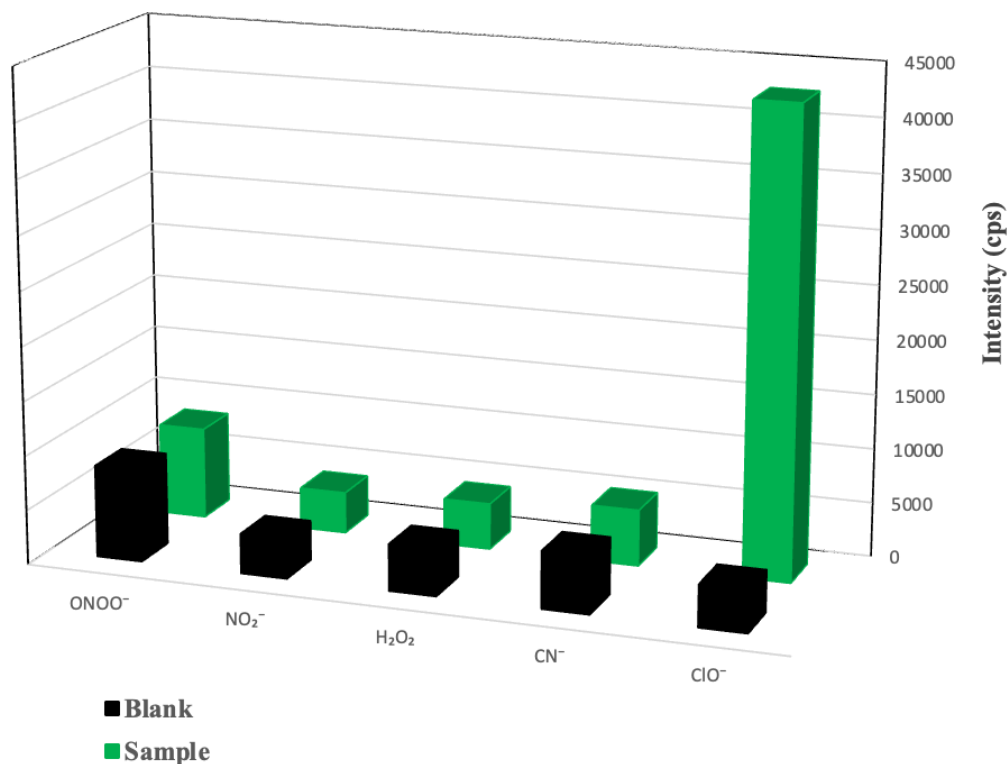


**Figure 15.** Fluorescence intensity of probe (5  $\mu\text{M}$ ) in the presence of various analytes (200  $\mu\text{M}$ ) at 513 nm in deionized water.

### 3.4.5 Analytical applications

The World Health Organization (WHO) proposed that the minimum residual concentration of  $\text{OCl}^-$  in drinking water should be 3.3  $\mu\text{M}$  [129] and the maximum  $\text{OCl}^-$  in pool water should be 67  $\mu\text{M}$  (5 mg/l) [130, 131].

Two types of real-life samples (tap water, and swimming pool) were chosen to study the practical application of probes. Tap water was collected from our lab. The pool water was collected from Wellness center swimming pool from South Dakota State

University. The levels of  $\text{ClO}^-$  in real water samples were obtained by the same method, except that the standard hypochlorite solutions were replaced by sample solutions. A standard addition method, in which different concentrations (10, 20, and 50  $\mu\text{M}$ ) of  $\text{ClO}^-$  were added into the samples, was used for further evaluation of the assay.

The  $\text{ClO}^-$  concentrations of tap water and pool water are 13.8  $\mu\text{M}$ , and 56.9  $\mu\text{M}$ , respectively. These satisfactory results demonstrate that probe has promise for the determination of  $\text{ClO}^-$  in practical application.

### **3.5 Conclusions**

In summary, we designed, synthesized, and evaluated a water-soluble fluorescence probe, FSH, for rapid analysis of aqueous  $\text{ClO}^-$ . FSH exhibited a fast response (1 min) and high selectivity over other analytes. The probe is easily synthesized by a one-step procedure and is excellent at determining aqueous  $\text{ClO}^-$  because of its high selectivity, excellent sensitivity, good water-solubility, fast response, and fluorometric determination.

### **3.6 Acknowledgments**

We gratefully acknowledge support from the CounterACT Program, National Institutes of Health Office of the Director, and the National Institute of Environmental Health Sciences (NIEHS), Grant number U54 ES027698 (CWW). The opinions or assertions contained herein are the private views of the authors. They are not to be construed as official or reflecting the views of the National Institutes of Health or the CounterACT Program.

## 4 CHAPTER 4. PHARMACOKINETICS OF NEXT GENERATION CYANIDE ANTIDOTE DIMETHYL TRISULFIDE FOLLOWING INTRANASAL AND INTRAMUSCULAR ADMINISTRATION OF DMTS IN RATS AND SWINE

### 4.1 Abstract

**Aim:** Dimethyl trisulfide (DMTS) is a promising sulfur donor cyanide antidote, which converts CN to less toxic SCN as a byproduct and is a more powerful sulfur donor than thiosulfate, the current FDA-approved sulfur donor. The current study was performed to determine the pharmacokinetic (PK) behavior of DMTS in rats and swine and to compare it to other US FDA-approved cyanide therapeutics. The PK behavior of DMTS was evaluated in both non-exposed and cyanide-exposed animals. **Methods:** We studied the PK behavior of intranasal (IN) and intramuscular (IM) administered DMTS in 47 rats and 35 swine. Blood DMTS and DMDS concentrations were monitored using dynamic headspace gas chromatography-mass spectrometry (DHS-GC-MS). **Results:** Concentrations of both DMTS and DMDS rapidly increased following both IM and IN DMTS administration, with IN distribution being particularly rapid. Elimination of DMTS was also relatively rapid during the initial elimination phase, but there also appears to be a second phase where a relatively consistent concentration of DMTS above the baseline is observed. The PK behavior of cyanide-exposed animals was starkly different than non-exposed animals, with blood DMTS concentrations greatly reduced when animals were exposed to cyanide. The calculated half-life of DMTS was approximately 300 min following IM administration. For IN administration, the half-lives of DMTS was approximately 252 min. **Conclusion:** Overall, the PK characteristics of DMTS were well-suited for the rapid treatment of cyanide poisoning and are comparable to current U.S.

FDA-approved antidotes (thiosulfate, sodium nitrite, and hydroxocobalamin). The establishment of DMTS PK behavior helps elaborate guidelines for administering DMTS and provides information vital to eventual FDA approval.

## 4.2 Introduction

As HCN or  $\text{CN}^-$ , cyanide is a poisonous and deadly chemical. Exposure to cyanide can occur from various sources, including food items (e.g., cassava, spinach), smoke from cigarettes or fires, occupational exposure from industrial operations (e.g., polymer production, pesticide production, synthetic fiber fabrication, mineral extractions, electrolysis, and electroplating), terrorist activities, and catastrophic events resulting in the release of cyanide (e.g., the warehouse explosion in Tianjin, China) [35-37, 132-139].

Cyanide exposure occurs by inhalation, ingestion, and/or absorption through the skin. Once cyanide reaches cells, it inhibits mitochondrial cytochrome oxidase, thus blocking electron transport and decreasing oxidative metabolism and oxygen utilization. This anaerobic metabolism causes lactic acidosis (i.e., accumulation of lactic acid) as glycolysis becomes the preferred method of energy production. As a result, cellular hypoxia, cytotoxic anoxia, and potential death results [35-38, 140].

There are currently three U.S. FDA-approved cyanide antidotes available to treat cyanide exposure. They are hydroxocobalamin (direct binding agent), sodium nitrite (indirect binding agent), and sodium thiosulfate (a sulfur donor). They are commercially available as Cyanokit<sup>®</sup> (hydroxocobalamin) and Nithiodote<sup>®</sup> (the combination of sodium thiosulfate and sodium nitrite), and both are administered intravenously (IV) [31, 141].

Hydroxocobalamin forms cyanocobalamin (Vitamin B<sub>12</sub>) after binding with cyanide. Because cyanocobalamin is water soluble and readily excreted from the body, it

is generally safe to use. However, it has some drawbacks, including a large recommended dose (5 g administered by IV infusion over 15 min), it is expensive, on-site reconstitution and delivery by trained personnel is required, and a second dose of 5 g is sometimes needed depending on the severity of exposure [142-144].

Sodium nitrite, frequently used with sodium thiosulfate, produces methemoglobin by oxidizing  $\text{Fe}^{2+}$  to  $\text{Fe}^{3+}$  in hemoglobin. Methemoglobin then binds with cyanide to form cyanomethemoglobin. It also works to rapidly compete with cyanide for the heme A group in cytochrome C oxidase, allowing some metabolic activity and reducing CN toxicity [144-146]. Sodium nitrite is given via IV administration (300 mg/10 mL vial at a rate of 2.5-5 mL/min) in combination with sodium thiosulfate (Nithiodote<sup>®</sup>), and a second dose is sometimes required depending on the severity of the exposure [144]. The drawbacks of this treatment include the inefficiency of methemoglobin to carry oxygen relative to hemoglobin. Therefore, excessive production of methemoglobin (>30%) can cause headaches, cyanosis, fatigue, coma, and potentially death. To convert methemoglobin back to hemoglobin, methylene blue and supplemental oxygen can be given in combination with sodium nitrite [37, 142, 144-147].

In the presence of rhodanese (i.e., a mitochondrial thiosulfate sulfur transferase enzyme), sodium thiosulfate acts as a sulfur donor by donating sulfur to cyanide and converts into less harmful thiocyanate, which can be readily excreted from the body. However, while effective and relatively non-toxic, it has a slow onset of action and requires a large dose (12.5 g administered by IV infusion over 10 min), with a second dose of 6.25 g likely needed. To mitigate this drawback, sodium thiosulfate is typically given in combination with more rapidly acting sodium nitrite [37, 132, 143, 144].

Because of the drawbacks of the current U.S. FDA-approved cyanide antidotes, including the requirement of trained medical personnel to administer each, they are not effective, especially in the event of mass exposure to cyanide. Because of the limitations of the currently available antidotes, it is essential to search for a next-generation cyanide antidote. Several candidate antidotes are being developed, including dimethyl trisulfide (DMTS).

DMTS acts as a sulfur donor, similar to thiosulfate, reacting with cyanide to form thiocyanate and dimethyl disulfide (DMDS), as shown in **Figure 16**. DMTS has shown great effectiveness in treating cyanide exposure [36, 148, 149]. DMTS is 43 times more powerful than thiosulfate as a sulfur donor in the presence of rhodanese and 79 times more powerful in the absence of rhodanese. Its antidotal potency ratio (APR) indicates that DMTS is about three times more effective at treating cyanide poisoning than sodium thiosulfate [142, 150-155]. Moreover, intramuscular (IM) administration, a more effective route of administration than IV for mass CN exposures, was shown effective for the administration of DMTS [31].

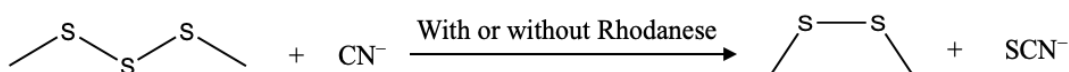


**Figure 16.** Schematic representation of the reaction of DMTS and cyanide to form dimethyl disulfide (DMDS) and thiocyanate.

Little has been published about the pharmacokinetics of antidotal doses of DMTS. Bhadra et al. [31] did publish a preliminary pharmacokinetic analysis of DMTS which showed that DMTS is absorbed and distributed very quickly, producing a  $C_{\max}$  (the maximum concentration of a drug achieved in the blood following dose administration)

and  $t_{\max}$  (the time at which  $C_{\max}$  is attained) of  $0.89 \pm 0.09 \mu\text{M}$  and 10 min, respectively. This quick distribution of IM-administered DMTS is promising since it may allow treatment of CN poisoning by untrained personnel, which is essential for mass casualty situations. Additionally, DMTS showed a long elimination half-life ( $t_{1/2} = 630$  min or 10.5 h), with an estimated elimination rate constant ( $k_E$ ) of  $0.0011 \text{ min}^{-1}$ . This behavior allows early and continuous protection for long periods after DMTS treatment. Overall, this preliminary pharmacokinetic data revealed impressive behavior of DMTS for treating CN poisoning, most notably quick distribution, and lasting blood concentrations. While the PK values were promising, Bhadra et al. [31] study only evaluated 5 rats. Multiple studies must be executed to translate DMTS towards FDA approval, including verification of the pharmacokinetic (PK) behavior of DMTS in multiple animal models, determination of its stability, and verification of its in-vivo mechanism of action.

The primary goal of this work was to define the PK behavior of DMTS from multiple animal models (rat and swine) to contribute to studies of the effectiveness of intranasal (IN) and intramuscular (IM)-delivered DMTS as a cyanide therapeutic.

### **4.3 Materials and Methods**

#### **4.3.1 Materials**

Methanol (LC-MS grade) and sulfuric acid (certified ACS plus) were purchased from Fisher Scientific (Fair Lawn, NJ, USA). Reverse-osmosis water was purified to  $18.2 \text{ M}\Omega\text{-cm}$  through a polishing unit (Lab Pro, Lab-conco, Kansas City, KS, USA). DMTS and internal standard (IS) dimethyl-d6 trisulfide (DMTS-d6) were obtained from Millipore-Sigma (St. Louis, MO, USA) and US Biological Life Sciences (Salem, MA, USA), respectively. DMDS and internal standard (IS) dimethyl-d6 disulfide (DMDS-d6) were

obtained from Alfa Aesar (Tewksbury, MA, USA) and Toronto Research Chemicals (North York, ON, Canada), respectively. For every experiment, DMTS and DMDS stock solution (200 mM) were freshly prepared in methanol; the standard DMTS and DMDS containers were stored in the dark at ambient temperature. The internal standards DMTS-d6 and DMDS-d6 were diluted in methanol to produce a stock solution of 100 mM, which was further diluted to 1 mM in DI water. The stock solutions of DMTS-d6 and DMDS-d6 were stored in a -80 °C freezer (Isotemp plus freezer, Fisher Scientific, NJ, USA) and in a flammable material storage refrigerator, respectively. The thermal desorption (TD) tube, filled with Tenax® TA sorptive material, was purchased from Gerstel Inc. (Linthicum, MD, USA). With a TC 2 tube conditioner and Aux-controller 163 (Gerstel Inc., MD, USA), the new TD tube was treated for 8 h at 315 °C under 68 psi of ultra-high purity (UHP) 5.0-grade nitrogen gas (A-OX Welding Supply Co., Sioux Falls, SD, USA) and the same TU tube was used for the entire study.

#### **4.3.2 Biological samples**

##### **4.3.2.1 Swine model of DMTS administration**

Swine studies were performed at the University of Colorado Anschutz Medical Campus and approved by the Institutional Animal Care and Use Committee (IACUC). All experiments complied with the regulations and guidelines of the Animal Welfare Act and the American Association for Accreditation of Laboratory Animal Care. Adolescent female Yorkshire cross swine weighing 45-55 kg (N=35) were used for this study. Pharmacokinetic analysis was completed in cyanide (n=25) and non-cyanide exposed (n=10) swine. At first, anesthesia was induced with intramuscular (IM) ketamine and sedation maintained with inhaled isoflurane. Following induction, swine were intubated

and instrumented for continuous monitoring of vital signs. Following instrumentation anesthesia was weaned to ensure spontaneous respirations. Throughout the experimental procedures sedation was maintained with 1-2% isoflurane to minimize pain and discomfort. Following a 10-minute acclimation period, animals were randomized into one of two groups, cyanide exposed or a non-cyanide group. The exposure dose of KCN was 7.5 mg/kg. All animals received IM DMTS at various doses (5-25 mg/kg; n=18) or 500  $\mu$ L of intranasal (IN) DMTS (10%, n=1; or neat, n=6) at 6 minutes post apnea. A subset of animals receiving IM DMTS received a second dose of DMTS if there was no physiologic response to the first treatment. All intramuscular injections were administered using a 1.5-inch, 500  $\mu$ L 22 gauge needle into the left or right gluteal muscle. If the injection volume exceeded 5 mL or two doses of DMTS were given, IM injection occurred in alternating gluteal muscles. Intravenous DMTS (10 mg/kg) was administered into the right external jugular vein and IN DMTS was administered using the SipNose nose-to-brain delivery device (developed by SipNose LTD). All animals were observed for 90 minutes post treatment or until death occurred, which was characterized by sustaining a mean arterial pressure <30 mmHg for 10 continuous minutes.

Multiple blood draws were performed from each catheterized swine. The blood samples were collected at baseline (i.e., before exposure and/or treatment) and 1, 2, 5, 10, 20, 30, 40, 50, 60, 70, 80, and 90 min post-DMTS administration from each animal. The stock concentration of the internal standard (420  $\mu$ M DMTS/DMDS in methanol) was shipped to University of Colorado Anschutz Medical Campus and stored at -30 °C before performing an individual animal study. Before starting the animal experiment, the stock IS solution was placed in an ice bath and diluted into deionized water to prepare the final

working IS concentration of 42  $\mu\text{M}$  DMTS/DMDS. Centrifuge tubes (2 mL) were prepared for each blood draw by adding 1000  $\mu\text{L}$  of 0.4% sulfuric acid. When ready for sample collection, 500  $\mu\text{L}$  of blood from the animal was pipetted into the designated sample collection tube containing acid. The IS (25  $\mu\text{L}$  of the 42  $\mu\text{M}$ ) was accurately spiked to the mixture (blood and acid) and then vortexed at 3000 rpm for 10 s to ensure proper mixing. The prepared samples were then flash-frozen and shipped to South Dakota State University (Brookings, SD, USA) on dry ice for analysis. Samples were kept at  $-80^\circ\text{C}$  until analyzed.

#### **4.3.2.2 Rat model of DMTS administration**

Rat studies were performed at the United States Army Medical Research Institute of Chemical Defense (USAMRICD, Aberdeen Proving Ground, MD). Rats (average weight of swine is 0.28 to 0.32 kg) were administered a proprietary formulation of DMTS via both IM and IN routes. For some studies, rats were exposed to CN before the treatment with DMTS at 7.5 mg/kg. For IM administration, 31 rats were treated with neat DMTS (25 mg/kg or 5 mg/kg). For IN administration, 16 rats were treated with DMTS (120 mg/kg or 30  $\mu\text{L}$  of neat DMTS). Multiple blood draws were performed from each catheterized rat. The blood samples were collected baseline (before exposure and/ or treatment) and after 1, 2, 5, 10, 20, 30, 40, 50, 60, 70, 80, and 90 min post-DMTS IN administration. The stock concentration of the internal standard (60  $\mu\text{M}$  DMTS/DMDS in methanol) was shipped to USMRICD before each experiment and was stored at  $-30^\circ\text{C}$ . Before use, the IS was placed in an ice bath and diluted in deionized water to prepare the final working IS concentration of 6  $\mu\text{M}$  DMTS/DMDS. Centrifuge tubes (2 mL) were prepared for each blood draw by adding 950  $\mu\text{L}$  of 0.4% sulfuric acid. Following blood sample collection, 50  $\mu\text{L}$  of blood was pipetted with acid into the designated sample collection tube. The IS (25  $\mu\text{L}$  of the 6

$\mu\text{M}$ ) was accurately spiked to the mixture (blood and acid), and the solution was vortexed at 3000 rpm for 10 s to ensure proper mixing. The prepared samples were then flash-frozen and shipped to South Dakota State University (Brookings, SD, USA) on dry ice for analysis. Samples were kept at  $-80^\circ\text{C}$  until analyzed. All animals were handled and housed by the Guide for the Care and Use of Laboratory Animals published by the United States National Institutes of Health (NIH Publication No. 85-23, Revised 1996). All experiments were approved by the USAMRICD's Institutional Animal Care and Use Committee (IACUC) and complied with the regulations and guidelines of the Animal Welfare Act and the American Association for Accreditation of Laboratory Animal Care.

#### **4.3.3 Preparation of DMTS standards and samples**

For calibration curve preparation, swine, and rat whole blood (non-sterile with sodium EDTA) were purchased from Pel-Freez Biological (Rogers, AR, USA) and kept in a  $-80^\circ\text{C}$  freezer (Thermo Scientific, NJ, USA) until used. To prepare the calibration curves for blood sample analysis, a stock solution of DMTS and DMDS mixture (200 mM each) and the corresponding IS were prepared in methanol, and the calibration standards for DMTS (0.2 – 50  $\mu\text{M}$ ) and DMDS (0.1 – 200  $\mu\text{M}$ ) were diluted in deionized water. The internal standards (DMTS-d6 and DMDS-d6) were diluted in deionized water to prepare the final working concentration (42  $\mu\text{M}$  for swine and 6  $\mu\text{M}$  for rats) for both DMTS-d6 and DMDS-d6. Each calibration standard was prepared in triplicate. To prepare blood samples as calibration standards for DHS analysis, whole blood (475  $\mu\text{L}$  for swine and 25  $\mu\text{L}$  for rats) was transferred to a 4-mL glass vial containing 0.4 % aqueous sulfuric acid (1000  $\mu\text{L}$  for swine and 950  $\mu\text{L}$  for rats). The mixture was then vortexed for 10 s at 3000  $\times$  rpm to ensure proper coagulation and denaturation of proteins. Note that acid

denaturation before adding DMTS/DMDS, both unlabeled and IS, is a crucial step in sample preparation to mitigate the quick and irreproducible degradation of DMTS/DMDS in non-denatured blood [31]. Finally, 25  $\mu\text{L}$  of a diluted calibration standard of DMTS/DMDS and 25  $\mu\text{L}$  of (42  $\mu\text{M}$  for swine and 6  $\mu\text{M}$  for rat) IS DMTS-d6/DMDS-d6 mixture was added to the acidified blood (1475  $\mu\text{L}$  for swine and 975  $\mu\text{L}$  for rat). The mixture (1525  $\mu\text{L}$  for swine and 1025  $\mu\text{L}$  for rats) was vortexed for 10 s at 3000  $\times$  rpm. An aliquot of the sample solution (150  $\mu\text{L}$  for swine and 900  $\mu\text{L}$  for rats) was placed in a 20-mL HS vial with a polytetrafluoroethylene-lined septum for analysis.

To analyze blood samples from treated animals, previously denatured and coagulated blood samples were thawed and vortexed for 10 s at 3000  $\times$  rpm. The aliquot (150  $\mu\text{L}$  for swine and 900  $\mu\text{L}$  for rat) of blood samples was then transferred to a 20-mL HS vial with a polytetrafluoroethylene-lined septum for analysis.

#### **4.3.4 Dynamic headspace GC-MS analysis of DMTS**

The prepared samples were analyzed using DHS-GC-MS via the method developed by Bhadra et al. [31]. Briefly, Gerstel MPS sampler (Gerstel Inc., Linthicum, MD, USA) with an Agilent GC-MS (Agilent Technologies, Wilmington, DE, USA) consisting of a 6890N series gas chromatograph and a 5975 series mass spectrometry (MS) detector was used for the analysis. The DHS was used to transfer the DMTS and DMDS from the sample to the adsorptive material (Tenax® TA) by incubating the HS vial at 40 °C for 1 min and then puncturing the septum with dual needles. Next, nitrogen was delivered through the headspace of the vial to a TDU tube with sorbent for trapping the DMTS and DMDS. The trapping and transfer heater temperatures were set at 28 and 75 °C, respectively. Following 10 min of trapping, the TDU tube was inserted into the TDU and was heated from 30 °C

to 280 °C at a rate of 12 °C/s to the analysis to a cooled injection system (CIS) PTV-type inlet with a quartz wool liner at -100 °C. To transfer the analytes into the GC column, the CIS liner was heated to 275 °C at a rate of 120 °C/s.

A DB5-MS bonded-phase column (30 m x 0.25 mm i.d., 0.25 µm film thickness; J&W Scientific, Folsom, CA, USA) was used to separate the analytes. With a column head pressure of 10.0 psi, the carrier gas helium was used at a 1.0 mL/min flow rate. The GC oven temperature was initially held at 30 °C for 1 min, then elevated at a rate of 120 °C/min up to 250 °C. It was held constant for 2 min before returning to its initial temperature. The retention time for both DMTS and DMTS-d6 was 3.1 min. Because one of the products of the reaction between DMTS with cyanide is the DMDS [156], the level of DMDS generation was also monitored. The retention time for both DMDS and DMDS-d6 were 2.2 min. Electron ionization (EI) was used with an electron energy of 70 eV. Selective ion monitoring (SIM) was used to monitor the quantification and identification ions of DMTS (m/z of 126 and 111, respectively), DMTS-d6 (m/z of 132 and 114, respectively), DMDS (m/z of 94 and 79, respectively), and DMDS-d6 (m/z of 100 and 82, respectively).

#### **4.3.5 Pharmacokinetic studies**

The primary goal of this work was to analyze biological samples from animal studies (performed at USAMRICD on rats and UC-Denver on Swine) for DMTS and DMDS utilizing the current gold-standard DHS-GC-MS technique [31] to contribute to studies of the effectiveness of IN-and IM-delivered DMTS as a cyanide therapeutic. For the entirety of the project, DMTS and DMDS were analyzed from 16 (non-exposed) and 11 (7 exposed and 4 non-exposed) IN-treated rats and swine, respectively. IM-treated rats (N=31; 3 exposed and 28 non-exposed) and swine (N=24; 19 exposed and 4 non-exposed)

were also evaluated. In addition, IV-treated swine (N=4; non-exposed) were evaluated.

#### 4.3.6 Pharmacokinetics & data analysis

PK analysis of DMTS and DMDS was completed to determine the most appropriate distribution model and to evaluate standard PK parameters, such as distribution half-life ( $t_{1/2 \alpha}$ ), elimination half-life ( $t_{1/2 \beta}$ ), area under the curve (AUC), and the elimination constants ( $K_E$ ). These parameters were obtained by evaluating the whole blood concentration of DMTS and DMDS over time and using the standard method to calculate the individual parameters [157]. The  $C_{\max}$  was defined as the maximum concentration of a drug achieved in the blood following dose administration, and  $t_{\max}$  was associated with the time at which  $C_{\max}$  was attained.  $C_{\max}$  and AUC were divided by the dose to compare normalized values of  $C_{\max}$  and AUC. The data are expressed as mean  $\pm$  standard error of the mean (SEM).

### 4.4 Results and Discussion

#### 4.4.1 PK behavior of Intravenous DMTS-treated Swine

Intravenous (IV) injection of DMTS (i.e., injection directly into the bloodstream) allows surety that a drug (DMTS in this case) is making it into the blood at a controllable amount. This type of dosing allows direct evaluation of the elimination behavior of a compound, free from artifacts of inefficient distribution that may occur with other routes of administration. IV administration also allows the rapid attainment of blood concentrations at which drugs are clinically effective [158].

Non-cyanide-exposed swine (N=4; average weight 45 to 48 kg) were IV-treated with DMTS at 10 mg/kg DMTS using a 10% aqueous formulation of DMTS. **Figure 17.** shows the blood concentrations of DMTS and DMDS, respectively. As seen in **Figure**

**17.A**, the blood DMTS concentration started at a maximum blood concentration of about 37.6  $\mu\text{M}$  at approximately 1 min post-administration. The concentrations then decreased as DMTS was eliminated from the body. The AUC of DMTS was calculated using blood DMTS concentration from 1 to 90 min, as 354  $\mu\text{M}\cdot\text{min}$ . The two-phase distribution model was used to describe the other PK behavior of IV-treated DMTS. The  $\alpha$ -phase distribution model was calculated using blood DMTS concentration from 1 to 40 min (**Figure 17.A** inset). Using this data, the  $K_E \alpha$  and  $t_{1/2} \alpha$  were 0.078  $\text{min}^{-1}$ , and 8.94 min, respectively. The  $\beta$ -phase distribution model was defined by a clear trend change from the  $\alpha$ -phase from 40 to 90 min (**Figure 17.A** inset). However, the  $K_E \beta$  and  $t_{1/2} \beta$  were not calculated since a consistent concentration above baseline was reached, and active elimination was not observed following the  $\alpha$ -elimination phase.

As seen in **Figure 17.B**, the blood DMDS concentration started at about 7.5  $\mu\text{M}$  at approximately 0.5 min post-administration. The concentrations then rapidly decreased as DMTS and DMDS were eliminated. The AUC of DMTS was calculated using blood DMDS concentrations from 0.5 to 90 min, as 168  $\mu\text{M}\cdot\text{min}$ . As with DMTS, a two-phase distribution model was used to describe the other PK behavior for blood DMDS concentration. The  $\alpha$ -phase distribution model was calculated using blood DMDS concentration from 0.5 to 10 min (**Figure 17.B** inset). Using this data, the  $K_E \alpha$  and  $t_{1/2} \alpha$  were 0.179  $\text{min}^{-1}$ , and 3.87 min, respectively. The  $\beta$ -phase 10 to 90 min (**Figure 17.B** inset). As with DMTS, active elimination was not observed following the  $\alpha$ -elimination phase for the time period studied.

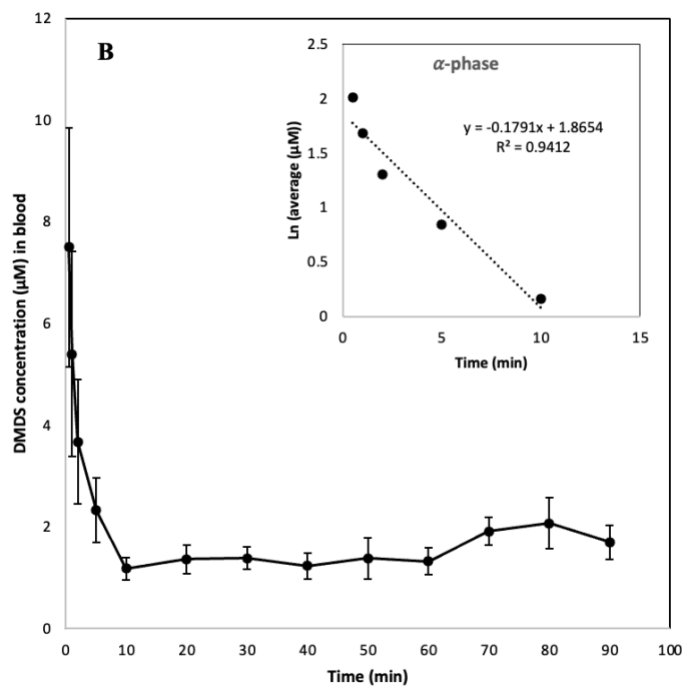
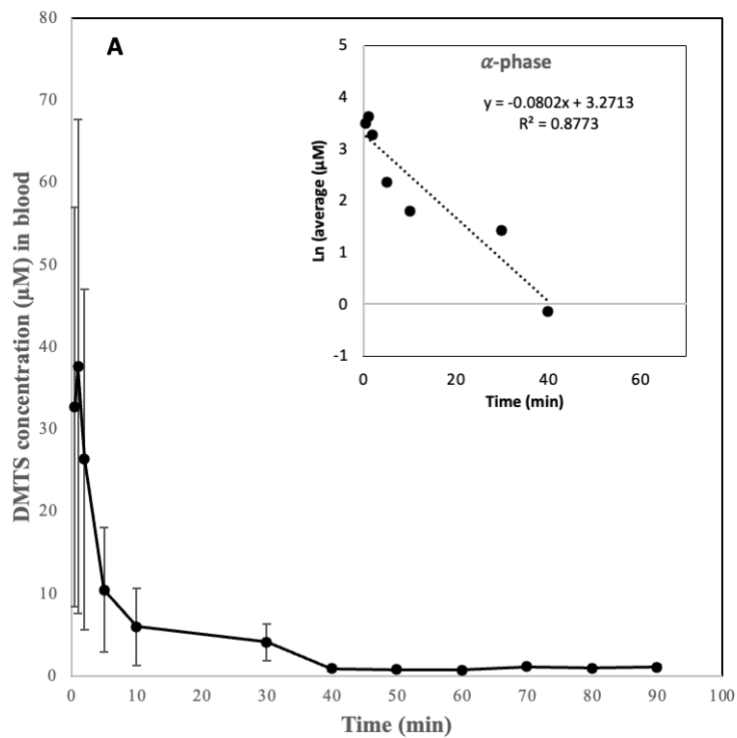


**Figure 17.** Blood concentration of DMTS (A) and DMDS (B) after IV administration of 10 mg/kg DMTS (10% aqueous) in non-exposed swine. Error bars represent the standard error of the mean (N=4).

#### 4.4.2 PK behavior of IM-administered DMTS

IM injection is a desirable mode of drug delivery in mass casualty situations since the drug is injected directly into the muscle, allowing autoinjector formulations and untrained individuals to administer the drug (including self-administration). This is in stark contrast to IV administration, which requires trained medical personnel to handle and administer antidotes. IM administration of DMTS has been shown effective for the administration of DMTS in multiple animal models [31, 155, 159].

##### 4.4.2.1 Rats treated with Intramuscular DMTS

Rats (N=31; average weight 0.28 to 0.32 kg) were intramuscularly treated with DMTS (10% aq DMTS) at two different dose levels, 25 and 5 mg/kg. This includes one group of rats (N=3) previously exposed to 7.5 mg/kg cyanide before treatment with DMTS. For rats administered 25 mg/kg DMTS in the absence of KCN, **Figure 18.A** shows the blood DMTS concentration rapidly increased to a maximum ( $C_{max}$ ) of about 0.87  $\mu\text{M}$  at approximately 2 min postadministration ( $t_{max}$ ). The concentrations then decreased generally consistently over time. The  $K_E$ ,  $t_{1/2}$ , and AUC of DMTS were calculated using blood DMTS concentrations from 60 to 360 min (**Figure 18.A** inset). Using this data, the  $K_E$ ,  $t_{1/2}$ , and AUC were 0.00275  $\text{min}^{-1}$ , 252 min, and 198  $\mu\text{M}\cdot\text{min}$ , respectively. For rats administered 5 mg/kg in the absence of KCN, **Figure 18.B** shows similar behavior of DMTS, with the blood DMTS concentrations rapidly increasing to a maximum ( $C_{max}$ ) of about 0.26  $\mu\text{M}$  at approximately 15 min postadministration ( $t_{max}$ ). The concentrations then generally decreased DMTS was eliminated. As expected, the blood concentration of DMTS was much lower (approximately 3.5 x) for the 5 mg/kg dose than 25 mg/kg (i.e., 5x lower

DMTS dose) (**Figure 19**). The  $K_E$ ,  $t_{1/2}$ , and AUC of DMTS were calculated using blood DMTS concentrations from 15 to 240 min (**Figure 18.B** inset) as  $0.00202 \text{ min}^{-1}$ , 343 min, and  $76.4 \text{ } \mu\text{M}\cdot\text{min}$ , respectively. When treating rats with DMTS (25 mg/kg) following exposure to KCN (7.5 mg/kg), the blood DMTS concentration increased slowly throughout the experiment, producing a maximum concentration of about  $0.25 \mu\text{M}$  at the final time point (**Figure 20**). Because there was no clear elimination phase, PK parameters weren't calculated. The behavior of DMTS is quite different in the animals exposed to cyanide. **Figure 20**. inset shows a comparison of the blood concentration of DMTS in cyanide-exposed and non-exposed rats. It is clear that the blood concentration of DMTS is very low in the CN-exposed rats compared to those non-exposed, with DMTS concentration not reaching even the lowest levels of the non-exposed rats. Also, the initial rapid increase in DMTS in non-exposed rats does not occur in the CN-exposed rats. Each of these behaviors may be explained by the reactions of DMTS in the presence of cyanide to produce SCN and potentially other products.

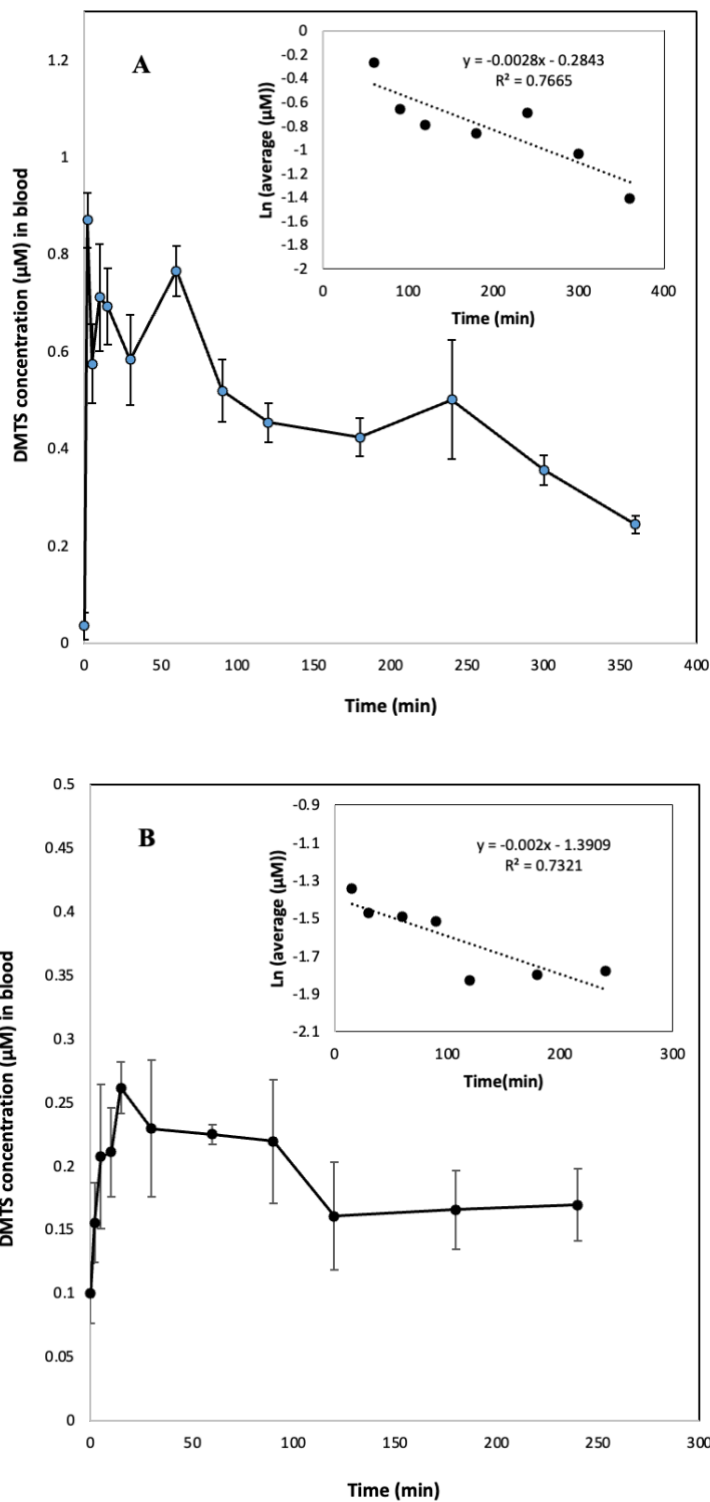


**Figure 18.** Blood DMTS concentration after IM administration of DMTS with 25 mg/kg (A) and 5 mg/kg (B) in non-exposed rats. Error bars represent the standard error of the mean (N=7 for A, N=6 for B).

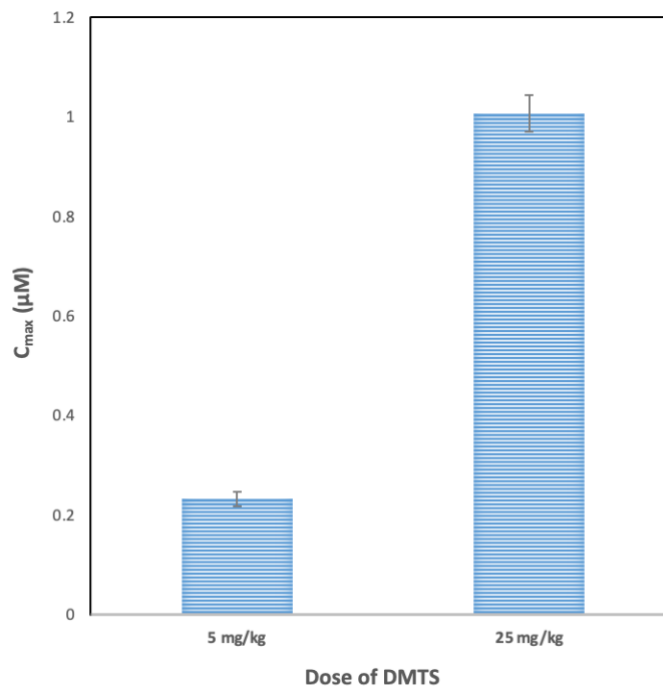


**Figure 19.** C<sub>max</sub> versus dose (25 and 5 mg/kg) of IM administration in non-exposed rats. Error bars represent the standard error of the mean (N=7, for each dose).

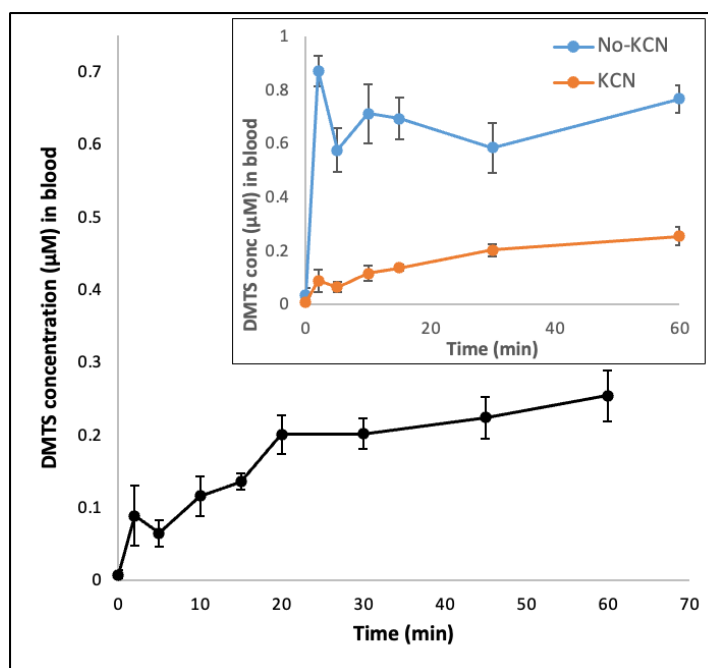


**Figure 20.** Blood DMTS concentration after IM administration of 25 mg/kg DMTS in CN-exposed (7.5 mg/kg) rats. Error bars represent the standard error of the mean. (N=3 for CN-exposed, N=7 for No-KCN). Inset shows the comparison concentration of CN-exposed and non-exposed rats after 25 mg/kg (data from **Figure 18A**).

#### 4.4.2.2 Swine treated with Intramuscular DMTS

Swine were used as an alternate model for the PK studies for DMTS. Initially, a single pig was administered a relatively large DMTS dose to evaluate the swine model's validity and to help identify an effective DMTS dose that rescues cyanide-exposed swine. Three doses of DMTS (25 mg/kg, 12.5 mg/kg, and 7.5 mg/kg) were administered to one pig each following exposure to KCN (7.5 mg/kg). As seen in **Figure 21.A**, the blood DMTS concentration increases rapidly to a maximum ( $C_{max}$ ) of about 5.76  $\mu$ M at approximately 10 min post administration ( $t_{max}$ ) when treated with 25 mg/kg DMTS in the presence of KCN. The concentration then decreased rapidly to a level well above the baseline. The DMTS concentration then slowly decreased for the rest of the experiment. Because only 1 swine was used for each DMTS dose, the PK parameters were not calculated. **Figure 21.B** also shows the blood DMTS concentration for a 12.5 mg/kg DMTS dose. Again, the blood DMTS concentration rapidly increased to a maximum ( $C_{max}$ ) of about 0.37  $\mu$ M at approximately 20 min post administration ( $t_{max}$ ) and stayed generally consistent. With the dose of 7.5 mg/kg of DMTS in the presence of KCN, the blood DMTS was not detected for all the time points.

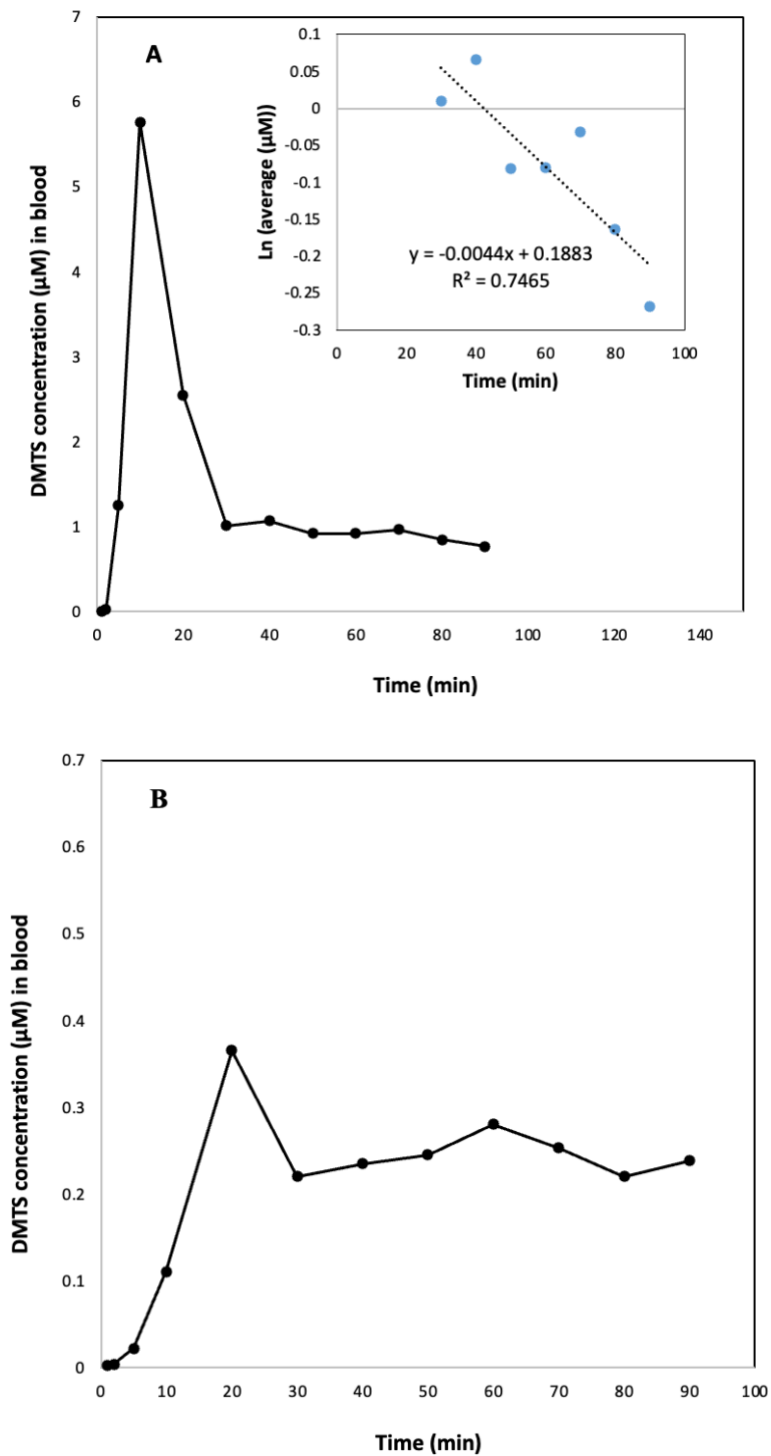


**Figure 21.** Blood DMTS concentrations after IM administration of DMTS with 25 mg/kg (A) and 12.5 mg/kg (B) in CN-exposed (7.5 mg/kg) swine. (N=1)

Following the preliminary dose-finding study, the effective dose to treat the clinical effect of cyanide poisoning was postulated as a single 10 mg/kg dose or two doses of 7.5 mg/kg for a 15 mg/kg total dose. **Figure 22.** and **Figure 23.** show the DMTS and DMDS blood concentrations for both doses following CN exposure. Unfortunately, as seen previously for KCN-exposed animals, the DMTS and DMDS concentrations in the blood were very low and generally increased slowly or remained constant throughout the experiment. This behavior was not amenable to elucidating the PK behavior of DMTS. Specifically, the  $C_{max}$  for DMTS was 0.48  $\mu\text{M}$  for the 10 mg/kg dose and 0.12  $\mu\text{M}$  for the 15 mg/kg dose. It should be noted that the low concentration of DMTS and DMDS contributed to high variability in the data. Because of the highly variable and a typical PK behavior, no other PK parameters were calculated. For accurate evaluation of PK behavior, these studies should be attempted on non-exposed swine.

The PK parameters which could be calculated describing the behavior of IM-DMTS in swine were evaluated in the presence of cyanide, and all DMTS parameters were calculated from cyanide-exposed animals. Because cyanide exposure greatly affects the PK behavior of DMTS, follow on studies should be completed with non-exposed swine. Also note that only a single pig was used for the 25 mg/kg dose.

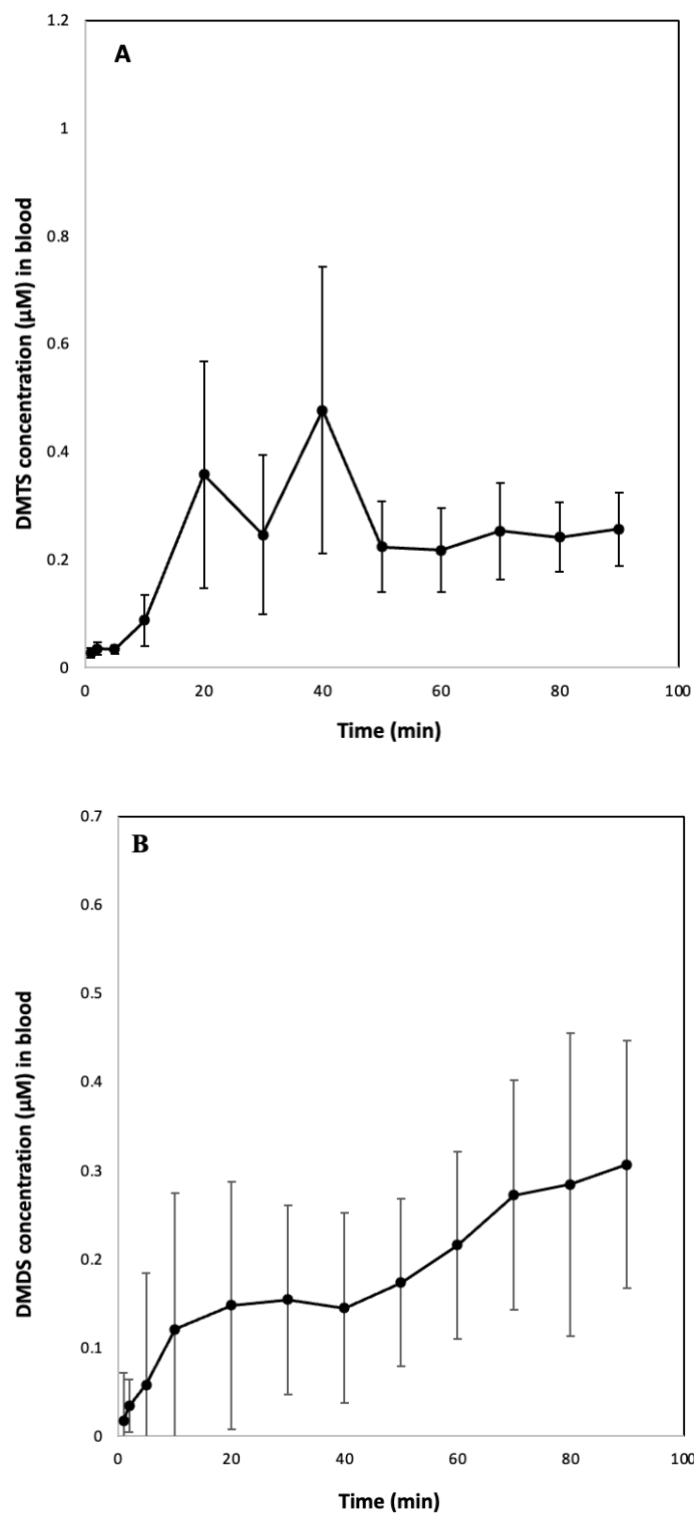


**Figure 22.** Blood DMTS (A) and DMDS (B) concentrations after IM administration of 10 mg/kg DMTS in CN-exposed (7.5 mg/kg) swine. Error bars represent the standard error of the mean (N=7 for A, N=4 for B).

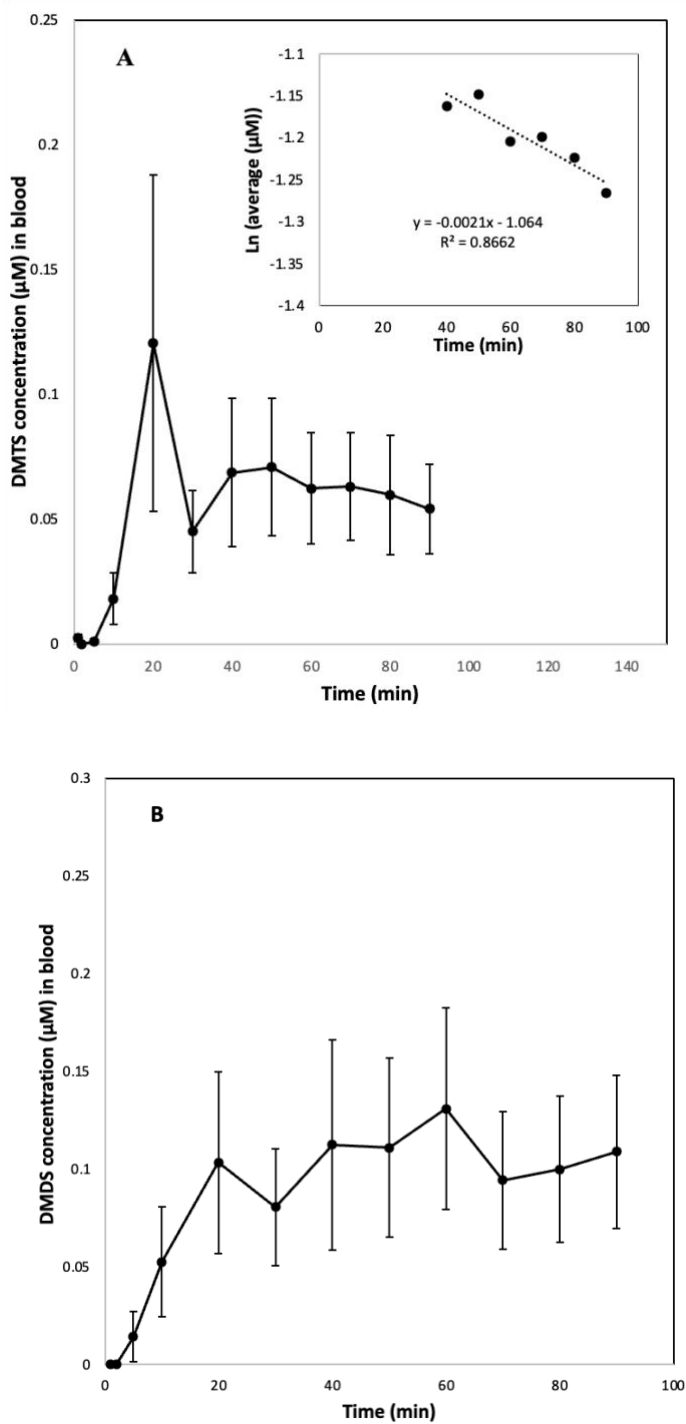


**Figure 23.** Blood DMTS (A) and DMDS (B) concentrations after IM administration of a double dose of DMTS (each dose was 7.5 mg/kg) in CN-exposed (7.5 mg/kg) swine. Error bars represent the standard error of the mean (N= 6).

### 4.4.3 PK behavior of Intranasal-treated DMTS

IN administration is a rare but sometimes effective option to deliver therapeutic medications to the patient's bloodstream to achieve the desired clinical effect. The nasal route can be advantageous as it is painless, the drug can be self-administered, and it promotes high patient compliance [160]. Therefore, IN administration of DMTS may be an effective alternative route of administration for massive CN exposure events.

#### 4.4.3.1 Rats treated with Intranasal DMTS

Rats were IN treated with 120 mg/kg (30  $\mu$ L of neat) DMTS in the absence of KCN. **Figure 24.** shows the blood concentrations of DMTS and DMDS from IN-treated rats. As seen in **Figure 24.A**, the blood DMTS concentration increased to a maximum ( $C_{max}$ ) of about 14.3  $\mu$ M at approximately 5 min postadministration ( $t_{max}$ ). The concentration then decreased rapidly as DMTS was eliminated. The AUC of DMTS was calculated using blood DMTS concentration from 5 to 300 min, as 383  $\mu$ M·min. The three-phase distribution model was used to describe the PK behavior of IN-treated DMTS in rats. The  $\alpha$ -phase distribution model was calculated using blood DMTS concentration from 5 to 15 min (**Figure 24.A** inset). Using this data, the  $K_E \alpha$  and  $t_{1/2 \alpha}$  were 0.136  $\text{min}^{-1}$ , and 5.10 min, respectively. The  $\beta$ -phase distribution model was calculated using blood DMTS concentrations from 15 to 120 min (**Figure 24.A** inset). Using this data, the  $K_E \beta$  and  $t_{1/2 \beta}$  were 0.0164  $\text{min}^{-1}$ , and 42.3 min, respectively. The  $\gamma$ -phase distribution model was calculated using blood DMTS concentration from 120 to 300 min (**Figure 24.A** inset). Using this data, the  $K_E \gamma$  and  $t_{1/2 \gamma}$  were 0.0027  $\text{min}^{-1}$ , and 252 min, respectively.

As seen in **Figure 24.B**, the blood DMDS concentration increased to a maximum ( $C_{max}$ ) of about 144.15  $\mu$ M at approximately 5 min postadministration ( $t_{max}$ ). The

concentrations then decreased rapidly as with DMTS. The AUC of DMDS was calculated using blood DMDS concentrations from 5 to 300 min, as 2177  $\mu\text{M}\cdot\text{min}$ . Similar to blood DMTS, the three-phase distribution model was also used to describe the other PK behavior of blood DMDS. The  $\alpha$ -phase distribution model was calculated using blood DMDS concentration from 5 to 30 min (**Figure 24.B** inset). Using this data, the  $K_E \alpha$  and  $t_{1/2} \alpha$  were 0.0923  $\text{min}^{-1}$ , and 7.51 min, respectively. The  $\beta$ -phase distribution model was calculated using blood DMTS concentration from 30 to 180 min (**Figure 24.B** inset). Using this data, the  $K_E \beta$  and  $t_{1/2} \beta$  were 0.0119  $\text{min}^{-1}$ , and 58.2 min, respectively. The  $\gamma$ -phase distribution model was calculated using blood DMTS concentration from 180 to 300 min (**Figure 24.B** inset). Using this data, the  $K_E \gamma$  and  $t_{1/2} \gamma$  were 0.00279  $\text{min}^{-1}$ , and 248 min, respectively.

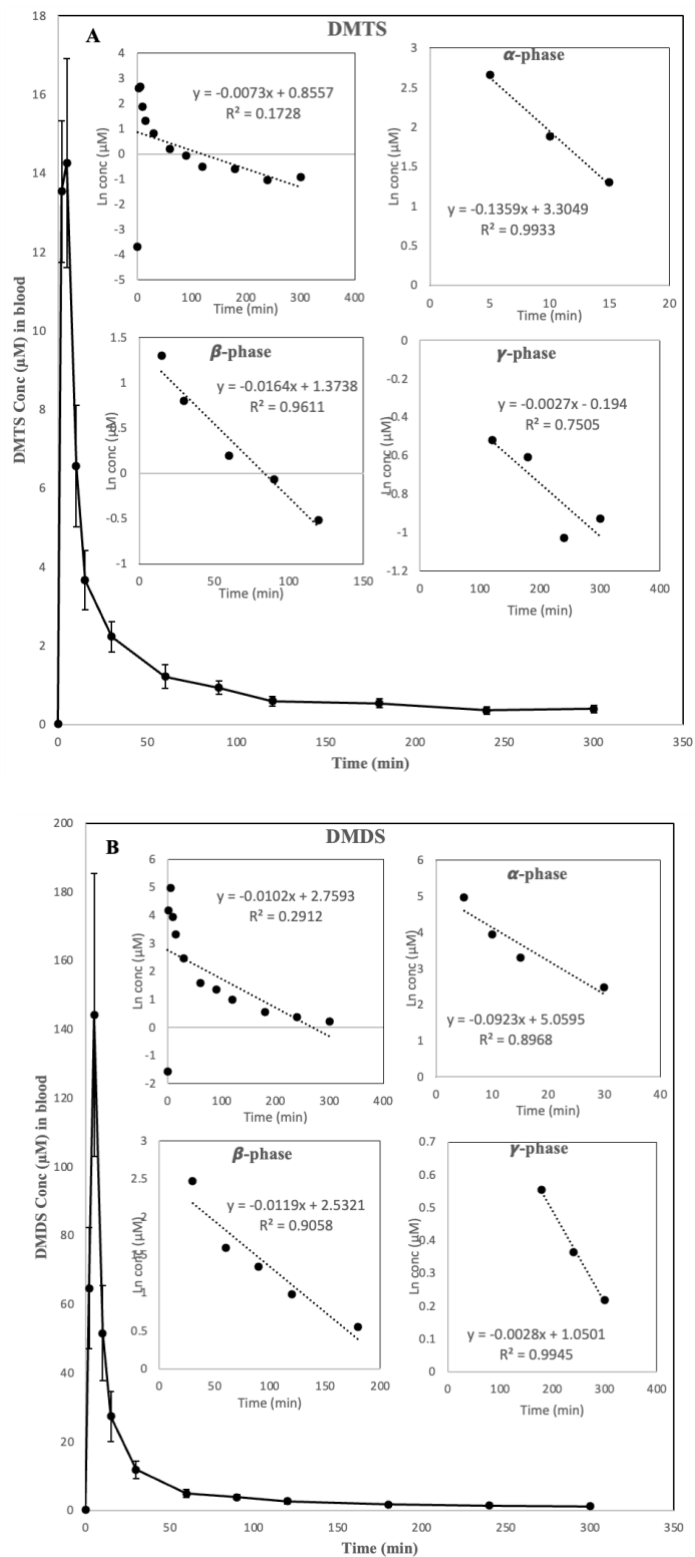


**Figure 24.** Blood DMTS (A) and DMDS (B) concentrations after IN administration of 100 mg/kg DMTS in non-exposed rats. Error bars represent the standard error of the mean (N = 9 for A, N=5 for B).

#### 4.4.3.2 Swine treated with Intranasal DMTS

This study was started with a single animal per DMTS dose to identify the effective dose of DMTS in swine. Three doses of DMTS (500  $\mu\text{L}$  of neat DMTS, 500  $\mu\text{L}$  of 10% DMTS, and 250  $\mu\text{L}$  of neat DMTS) were administered to KCN-exposed pigs. The blood DMTS and DMDS concentrations were below the LLOQ except for the administration of 500  $\mu\text{L}$  of neat DMTS. Therefore, follow-on studies utilized a dose of 550  $\mu\text{L}$  of neat DMTS.

Non-exposed swine (N=4; 45 to 48 kg) were IN-treated with 550  $\mu\text{L}$  of neat DMTS. **Figure 25.** shows the calculated blood concentrations of DMTS and DMDS, respectively. While the blood DMTS concentration was above the LLOQ of the method, it was variable and generally consistent. Therefore, no PK parameters could be confidently calculated. Conversely, the blood DMDS concentration increased rapidly to a maximum ( $C_{\text{max}}$ ) of about 15.81  $\mu\text{M}$  at approximately 5 min postadministration ( $t_{\text{max}}$ ). The  $K_E$  and  $t_{1/2}$  of DMDS were calculated using blood concentrations from 10 to 90 min (**Figure 25.B** inset) as 0.00964  $\text{min}^{-1}$ , and 71.9 min, respectively. The AUC was 693  $\mu\text{M}\cdot\text{min}$ .

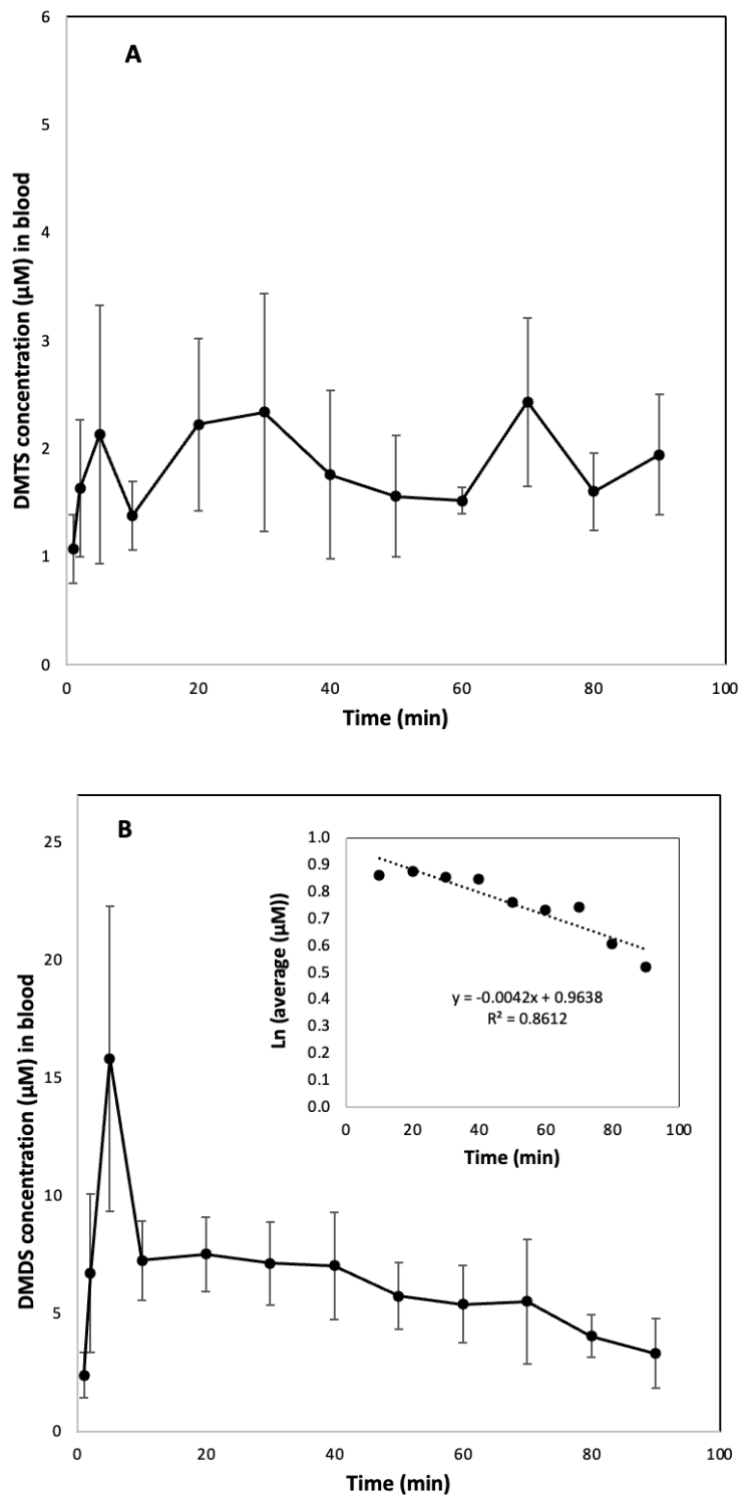


**Figure 25.** Blood DMTS (A) and DMDS (B) concentrations after IN administration of 550 µL of neat DMTS in non-exposed swine. Error bars represent the standard error of the mean (N = 4).

Four cyanide-exposed (7.5 mg/kg) swine were treated with intranasal administration of 550  $\mu\text{L}$  of neat DMTS. Because DMTS concentrations were below the LLOQ of the method, they were not plotted. As seen in **Figure 26.A**, the blood DMDS concentration was close to the LLOQ but was able to be quantified. It increased to a maximum ( $C_{\text{max}}$ ) of about 0.114  $\mu\text{M}$  at approximately 5 min postadministration ( $t_{\text{max}}$ ), and concentrations then decreased as DMTS was eliminated. The  $K_E$ ,  $t_{1/2}$ , and AUC were 0.015  $\text{min}^{-1}$ , 46.2 min, and 5.7  $\mu\text{M}\cdot\text{min}$ , respectively, as calculated from DMDS concentration from 20 min to 90 min (**Figure 26.A** inset).

As with IM-treated rats, the presence of KCN greatly decreased the DMTS and DMDS concentrations to the extent that the DMTS concentrations were not quantifiable, and the DMDS concentrations decreased by approximately 110 times (**Figure 26.B**).

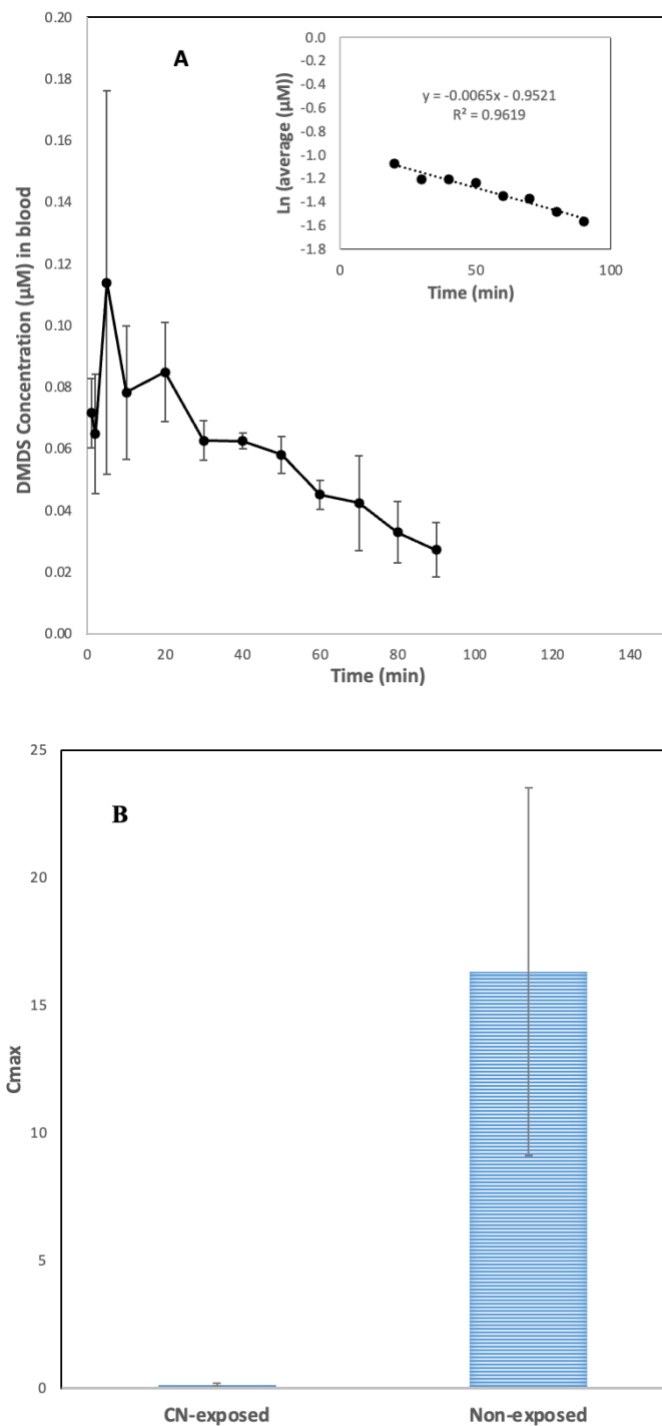


**Figure 26.** Blood DMDS concentration after IN administration of 550  $\mu\text{L}$  of neat DMTS in CN-exposure (7.5 mg/kg) swine. Error bars represent the standard error of the mean (N = 4). Blood DMTS concentration was below LLOQ (<0.2  $\mu\text{M}$ ).

#### 4.4.4 Discussion (IV, IM, and IN- administered DMTS in rats and swine)

The PK results of IV administration of DMTS reveal that DMTS is distributed very quickly, as seen by rapidly decreasing blood concentrations from a  $C_{\max}$  of 37.6  $\mu\text{M}$ . The  $C_{\max}$  of DMDS was 7.5  $\mu\text{M}$  for comparison. Additionally, DMTS and DMDS  $\alpha$ -phase half-lives 8.94 min and 3.87 min, respectively, with elimination rate constants of 0.078  $\text{min}^{-1}$  and 0.179  $\text{min}^{-1}$ , respectively. The  $\beta$ -phase elimination half-lives could not be estimated since no clear elimination was observed from the measured blood concentrations.

The PK behavior of DMTS following IM administration in rats reveals that DMTS is quickly absorbed and distributed. Most IM-DMTS doses produced the maximum blood DMTS concentrations at earliest 2-15 min (except 25 mg/kg DMTS with KCN). This quick distribution of DMTS from IM administration is promising in that it should allow prompt treatment of CN throughout the body by untrained personnel. Additionally, DMTS showed a comparable elimination half-life ( $t_{1/2} = 252$  to 343 min) to the approved antidotes (see **Table 8**). This behavior should allow rapid protection from cyanide exposure compared to other antidotes. The PK behavior of IM-DMTS in swine was evaluated in the presence of cyanide. Because cyanide exposure greatly affects the PK behavior of DMTS, quantification of the PK behavior of DMTS was not possible. Follow on studies should be completed with non-exposed swine. Overall, this pharmacokinetic data of IM-treated rats showed impressive behavior of DMTS for the treatment of CN poisoning, most notably quick onset of action, which is essential for treatment of cyanide exposure.

The PK results of IN-administered DMTS in rats revealed that DMTS is absorbed and distributed very quickly with a  $t_{\max}$  of 5 min at a  $C_{\max}$  of 14.3  $\mu\text{M}$ . The  $C_{\max}$  of DMDS was 144.15  $\mu\text{M}$  for comparison, likely showing a rapid conversion of DMTS. Moreover,

the maximum concentration of blood DMTS and DMDS are at the earliest point of 5 min. This quick distribution of DMTS and DMDS from IN administration is promising in that it should allow rapid reaction of DMTS with CN. While swine were cyanide exposed, the PK results of IN administration of DMTS in swine reveal that DMTS and DMDS are also quickly absorbed and distributed. Unfortunately, the blood DMTS concentration for swine either did not show the expected eliminating trend or was below the LLOQ. Therefore, it is clear that the blood DMTS and DMDS concentrations were significantly reduced from well above the LLOQ for non-cyanide-exposed animals to near or below the LLOQ for cyanide-exposed animals. The potential reason is as DMTS treats cyanide-exposed animals by the reaction of DMTS and cyanide to form DMDS and thiocyanate [142]. Therefore, DMTS may be rapidly converted to DMDS and other byproducts in the presence of cyanide. Overall, this pharmacokinetic data for IN-treated rats and swine showed impressive behavior of DMTS for the treatment of CN poisoning, most notably rapid distribution.

#### **4.4.5 Comparing current US FDA-approved antidotes with a novel antidote (DMTS)**

The absorption of DMTS, following IV, IM, or IN-administration of DMTS, is rapid, with the detection of DMTS and DMDS in the first blood sample collected via all routes.

Compared with DMTS, sodium thiosulfate has a slow rate of distribution, as it must distribute into the mitochondria of the liver and kidney to be effective [161]. As cyanide requires a fast onset of action, this slow rate of distribution is not ideal for a cyanide antidote. However, sodium thiosulfate is commonly administered with sodium nitrite or

hydroxocobalamin. This combination was effective for cyanide poisoning [162]. In fact, sodium thiosulfate and sodium nitrite have been FDA-approved to be packaged together as Nithiodote™ [163-165].

While nitrile has been shown to be rapidly acting, and it has a short half-life compared to thiosulfate and hydroxocobalamin, it has other disadvantages such as, reducing the oxygen-carrying capacity in the blood [166]. Therefore, sodium nitrite alone is not ideal for treating smoke inhalation victims [145, 167-169].

While the  $\alpha$ -phase half-life of hydroxocobalamin is short (averaging 15–40 min), the  $\beta$ -phase half-life was much longer (averaging >360 min) [170-173]. The relatively long half-life (**Table 8**) is combined with a fast onset of action, hydroxocobalamin shows excellent PK properties. However, the large molecular weight and poor solubility make it challenging to administer rapidly in therapeutic doses. Additionally, it is very difficult to administer.

Overall, DMTS appears to have excellent PK properties for rapid treatment of early-onset symptoms of cyanide exposure without the complications inherent in sodium nitrite, or the practical disadvantages of hydroxocobalamin. Moreover, multiple modes of administration, IV, IM, and IN, showed promising behavior of DMTS for the treatment of CN poisoning, with IM and IN administration allowing prompt treatment of CN by untrained personnel for massive CN exposure events.

**Table 8.** The PK parameters of US FDA-approved and novel cyanide antidote (DMTS)

Therapeutic	Route	Animals	Dose	C <sub>max</sub> ( $\mu$ M)	t <sub>1/2</sub> $\alpha$ (min)	t <sub>1/2</sub> $\beta$ (min)	t <sub>1/2</sub> $\gamma$ (min)	Study Ref.	
DMTS	IV	Swine	10 mg/kg	37.6	8.94	$\Phi$		This study	
	IM	Rats	25 mg/kg	0.87	$\diamond$	252*			
			5 mg/kg	0.26	$\diamond$	343*			
	IN	Rats	120 mg/kg (30 $\mu$ L of neat DMTS)	14.3	5.10	42.3	252*		
			Swine	15 mg/kg (550 $\mu$ L of neat DMTS)	15.8 <sup>⊗</sup>	$\diamond$	71.9 <sup>⊗</sup>		
			Swine	15 mg/kg (550 $\mu$ L of neat DMTS) <sup>∇</sup>	0.114 <sup>⊗</sup>	$\diamond$	46.2 <sup>⊗</sup>		
IM	Rats	10 mg/kg	0.89	$\diamond$	630		Bhadra et al. [31]		
Sodium thiosulfate	IV	Humans	1 g, 150 mg/kg	6400	15-20	182		Schulz et al. [161, 174] Ivankovich et al. [175]	
Sodium nitrite	IV	Humans	550 $\mu$ g/kg	320	$\diamond$	42.1 $\pm$ 10.2 <sup>∞</sup> , 78 <sup>∞,δ</sup> , 168 <sup>∇,δ</sup>		Dejam et al. [176] Kirk et al. [146]	
Hydroxo cobalamin	IV	Humans	5g	212.4 $\pm$ 30.9	36	954,		Becker et al. [170]	
			N/A	111.6 $\pm$ 20.4 <sup>∇</sup>	1572 $\pm$ 162 <sup>∇</sup>		Houeto et al. [171]		
	IV	Dogs	70 mg/kg	316 $\pm$ 47,	18.6 $\pm$ 12	441.6 $\pm$ 47.4,		Marrs et al. [172]	
			140 mg/kg	604 $\pm$ 66	15.6 $\pm$ 12.6	360 $\pm$ 34.8		De La Coussaye et al. [173]	

\*The t<sub>1/2</sub>s denoted are considered relatively accurate to estimations, <sup>⊗</sup>DMDS formed from the administration of DMTS, <sup>∇</sup>PK analysis in the presence of Cyanide, <sup>◇</sup>Active distribution was not observed, <sup>Φ</sup>Active elimination was not observed, <sup>δ</sup>Methemoglobin formed from the administration of sodium nitrite, <sup>∞</sup>These studies reported a 'terminal half-life' and a two-phase distribution model. The table lists the terminal half-life as the t<sub>1/2</sub>  $\beta$  -phase, IV=Intravenous, IM= Intramuscular, IN=Intranasal.

#### **4.5 Conclusion**

We studied the pharmacokinetics of IM and IN DMTS in rats and swine. This study demonstrated that DMTS is rapidly absorbed into the blood stream, giving it the potential to quickly neutralize cyanide. It also decreases rapidly to a level well above the baseline and then remains fairly consistent. IM-DMTS and IN-DMTS have a comparable half-life (approximately 300 min and 252 min, respectively) relative to the terminal half-life of hydroxocobalamin but have a comparable half-life to Sodium thiosulfate and sodium nitrite. These results could help analyze pharmacokinetic data in poisoned humans and allow the physician with detailed guidelines for administering DMTS when repeated or continuous administration is required. The PK parameters found in this study help identify the distribution behavior, duration of effectiveness, effective dose, the design of follow-on PK studies, and the approval of DMTS as a cyanide antidote.

#### **4.6 Acknowledgments**

We gratefully acknowledge support from the CounterACT Program, National Institutes of Health Office of the Director, and the National Institute of Environmental Health Sciences (NIEHS) (AOD16026-001-00000/A120-B.P2016-01 and AOD18015-001-00000/MRICD-IAA-18-0129-00). The opinions or assertions contained herein are the private views of the authors. They are not to be construed as official or reflecting the views of the National Institutes of Health or the CounterACT Program.

## **5 CHAPTER 5. CONCLUSIONS, BRODER IMPACTS, AND FUTURE WORKS**

### **5.1 Conclusions**

A novel chlorotyrosine protein adduct, 2,6-DCP, was found based on the interaction of tyrosine and chlorine utilizing base hydrolysis, and a simple and sensitive UHPLC-MS/MS method was successfully developed and validated to analyze the novel compound, 2,6-DCP. The detection of 2,6-DCP in NaOCl-spiked rat plasma protein and plasma protein isolated from chlorine-exposed rats indicates that 2,6-DCP is a promising biomarker for chlorine exposure. A fluorescence probe called FSH was synthesized for water's OCl<sup>-</sup> detection. The probe could be easily synthesized in one step and exhibited a fast response, high selectivity, and excellent sensitivity for OCl<sup>-</sup>. The pharmacokinetics of DMTS, a cyanide antidote, has been studied for IN- and IM- administration in rats and swine. Overall, IM- and IN-administration of DMTS have excellent PK properties with the early onset symptoms of cyanide exposure and a comparable half-life against the currently U.S. FDA-approved antidotes. The findings will help to identify the doses needed to prevent cyanide poisoning.

### **5.2 Broder impacts**

TIAs exposure can be harmful, as they are extremely poisonous and can cause death. However, those TIAs have a significant role in our modern world. They are used in many sectors, including automotive, electronics, disinfectants, and pharmaceuticals. Therefore, transportation mishaps are leading possibilities of TIAs exposure. Hence, it is essential to understand the toxicology of those agents by developing technologies to determine the level of exposure and identify the therapeutic agents to defend against the adverse health effects of the exposure. The detection of the novel biomarker, 2,6-DCP, formed from strong

base hydrolysis of chlorotyrosine protein adduct, can confirm the chlorine exposure. Additionally, detecting hypochlorite in groundwater by utilizing the fluorescence probe FSH will provide insight into the level of community exposure during chlorine exposure. Furthermore, the pharmacokinetic study of DMTS will help identify the onset of action, duration of effectiveness, and necessary doses to prevent cyanide poisoning. Ultimately, this can help to get the U.S. FDA approval of DMTS as a cyanide antidote.

### **5.3 Future work**

Future work should include applying the 2,6-DCP method to analyze 2,6-DCP from more animals exposed to chlorine and compare it to exposure by inhalation. In addition, more animal studies should be performed to confirm the effectiveness of 2,6-DCP as a biomarker. Also, applying the fluorescence probe FSH to analyze  $\text{ClO}^-$  from groundwater (e.g., pool water, lake water, etc.) should be included. Additionally, future work should include the development of a method with the probe FSH for  $\text{OCl}^-$  in biological samples. Lastly, more PK studies of DMTS with different doses of IN- and IM administration needs to perform before extending the development toward clinical trials.

## 6 REFERENCES

1. Guidotti, T.L., *An international registry for toxic inhalation and pulmonary edema: notes from work in progress*. International archives of occupational and environmental health, 1996. **68**(6): p. 380-386.
2. Bessac, B.F. and S.-E. Jordt, *Sensory detection and responses to toxic gases: mechanisms, health effects, and countermeasures*. Proceedings of the American Thoracic Society, 2010. **7**(4): p. 269-277.
3. Rosenstock, L., et al., *Textbook of clinical occupational and environmental medicine*. 2004.
4. Albert, R.K., S.G. Spiro, and J.R. Jett, *Clinical respiratory medicine*. 2008: Elsevier Health Sciences.
5. Gorguner, M. and M. Akgun, *Acute inhalation injury*. The Eurasian journal of medicine, 2010. **42**(1): p. 28.
6. Lawson, J., *Chlorine exposure: a challenge to the physician*. American Family Physician, 1981. **23**(1): p. 135-138.
7. Mackie, E., et al., *Management of chlorine gas-related injuries from the Graniteville, South Carolina, train derailment*. Disaster medicine and public health preparedness, 2014. **8**(5): p. 411-416.
8. Evans, R.B., *Chlorine: state of the art*. Lung, 2005. **183**(3): p. 151-167.
9. Sidell, F.R., E.T. Takafuji, and D.R. Franz, *Medical aspects of chemical and biological warfare*. 1997, Office of the Surgeon General (ARMY) Falls Church VA.
10. Cooke, R., *PSU alumnus recalls 1982 Tylenol murders*. The Digital Collegian, 2002.
11. Markel, H., *How the Tylenol murders of 1982 changed the way we consume medication*. 2014.
12. Layton, D., *Seductive poison: A Jonestown survivor's story of life and death in the Peoples Temple*. 2010: Anchor.
13. AH, Ç., *İnhalasyona Bağlı Akciğer Zedelenmesi*. Göğüs Hastalıkları Acilleri. Ankara: Bilimsel Tıp Yayınevi, 2000: p. 107-117.
14. Conn, H.F. and R.B. Conn, *Current diagnosis 6*, in *Current diagnosis 6*. 1980, WB Saunders.
15. Duncan, M.A., et al., *Follow-up assessment of health consequences after a chlorine release from a train derailment—Graniteville, SC, 2005*. Journal of Medical Toxicology, 2011. **7**: p. 85-91.
16. Chasis, H., et al., *Chlorine accident in Brooklyn*. Occupational Medicine, 1947. **4**(2): p. 152-76.
17. JOYNER, R.E. and E.G. DUREL, *Accidental liquid chlorine spill in a rural community*. Journal of Occupational Medicine, 1962. **4**(3): p. 152-154.
18. Fleta, J., et al., *Intoxication of 76 children by chlorine gas*. Human toxicology, 1986. **5**(2): p. 99-100.
19. Charan, N.B., et al., *Effects of accidental chlorine inhalation on pulmonary function*. Western Journal of Medicine, 1985. **143**(3): p. 333.

20. Hasan, F.M., A. Gehshan, and F.J. Fuleihan, *Resolution of pulmonary dysfunction following acute chlorine exposure*. Archives of Environmental Health: An International Journal, 1983. **38**(2): p. 76-80.
21. Kaufman, J. and D. Burkons, *Clinical, roentgenologic, and physiologic effects of acute chlorine exposure*. Archives of Environmental Health: An International Journal, 1971. **23**(1): p. 29-34.
22. Weiul, H., et al., *Late evaluation of pulmonary function after acute exposure to chlorine gas*. American Review of Respiratory Disease, 1969. **99**(3): p. 374-9.
23. Beach, F., E.S. Jones, and G. Scarrow, *Respiratory effects of chlorine gas*. Occupational and Environmental Medicine, 1969. **26**(3): p. 231-236.
24. Ploysongsang, Y., B. Beach, and R. DiLisio, *Pulmonary function changes after acute inhalation of chlorine gas*. Southern medical journal, 1982. **75**(1): p. 23-26.
25. White, C.W. and J.G. Martin, *Chlorine gas inhalation: human clinical evidence of toxicity and experience in animal models*. Proceedings of the American Thoracic Society, 2010. **7**(4): p. 257-263.
26. Van Der Vliet, A., et al., *Formation of reactive nitrogen species during peroxidase-catalyzed oxidation of nitrite: a potential additional mechanism of nitric oxide-dependent toxicity*. Journal of Biological Chemistry, 1997. **272**(12): p. 7617-7625.
27. Winder, C., *The toxicology of chlorine*. Environmental research, 2001. **85**(2): p. 105-114.
28. Chang, J. and C. Barrow, *Sensory irritation tolerance and cross-tolerance in F-344 rats exposed to chlorine or formaldehyde gas*. Toxicology and applied pharmacology, 1984. **76**(2): p. 319-327.
29. Nodelman, V. and J.S. Ultman, *Longitudinal distribution of chlorine absorption in human airways: a comparison to ozone absorption*. Journal of applied physiology, 1999. **87**(6): p. 2073-2080.
30. Nodelman, V. and J.S. Ultman, *Longitudinal distribution of chlorine absorption in human airways: comparison of nasal and oral quiet breathing*. Journal of Applied Physiology, 1999. **86**(6): p. 1984-1993.
31. Bhadra, S., et al., *Analysis of potential cyanide antidote, dimethyl trisulfide, in whole blood by dynamic headspace gas chromatography–mass spectroscopy*. Journal of Chromatography A, 2019. **1591**: p. 71-78.
32. Jiang, J., et al., *Hydrogen sulfide—mechanisms of toxicity and development of an antidote*. Scientific reports, 2016. **6**(1): p. 20831.
33. Anantharam, P., et al., *Midazolam efficacy against acute hydrogen sulfide-induced mortality and neurotoxicity*. Journal of medical toxicology, 2018. **14**: p. 79-90.
34. Hendry-Hofer, T.B., et al., *Intramuscular aminotetrazole cobinamide as a treatment for inhaled hydrogen sulfide poisoning in a large swine model*. Annals of the New York Academy of Sciences, 2020. **1479**(1): p. 159-167.
35. Jackson, R., et al., *Development of a fluorescence-based sensor for rapid diagnosis of cyanide exposure*. Analytical chemistry, 2014. **86**(3): p. 1845-1852.
36. Bhandari, R.K., et al., *Simultaneous determination of cyanide and thiocyanate in plasma by chemical ionization gas chromatography mass-spectrometry (CI-GC-MS)*. Analytical and bioanalytical chemistry, 2012. **404**(8): p. 2287-2294.

37. Leybell, I., *Cyanide Toxicity*, in, *Medscape*. Emergency Medicine, 2018. **488**.
38. Beasley, D. and W. Glass, *Cyanide poisoning: pathophysiology and treatment recommendations*. Occupational Medicine, 1998. **48**(7): p. 427-431.
39. Bryson, P.D., *Comprehensive reviews in toxicology: for emergency clinicians*. 1996: CRC press.
40. Feeney, J., A.S. Burgen, and E. Grell, *Cyanide Binding to Carbonic Anhydrase: A <sup>13</sup>C-Nuclear-Magnetic-Resonance Study*. European Journal of Biochemistry, 1973. **34**(1): p. 107-111.
41. Dychdala, G.R., *Chlorine and chlorine compounds*. Disinfection, sterilization and preservation, 2001. **2**: p. 167-195.
42. Fauvarque, J., *The chlorine industry*. Pure and applied chemistry, 1996. **68**(9): p. 1713-1720.
43. McCord, C.P., *Industrial poisoning from low concentrations of chlorine gas*. Journal of the American Medical Association, 1926. **86**(22): p. 1687-1688.
44. Koontz, A., *After effects of irritant gases: Residual pulmonary lesions*. South. Med. J, 1934. **27**: p. 676-679.
45. Torén, K. and P.D. Blanc, *The history of pulp and paper bleaching: respiratory-health effects*. The Lancet, 1997. **349**(9061): p. 1316-1318.
46. Adelson, L. and J. Kaufman, *Fatal chlorine poisoning: report of two cases with clinicopathologic correlation*. American Journal of Clinical Pathology, 1971. **56**(4): p. 430-442.
47. Murphy, D.M., et al., *Severe airway disease due to inhalation of fumes from cleansing agents*. Chest, 1976. **69**(3): p. 372-376.
48. Martinez, T.T. and C. Long, *Explosion risk from swimming pool chlorinators and review of chlorine toxicity*. Journal of Toxicology: Clinical Toxicology, 1995. **33**(4): p. 349-354.
49. Faigel, H.C., *Mixtures of household cleaning agents*. New England Journal of Medicine, 1964. **271**(12): p. 618-618.
50. Jones, F.L., *Chlorine poisoning from mixing household cleaners*. JAMA, 1972. **222**(10): p. 1312-1312.
51. Goulding, R., G. Ashforth, and H. Jenkins, *Household products and poisoning*. British medical journal, 1978. **1**(6108): p. 286.
52. Gapany-Gapanavičius, M., et al., *Pneumomediastinum: a complication of chlorine exposure from mixing household cleaning agents*. Jama, 1982. **248**(3): p. 349-350.
53. Mrvos, R., B. Dean, and E.P. Krenzelok, *Home exposures to chlorine/chloramine gas: review of 216 cases*. Southern medical journal, 1993. **86**(6): p. 654-657.
54. Dewhirst, F., *Voluntary chlorine inhalation*. British Medical Journal (Clinical research ed.), 1981. **282**(6263): p. 565.
55. Decker, W.J. and H. Frederick Koch, *Chlorine poisoning at the swimming pool: an overlooked hazard*. Clinical Toxicology, 1978. **13**(3): p. 377-381.
56. Edwards, I., W. Temple, and T. Dobbins, *Acute chlorine poisoning from a high school experiment*. The New Zealand medical journal, 1983. **96**(740): p. 720-721.
57. Sexton, J.D. and D.J. Pronchik, *Chlorine inhalation: the big picture*. Journal of Toxicology: Clinical Toxicology, 1998. **36**(1-2): p. 87-93.

58. Rafferty, P., *Voluntary chlorine inhalation: a new form of self-abuse?* British Medical Journal, 1980. **281**(6249): p. 1178.
59. Paull, J.M., *The origin and basis of threshold limit values.* American Journal of Industrial Medicine, 1984. **5**(3): p. 227-238.
60. Donkor, A.B., *Analysis of Metabolites and Therapeutics for Toxic Inhaled Agent Exposure.* 2021: South Dakota State University.
61. Barrow, C.S., et al., *Comparison of the sensory irritation response in mice to chlorine and hydrogen chloride.* Archives of Environmental Health: An International Journal, 1977. **32**(2): p. 68-76.
62. Gautrin, D., et al., *Is reactive airways dysfunction syndrome a variant of occupational asthma?* Journal of Allergy and Clinical Immunology, 1994. **93**(1): p. 12-22.
63. Alberts, W.M. and A. Guillermo, *Reactive airways dysfunction syndrome.* Chest, 1996. **109**(6): p. 1618-1626.
64. Hureiki, L., J.-P. Croué, and B. Legube, *Chlorination studies of free and combined amino acids.* Water research, 1994. **28**(12): p. 2521-2531.
65. Domigan, N.M., et al., *Chlorination of tyrosyl residues in peptides by myeloperoxidase and human neutrophils.* Journal of Biological Chemistry, 1995. **270**(28): p. 16542-16548.
66. Crow, B.S., et al., *Simultaneous Measurement of 3-Chlorotyrosine and 3, 5-Dichlorotyrosine in Whole Blood, Serum and Plasma by Isotope Dilution HPLC-MS-MS.* Journal of analytical toxicology, 2016. **40**(4): p. 264-271.
67. Sochaski, M.A., et al., *3-chlorotyrosine and 3, 5-dichlorotyrosine as biomarkers of respiratory tract exposure to chlorine gas.* Journal of analytical toxicology, 2008. **32**(1): p. 99-105.
68. Hazen, S.L., et al., *Human neutrophils employ chlorine gas as an oxidant during phagocytosis.* The Journal of clinical investigation, 1996. **98**(6): p. 1283-1289.
69. Kettle, A.J., *Neutrophils convert tyrosyl residues in albumin to chlorotyrosine.* FEBS letters, 1996. **379**(1): p. 103-106.
70. Hazen, S.L., et al., *Mass spectrometric quantification of 3-chlorotyrosine in human tissues with attomole sensitivity: a sensitive and specific marker for myeloperoxidase-catalyzed chlorination at sites of inflammation.* Free Radical Biology and Medicine, 1997. **23**(6): p. 909-916.
71. Hazen, S.L. and J.W. Heinecke, *3-Chlorotyrosine, a specific marker of myeloperoxidase-catalyzed oxidation, is markedly elevated in low density lipoprotein isolated from human atherosclerotic intima.* The Journal of clinical investigation, 1997. **99**(9): p. 2075-2081.
72. Himmelfarb, J., et al., *Myeloperoxidase-catalyzed 3-chlorotyrosine formation in dialysis patients.* Free Radical Biology and Medicine, 2001. **31**(10): p. 1163-1169.
73. Mocatta, T.J., et al., *Plasma concentrations of myeloperoxidase predict mortality after myocardial infarction.* Journal of the American College of Cardiology, 2007. **49**(20): p. 1993-2000.
74. Kettle, A.J., et al., *Myeloperoxidase and protein oxidation in the airways of young children with cystic fibrosis.* American journal of respiratory and critical care medicine, 2004. **170**(12): p. 1317-1323.

75. Chapman, A.L., et al., *Comparison of mono-and dichlorinated tyrosines with carbonyls for detection of hypochlorous acid modified proteins*. Archives of biochemistry and biophysics, 2000. **377**(1): p. 95-100.
76. de Bruin-Hoegée, M., et al., *Elucidation of in Vitro Chlorinated Tyrosine Adducts in Blood Plasma as Selective Biomarkers of Chlorine Exposure*. Chemical Research in Toxicology, 2022. **35**(6): p. 1070-1079.
77. Davies, M., et al., *Reactions of hypochlorous acid with tyrosine and peptidyl-tyrosyl residues give dichlorinated and aldehydic products in addition to 3-chlorotyrosine*. Journal of Biological Chemistry, 2000. **275**(15): p. 10851-10858.
78. Logue, B.A., et al., *Determination of methyl isopropyl hydantoin from rat erythrocytes by gas-chromatography mass-spectrometry to determine methyl isocyanate dose following inhalation exposure*. Journal of Chromatography B, 2018. **1093**: p. 119-127.
79. Bockstaele, E., I. Taverniers, and M. Loose, *Analytical Method Validation and Quality Assurance. Pharmaceutical Sciences Encyclopedia: Drug Discovery, Development, and Manufacturing*, 2010.
80. Shah, V.P., et al., *Bioanalytical method validation—a revisit with a decade of progress*. Pharmaceutical research, 2000. **17**: p. 1551-1557.
81. Davies, M.J., et al., *Stable markers of oxidant damage to proteins and their application in the study of human disease*. Free Radical Biology and Medicine, 1999. **27**(11-12): p. 1151-1163.
82. Thomson, K., *Investigating and detecting biomarkers for oxidative stress*. 2011, University of Glasgow.
83. Logue, B.A. and E. Manandhar, *Percent residual accuracy for quantifying goodness-of-fit of linear calibration curves*. Talanta, 2018. **189**: p. 527-533.
84. Donkor, A.B., et al., *Identification and determination of phenyl methyl carbamate released from adducted hemoglobin for methyl isocyanate exposure verification*. Journal of Chromatography A, 2022. **1681**: p. 463454.
85. Capone, D., et al., *Identification and analysis of 2-chloro-6-methylphenol, 2, 6-dichlorophenol and indole: causes of taints and off-flavours in wines*. Australian Journal of Grape and Wine Research, 2010. **16**(1): p. 210-217.
86. Jáuregui, O., E. Moyano, and M. Galceran, *Capillary electrophoresis–electrospray ion-trap mass spectrometry for the separation of chlorophenols*. Journal of Chromatography A, 2000. **896**(1-2): p. 125-133.
87. Kalakuntla, R.R. and K.S. Kumar, *Bioanalytical method validation: A quality assurance auditor view point*. Journal of Pharmaceutical Sciences and Research, 2009. **1**(3): p. 1.
88. *Reviewer Guidance: Validation of Chromatographic Methods in: C.f.D.E.a.R. (CDER) (Ed.)*. 1994.
89. *Health and Safety Executive, Occupational exposure limits*. 1989.
90. Na, W., et al., *Acute chlorine poisoning caused by an accident at a swimming pool*. Toxicology and industrial health, 2021. **37**(9): p. 513-519.
91. Manual, E.G., *Alternative disinfectants and oxidants*. Disinfectant use in water treatment, Washington DC, 1999.
92. White, G., *Handbook of Chlorination and Alternative Disinfectants. Vol. 3*. 1992, Van Nostrand Reinhold Co. New York, NY.

93. Shamrukh, M. and Y. Hassan. *Chlorination and optimal chlorine dosage for Nile water*. in *Proc. First Ain Shams University Int. Conf. on Environmental Engineering, ASCEE*. 2005.
94. Buckley, R.L., et al., *A case study of chlorine transport and fate following a large accidental release*. *Atmospheric Environment*, 2012. **62**: p. 184-198.
95. Blanton, J., et al., *Transport and dispersion of a conservative tracer in coastal waters with large intertidal areas*. *Estuaries and coasts*, 2009. **32**: p. 573-592.
96. Hearn, J., et al., *Cl<sub>2</sub> deposition on soil matrices*. *Journal of hazardous materials*, 2012. **237**: p. 307-314.
97. Hearn, J.D., et al., *Deposition of Cl<sub>2</sub> on soils during outdoor releases*. *Journal of hazardous materials*, 2013. **252**: p. 107-114.
98. White, G.C., *Handbook of chlorination*. 1972.
99. Stout, G.L., *Chlorine injury to lettuce and other vegetation*. *Calif. Dept. Agric Month. Bull*, 1932. **21**: p. 340-344.
100. Hindawi, I.J., *Injury by sulfur dioxide, hydrogen fluoride, and chlorine as observed and reflected on vegetation in the field*. *Journal of the Air Pollution Control Association*, 1968. **18**(5): p. 307-312.
101. Brennan, E., I. Leone, and C. Holmes, *Accidental chlorine gas damage to vegetation*. *Plant disease reporter*, 1969.
102. Harger, J.R.E., *Damage to vegetation by chlorine gas*. *International Journal of Environmental Studies*, 1973. **4**(1-4): p. 93-108.
103. Booi, C., *The investigation into the spreading and dispersion of a heavy gas cloud by means of plant damages in the affected area*. Unpublished report, Landbouwhogeschool, Wageningen (The Netherlands), 1979: p. 343-356.
104. Nussey, C., A. Mercer, and R. Fitzpatrick, *The effect of uncertainty in chlorine toxicity data on risk estimation*. *Heavy Gas and Risk Assessment III*. Reidel, Dordrecht, 1986.
105. Griffiths, R. and L. Smith, *Development of a vegetation-damage indicator as a means of post-accident investigation for chlorine releases*. *Journal of hazardous materials*, 1990. **23**(2): p. 137-165.
106. Li, J., F. Huo, and C. Yin, *A selective colorimetric and fluorescent probe for the detection of ClO<sup>-</sup> and its application in bioimaging*. *RSC Advances*, 2014. **4**(84): p. 44610-44613.
107. Guo, Y., et al., *Colorimetric detection of hypochlorite in tap water based on the oxidation of 3, 3', 5, 5'-tetramethyl benzidine*. *Analytical Methods*, 2015. **7**(10): p. 4055-4058.
108. Soldatkin, A., et al., *New enzyme potentiometric sensor for hypochlorite species detection*. *Sensors and Actuators B: Chemical*, 1997. **43**(1-3): p. 99-104.
109. Wang, B. and J.I. Anzai, *A facile electrochemical detection of hypochlorite ion based on ferrocene compounds*. *Int. J. Electrochem. Sci*, 2015. **10**: p. 3260-3268.
110. Ordeig, O., et al., *Continuous detection of hypochlorous acid/hypochlorite for water quality monitoring and control*. *Electroanalysis: An International Journal Devoted to Fundamental and Practical Aspects of Electroanalysis*, 2005. **17**(18): p. 1641-1648.

111. Endo, T., T. Yoshimura, and K. Esumi, *Voltammetric study of sodium hypochlorite using dendrimer-stabilized gold nanoparticles*. Journal of colloid and interface science, 2004. **269**(2): p. 364-369.
112. Thiagarajan, S., Z.-Y. Wu, and S.-M. Chen, *Amperometric determination of sodium hypochlorite at poly MnTAPP-nano Au film modified electrode*. Journal of Electroanalytical Chemistry, 2011. **661**(2): p. 322-328.
113. Yap, Y.W., M. Whiteman, and N.S. Cheung, *Chlorinative stress: an under appreciated mediator of neurodegeneration?* Cellular signalling, 2007. **19**(2): p. 219-228.
114. Soundappan, T., et al., *Crumpled graphene oxide decorated SnO<sub>2</sub> nanocolumns for the electrochemical detection of free chlorine*. Applied Nanoscience, 2017. **7**: p. 645-653.
115. Claver, J.B., M.V. Mirón, and L. Capitán-Vallvey, *Determination of hypochlorite in water using a chemiluminescent test strip*. Analytica chimica acta, 2004. **522**(2): p. 267-273.
116. Yang, Y.-K., et al., *A rhodamine– hydroxamic acid-based fluorescent probe for hypochlorous acid and its applications to biological imagings*. Organic letters, 2009. **11**(4): p. 859-861.
117. Zhu, B., et al., *A highly selective colorimetric probe for fast and sensitive detection of hypochlorite in absolute aqueous solution*. Sensors and Actuators B: Chemical, 2014. **191**: p. 473-478.
118. Ding, S., et al., *Real-time detection of hypochlorite in tap water and biological samples by a colorimetric, ratiometric and near-infrared fluorescent turn-on probe*. Analyst, 2015. **140**(13): p. 4687-4693.
119. Song, H., et al., *A dual-function fluorescent probe: sensitive detection of water content in commercial products and rapid detection of hypochlorite with a large Stokes shift*. Dyes and Pigments, 2019. **162**: p. 160-167.
120. Taheri, M. and N. Mansour, *Functionalized silicon nanoparticles as fluorescent probe for detection of hypochlorite in water*. Journal of Photochemistry and Photobiology A: Chemistry, 2019. **382**: p. 111906.
121. Yin, B., et al., *Green synthesis of carbon dots with down-and up-conversion fluorescent properties for sensitive detection of hypochlorite with a dual-readout assay*. Analyst, 2013. **138**(21): p. 6551-6557.
122. Jantra, S., et al., *“Turn on” orange fluorescent probe based on styryl-BODIPY for detection of hypochlorite and its application in live cell imaging*. Dyes and Pigments, 2019. **162**: p. 189-195.
123. Wang, Z., et al., *Three novel camphor-based fluorescence probes for ratiometric detection of hypochlorite and bio-imaging in living cells*. Sensors and Actuators B: Chemical, 2019. **284**: p. 148-158.
124. Chen, L.-D., et al., *Two highly selective and sensitive fluorescent probes design and apply to specific detection of hypochlorite*. Dyes and Pigments, 2019. **161**: p. 510-518.
125. Zhu, B., et al., *A colorimetric and ratiometric fluorescent probe for thiols and its bioimaging applications*. Chemical communications, 2010. **46**(31): p. 5710-5712.
126. Fink, D.W. and W.R. Koehler, *pH effects on fluorescence of umbelliferone*. Analytical Chemistry, 1970. **42**(9): p. 990-993.

127. Martin, M.M. and L. Lindqvist, *The pH dependence of fluorescein fluorescence*. Journal of Luminescence, 1975. **10**(6): p. 381-390.
128. Zhujun, Z. and W.R. Seitz, *A fluorescence sensor for quantifying pH in the range from 6.5 to 8.5*. Analytica chimica acta, 1984. **160**: p. 47-55.
129. Goswami, S., et al., *A rhodamine-quinoline based chemodosimeter capable of recognising endogenous OCl<sup>-</sup> in human blood cells*. RSC advances, 2014. **4**(47): p. 24881-24886.
130. Rigas, F., A. Mavridou, and A. Zacharopoulos, *Water quality of swimming pools in Athens area*. International Journal of Environmental Health Research, 1998. **8**(3): p. 253-260.
131. Simard, S., R. Tardif, and M.J. Rodriguez, *Variability of chlorination by-product occurrence in water of indoor and outdoor swimming pools*. Water Research, 2013. **47**(5): p. 1763-1772.
132. Baskin, S., et al., *Insights on cyanide toxicity and methods of treatment*. Pharmacological perspectives of toxic chemicals and their antidotes, 2004: p. 105-146.
133. Kage, S., T. Nagata, and K. Kudo, *Determination of cyanide and thiocyanate in blood by gas chromatography and gas chromatography-mass spectrometry*. Journal of Chromatography B: Biomedical Sciences and Applications, 1996. **675**(1): p. 27-32.
134. Logue, B.A., et al., *The analysis of cyanide and its breakdown products in biological samples*. Critical Reviews in Analytical Chemistry, 2010. **40**(2): p. 122-147.
135. Barnes, C.D. and L.G. Eltherington, *Drug dosage in laboratory animals: a handbook*. 1973: Univ of California Press.
136. Cummings, T., *The treatment of cyanide poisoning*. Occupational medicine, 2004. **54**(2): p. 82-85.
137. Sudworth, J., *China explosions: What we know about what happened in Tianjin*. BBC News, August, 2015. **17**.
138. Randviir, E.P. and C.E. Banks, *The latest developments in quantifying cyanide and hydrogen cyanide*. TrAC Trends in Analytical Chemistry, 2015. **64**: p. 75-85.
139. Cardoso, L.M., F.B. Mainier, and J.A. Itabirano, *Analysis voltammetry of cyanide and process electrolytic removal of cyanide in effluents*. American Journal of Environmental Engineering, 2014. **4**(6): p. 182-188.
140. Conn, E.E., *Cyanogenesis, the production of hydrogen cyanide, by plants, in Effects of poisonous plants on livestock*. 1978, Elsevier. p. 301-310.
141. Stutelberg, M.W., et al., *Pharmacokinetics of next generation cyanide antidote sulfanegen in rabbits*. International journal of Pharmacokinetics, 2017. **2**(2): p. 105-111.
142. Manandhar, E., et al., *Determination of dimethyl trisulfide in rabbit blood using stir bar sorptive extraction gas chromatography-mass spectrometry*. Journal of Chromatography a, 2016. **1461**: p. 10-17.
143. Gracia, R. and G. Shepherd, *Cyanide poisoning and its treatment*. Pharmacotherapy: The Journal of Human Pharmacology and Drug Therapy, 2004. **24**(10): p. 1358-1365.

144. Hamel, J., *A review of acute cyanide poisoning with a treatment update*. Critical care nurse, 2011. **31**(1): p. 72-82.
145. Pearce, L.L., et al., *Reversal of cyanide inhibition of cytochrome c oxidase by the auxiliary substrate nitric oxide: an endogenous antidote to cyanide poisoning?* Journal of Biological Chemistry, 2003. **278**(52): p. 52139-52145.
146. Kirk, M.A., R. Gerace, and K.W. Kulig, *Cyanide and methemoglobin kinetics in smoke inhalation victims treated with the cyanide antidote kit*. Annals of emergency medicine, 1993. **22**(9): p. 1413-1418.
147. Yusim, Y., D. Livingstone, and A. Sidi, *Blue dyes, blue people: the systemic effects of blue dyes when administered via different routes*. Journal of clinical anesthesia, 2007. **19**(4): p. 315-321.
148. Kiss, L., et al., *From the cover: In vitro and in vivo blood-brain barrier penetration studies with the novel cyanide antidote candidate dimethyl trisulfide in mice*. Toxicological Sciences, 2017. **160**(2): p. 398-407.
149. Lee, J., et al., *Monitoring dose response of cyanide antidote dimethyl trisulfide in rabbits using diffuse optical spectroscopy*. Journal of Medical Toxicology, 2018. **14**(4): p. 295-305.
150. Fan, W., H. Shen, and Y. Xu, *Quantification of volatile compounds in Chinese soy sauce aroma type liquor by stir bar sorptive extraction and gas chromatography–mass spectrometry*. Journal of the Science of Food and Agriculture, 2011. **91**(7): p. 1187-1198.
151. Lawson, L.D., Z.-Y.J. Wang, and B.G. Hughes, *Identification and HPLC quantitation of the sulfides and dialk(en)yl thiosulfinates in commercial garlic products*. Planta medica, 1991. **57**(04): p. 363-370.
152. Frankenberg, L., *Enzyme therapy in cyanide poisoning: effect of rhodanese and sulfur compounds*. Archives of toxicology, 1980. **45**(4): p. 315-323.
153. Iciek, M.g. and L. Wlodek, *Biosynthesis and biological properties of compounds containing highly reactive, reduced sulfane sulfur*. Polish journal of pharmacology, 2001. **53**(3): p. 215-226.
154. Petrikovics, I., et al., *Encapsulated rhodanese with two new sulfur donors in cyanide antagonism*. Toxicology Letters, 2010(196): p. S144.
155. Rockwood, G.A., D.E. Thompson, and I. Petrikovics, *Dimethyl trisulfide: a novel cyanide countermeasure*. Toxicology and industrial health, 2016. **32**(12): p. 2009-2016.
156. Sorbo, B., *Crystalline rhodanese*. Acta chem. scand, 1953. **7**(8).
157. Shargel L, W.-P.S., Yu AB, *Applied Biopharmaceutics & Pharmacokinetics*. 2007.
158. Chris Young, J.J., *Everything to know about intravenous injections*. 2021.
159. Downey, I., et al. *In vivo efficacy and optimization of novel cyanide countermeasures*. in *NIH CounterACT 7th Annual Network Research Symposium, Washington, DC, USA*. 2013.
160. Salama, M.M. and A.O. Elzoghby, *Mucoadhesive nanoparticles as promising drug delivery systems*, in *Theory and Applications of Nonparenteral Nanomedicines*. 2021, Elsevier. p. 113-136.

161. Schulz, V., et al., *Cyanide toxicity of sodium nitroprusside in therapeutic use with and without sodium thiosulphate*. *Klinische Wochenschrift*, 1982. **60**(22): p. 1393-1400.
162. Hall, A.H., R. Dart, and G. Bogdan, *Sodium thiosulfate or hydroxocobalamin for the empiric treatment of cyanide poisoning?* *Annals of emergency medicine*, 2007. **49**(6): p. 806-813.
163. W Borron, S. and F. J Baud, *Antidotes for acute cyanide poisoning*. *Current Pharmaceutical Biotechnology*, 2012. **13**(10): p. 1940-1948.
164. Marraffa, J.M., V. Cohen, and M.A. Howland, *Antidotes for toxicological emergencies: a practical review*. *American Journal of Health-System Pharmacy*, 2012. **69**(3): p. 199-212.
165. Bebarta, V.S., et al., *Sodium nitrite and sodium thiosulfate are effective against acute cyanide poisoning when administered by intramuscular injection*. *Annals of emergency medicine*, 2017. **69**(6): p. 718-725. e4.
166. Baskin, S.I., A.M. Horowitz, and E.W. Nealley, *The antidotal action of sodium nitrite and sodium thiosulfate against cyanide poisoning*. *The Journal of Clinical Pharmacology*, 1992. **32**(4): p. 368-375.
167. Brenner, M., et al., *Sulfanegen sodium treatment in a rabbit model of sub-lethal cyanide toxicity*. *Toxicology and applied pharmacology*, 2010. **248**(3): p. 269-276.
168. Cambal, L.K., et al., *Acute, sublethal cyanide poisoning in mice is ameliorated by nitrite alone: complications arising from concomitant administration of nitrite and thiosulfate as an antidotal combination*. *Chemical research in toxicology*, 2011. **24**(7): p. 1104-1112.
169. DesLauriers, C.A., A.M. Burda, and M. Wahl, *Hydroxocobalamin as a cyanide antidote*. *American journal of therapeutics*, 2006. **13**(2): p. 161-165.
170. Forsyth, J.C., et al., *Hydroxocobalamin as a cyanide antidote: safety, efficacy and pharmacokinetics in heavily smoking normal volunteers*. *Journal of Toxicology: Clinical Toxicology*, 1993. **31**(2): p. 277-294.
171. Houeto, P., et al., *Pharmacokinetics of hydroxocobalamin in smoke inhalation victims*. *Journal of Toxicology: Clinical Toxicology*, 1996. **34**(4): p. 397-404.
172. Thompson, J.P. and T.C. Marrs, *Hydroxocobalamin in cyanide poisoning*. *Clinical Toxicology*, 2012. **50**(10): p. 875-885.
173. de La Coussaye, J., et al., *Pharmacokinetics of hydroxocobalamin in dogs*. *Journal of neurosurgical anesthesiology*, 1994. **6**(2): p. 111-115.
174. Schulz, V., *Clinical pharmacokinetics of nitroprusside, cyanide, thiosulphate and thiocyanate*. *Clinical pharmacokinetics*, 1984. **9**: p. 239-251.
175. Ivankovich, A.D., et al., *Sodium thiosulfate disposition in humans: relation to sodium nitroprusside toxicity*. *Anesthesiology*, 1983. **58**(1): p. 11-17.
176. Dejam, A., et al., *Nitrite infusion in humans and nonhuman primates: endocrine effects, pharmacokinetics, and tolerance formation*. *Circulation*, 2007. **116**(16): p. 1821-1831.